So many paths, that wind and wind,
While just the art of being kind
Is all the sad world needs
Ella Wilcox (1855-1919), The World's Needs

17

Tunneling

Tunneling processes govern the decay of metastable atomic and nuclear states, as well as the transition of overheated or undercooled thermodynamic phases to a stable equilibrium phase. Path integrals are an important tool for describing these processes theoretically. For high tunneling barriers, the decay proceeds slowly and its properties can usually be explained by a semiclassical expansion of a simple model path integral. By combining this expansion with the variational methods of Chapter 5, it is possible to extend the range of applications far into the regime of low barriers.

In this chapter we present a novel theory of tunneling through high and low barriers and discuss several typical examples in detail. A useful fundamental application arises in the context of perturbation theory since the large-order behavior of perturbation expansions is governed by semiclassical tunneling processes. Here the new theory is used to calculate perturbation coefficients to any order with a high degree of accuracy.

17.1 Double-Well Potential

A simple model system for tunneling processes is the symmetric double-well potential of Eq. (5.78). It may be rewritten in the form

$$V(x) = \frac{\omega^2}{8a^2}(x-a)^2(x+a)^2, \tag{17.1}$$

which exhibits the two degenerate symmetric minima at $x = \pm a$ (see Fig. 17.1). The coupling strength is

$$g = \omega^2/2a^2. \tag{17.2}$$

Near the minima, the potential looks approximately like a harmonic oscillator potential $V_\pm(x) = \omega^2(x \mp a)^2/2$:

$$V(x) = \frac{\omega^2}{2}(x \mp a)^2 \left(1 \pm \frac{x \mp a}{a} + \dots\right) \equiv V_\pm(x) + \Delta V_\pm(x) + \dots \ . \tag{17.3}$$

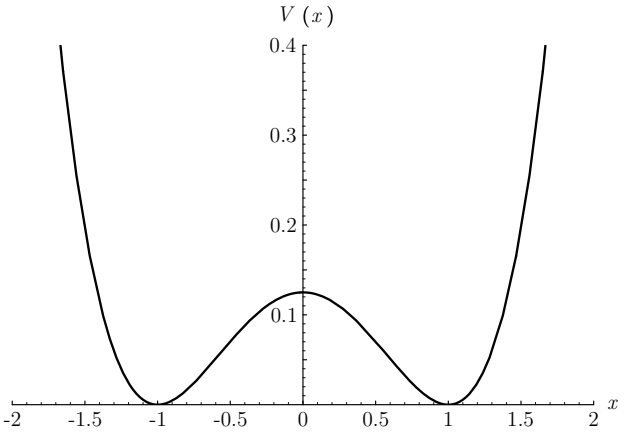

Figure 17.1 Plot of symmetric double-well potential $V(x) = (x-a)^2(x+a)^2\omega^2/8a^2$ for $\omega = 1$ and $a = 1$.

The height of the potential barrier at the center is

$$V_{\max} = \frac{(\omega a)^2}{8}. \tag{17.4}$$

In the limit $a \to \infty$ at a fixed frequency ω, the barrier height becomes infinite and the system decomposes into a sum of two independent harmonic-oscillator potentials widely separated from each other. Correspondingly, the wave functions of the system should tend to two separate sets of oscillator wave functions

$$\psi_n(\Delta x_\pm) \to \left(\frac{\omega}{\pi\hbar}\right)^{1/4} \frac{1}{2^{n/2}\sqrt{n!}} e^{-\omega(\Delta x_\pm)^2/2\hbar} H_n(\Delta x_\pm \sqrt{\omega/\hbar}), \tag{17.5}$$

where the quantities

$$\Delta x_\pm \equiv x \pm a \tag{17.6}$$

measure the distances of the point x from the respective minima.

A similar separation occurs in the time evolution amplitude which decomposes into the sum of the amplitudes of the individual oscillators

$$\begin{aligned} (x_b t_b | x_a t_a) &\xrightarrow{a\to\infty} (x_b t_b | x_a t_a)_- + (x_b t_b | x_a t_a)_+ \\ &\equiv \int \mathcal{D}x(t) \exp\left\{\frac{i}{\hbar}\int_{t_a}^{t_b} dt \frac{1}{2}[\dot{x}^2 - \omega^2(x+a)^2]\right\} + (a \to -a). \end{aligned} \tag{17.7}$$

For convenience, we have assumed a unit particle mass $M = 1$ in the Lagrangian of the system:

$$L = \frac{\dot{x}^2}{2} - V(x). \tag{17.8}$$

If a is no longer infinite, a particle in either of the two oscillator wells has a nonvanishing amplitude for tunneling through the barrier to the other well, and the wave functions of the right- and left-hand oscillators are mixed with each other. Since the action is symmetric under the mirror reflection $x \to -x$, the solutions of the Schrödinger equation

$$\hat{H}\psi(x,t) = H(-i\partial_x, x)\psi(x,t) = i\hbar\partial_t\psi(x,t), \tag{17.9}$$

with the Hamiltonian

$$H(p,x) = \frac{p^2}{2} + V(x), \tag{17.10}$$

can be separated into symmetric and antisymmetric wave functions. As usual, the symmetric states have a lower energy than the antisymmetric ones since a smaller number of nodes implies less kinetic energy for the particles.

If the distance parameter a is very large, then, to leading order in $a \to \infty$, the lowest two wave functions coincide approximately with the symmetric and antisymmetric combinations of the harmonic-oscillator wave functions

$$\psi_{\rm s,a} \approx \frac{1}{\sqrt{2}}[\psi_0(x-a) \pm \psi_0(x+a)]. \tag{17.11}$$

Due to tunneling, the lowest two energies show some deviation from the harmonic ground state value

$$E^{(0)}_{\rm s,a} = \frac{1}{2}\hbar\omega + \Delta E^{(0)}_{\rm s,a}. \tag{17.12}$$

At a large distance parameter a, this deviation is very small. In quantum mechanics, the level shifts $\Delta E_{\rm s,a}$ can be calculated in lowest-order perturbation theory by inserting the approximate wave functions (17.11) into the formula

$$\Delta E_{\rm s,a} = \int dx \psi_{\rm s,a}\hat{H}\psi_{\rm s,a}. \tag{17.13}$$

Since the wave functions $\psi_0(x \pm a)$ of the individual potential wells fall off exponentially like $e^{-x^2/2}$ at large x, the level shifts $\Delta E_{\rm s,a}$ are exponentially small in the square distance a^2.

In this chapter we derive the level shifts $\Delta E_{\rm s}, \Delta E_{\rm a}$ and the related tunneling amplitudes from the path integral of the system. For large a, this will be relatively simple since we can have recourse to the semiclassical approximation developed in Chapter 4 which becomes exact in the limit $a \to \infty$. As long as we are interested only in the lowest two states, the problem can immediately be simplified. We take the spectral representation of the amplitude

$$\begin{aligned}(x_b t_b | x_a t_a) &= \int \mathcal{D}x(t) e^{(i/\hbar)\int_{t_a}^{t_b} dt[\dot{x}^2/2 - V(x)]} \\ &= \sum_n \psi_n(x_b)\psi_n(x_a) e^{-iE_n(t_b-t_a)/\hbar}\end{aligned} \tag{17.14}$$

to imaginary times $t_{a,b} \to \tau_{a,b} = \mp iL/2$, where it becomes

$$\begin{aligned}(x_b\ L/2|x_a - L/2) &= \int \mathcal{D}x(\tau) e^{-(1/\hbar)\int_{-L/2}^{L/2} d\tau [x'^2/2 + V(x)]} \\ &= \sum_n \psi_n(x_b)\psi_n(x_a) e^{-E_n L/\hbar},\end{aligned} \tag{17.15}$$

with the notation $x'(\tau) \equiv dx(\tau)/d\tau$. In the limit of large L, the spectral sum (17.15) is obviously most sensitive to the lowest energies, the contributions of the higher energies E_n being suppressed exponentially. Thus, to calculate the small level shifts of the two lowest states, $\Delta E_{\rm s,a}$, we have only to find the leading and subleading exponential behaviors. Since the wave functions are largest close to the bottoms of the double well at $x \sim \pm a$, we may consider the amplitudes with the initial and final positions x_a and x_b lying precisely at the bottoms, once on the same side of the potential barrier,

$$(a\ L/2|a\ -L/2) = (-a\ L/2|\,-a\ -L/2), \tag{17.16}$$

and once on the opposite sides

$$(a\ L/2|\,-a\ -L/2) = (-a\ L/2|a\ -L/2). \tag{17.17}$$

For these amplitudes we now calculate the semiclassical approximation in the limit $L \to \infty$. The results will lead to level shift formula in Section 17.7.

17.2 Classical Solutions — Kinks and Antikinks

According to Chapter 4, the leading exponential behavior of the semiclassical approximation is obtained from the classical solutions to the path integral. The fluctuation factor requires the calculation of the quadratic fluctuation correction. The result has the form

$$\sum_{\text{class. solutions}} \exp\{-\mathcal{A}_{\rm cl}/\hbar\} \times F\ , \tag{17.18}$$

where $\mathcal{A}_{\rm cl}$ denotes the action of each classical solution and F the fluctuation factor.

The amplitude (17.16), which contains the bottom of the same well on either side, is dominated by a trivial classical solution which remains all the time at the same bottom:

$$x(\tau) \equiv \pm a. \tag{17.19}$$

Classical solutions exist also for the other amplitudes (17.17) which connect the different bottoms at $-a$ and a. These solutions cross the barrier and read, in the limit $L \to \infty$,

$$x(\tau) = x_{\rm cl}^{\pm}(\tau) \equiv \pm a \tanh[\omega(\tau - \tau_0)/2], \tag{17.20}$$

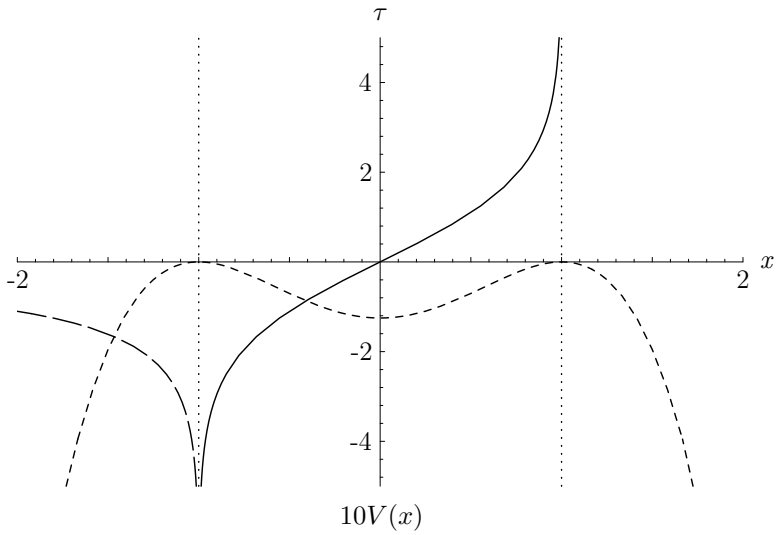

Figure 17.2 Classical kink solution (solid curve) in double-well potential (short-dashed curve with units marked on the lower half of the vertical axis). The solution connects the two degenerate maxima in the reversed potential. The long-dashed curve shows a solution which starts out at a maximum and slides down into the adjacent abyss.

with an arbitrary parameter τ_0 specifying the point on the imaginary time axis where the crossing takes place. The crossing takes place within a time of the order of $2/\omega$. For large positive and negative τ, the solution approaches $\pm a$ exponentially (see Fig. 17.2). Alluding to their shape, the solutions $x_{\rm cl}^{\pm}(\tau)$ are called *kink* and *antikink* solutions, respectively.[1]

To derive these solutions, consider the equation of motion in real time,

$$\ddot{x}(t) = -V'(x(t)), \tag{17.21}$$

where $V'(x) \equiv dV(x)/dx$. In the Euclidean version with $\tau = -it$, this reads

$$x''(\tau) = V'(x(\tau)). \tag{17.22}$$

Since the differential equation is of second order, there is merely a sign change in front of the potential with respect to the real-time differential equation (17.21). The Euclidean equation of motion corresponds therefore to a usual equation of motion of a point particle in real time, whose potential is turned upside down with respect to Fig. 17.1. This is illustrated in Fig. 17.3. The reversed potential allows obviously for a classical solution which starts out at $x = -a$ for $\tau \to -\infty$ and arrives at $x = a$ for $\tau \to +\infty$. The particle needs an infinite time to leave the initial potential mountain and to climb up to the top of the final one. The movement through the central valley proceeds within the finite time $\approx 2/\omega$. If the particle does not start

[1] In field-theoretic literature, such solutions are also referred to as instanton or anti-instanton solutions, since the valley is crossed within a short time interval. See the references quoted at the end of the chapter.

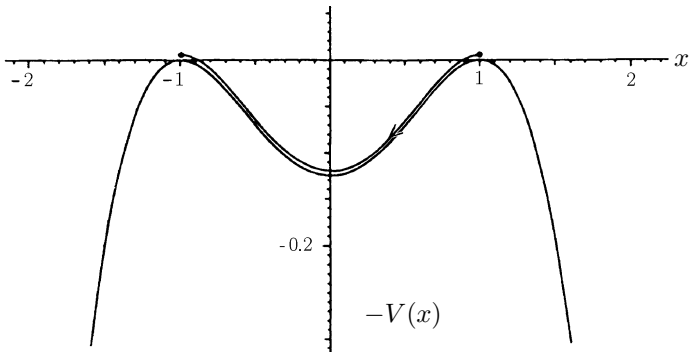

Figure 17.3 Reversed double-well potential governing motion of position x as function of imaginary time τ.

its movement exactly at the top but slightly displaced towards the valley, say at $x = -a+\epsilon$, it will reach $x = a-\epsilon$ after a finite time, then return to $x = -a+\epsilon$, and oscillate back and forth forever. In the limit $\epsilon \to 0$, the period of oscillation goes to infinity and only a single crossing of the valley remains.

To calculate this movement, the differential equation (17.22) is integrated once after multiplying it by $x' = dx/d\tau$ and rewriting it as

$$\frac{1}{2}\frac{d}{d\tau}x'^2 = \frac{d}{d\tau}V(x(\tau)). \tag{17.23}$$

The integration gives

$$\frac{x'^2}{2} + [-V(x(\tau))] = \text{const}\,. \tag{17.24}$$

If τ is reinterpreted as the physical time, this is the law of *energy conservation* for the motion in the reversed potential $-V(x)$. Thus we identify the integration constant in (17.24) as the total energy E in the reversed potential:

$$\text{const} \equiv E. \tag{17.25}$$

Integrating (17.24) further gives

$$\tau - \tau_0 = \pm\frac{1}{\sqrt{2}}\int_{x(\tau_0)}^{x(\tau)} \frac{dx}{\sqrt{E+V(x)}}. \tag{17.26}$$

A look at the potential in Fig. 17.3 shows that an orbit starting out with the particle at rest for $\tau \to -\infty$ must have $E = 0$. Inserting the explicit potential (17.1) into (17.26), we obtain for $|x| < a$

$$\begin{aligned} \tau - \tau_0 &= \pm\frac{2a}{\omega}\int_0^x \frac{dx'}{(a-x')(x'+a)} = \pm\frac{1}{\omega}\log\frac{a+x}{a-x} \\ &= \pm\frac{2}{\omega}\text{arctanh}\frac{x}{a}. \end{aligned} \tag{17.27}$$

Thus we find the kink and antikink solutions crossing the barrier:

$$x_{\rm cl}(\tau) = \pm a \tanh[(\tau - \tau_0)\omega/2]. \tag{17.28}$$

The Euclidean action of such a classical object can be calculated as follows [using (17.24) and (17.25)]:

$$\begin{aligned} \mathcal{A}_{\rm cl} &= \int_{-\infty}^{\infty} d\tau \left[\frac{{x'_{\rm cl}}^2}{2} + V(x_{\rm cl}(\tau)) \right] = \int_{-\infty}^{\infty} d\tau ({x'}^2_{\rm cl} - E) \\ &= -EL + \int_{-a}^{a} dx \sqrt{2[E + V(x)]}. \end{aligned} \tag{17.29}$$

The kink has $E = 0$, so that

$$\sqrt{2[E + V(x)]} = \frac{\omega}{2a}(a^2 - x^2), \tag{17.30}$$

and the classical action becomes

$$\mathcal{A}_{\rm cl} = \frac{\omega}{2a} \int_{-a}^{a} dx (a^2 - x^2) = \frac{2}{3} a^2 \omega = \frac{\omega^3}{3g}. \tag{17.31}$$

Note that for $E = 0$, the classical action is also given by the integral

$$\mathcal{A}_{\rm cl} = \int_{-\infty}^{\infty} d\tau \; {x'_{\rm cl}}^2. \tag{17.32}$$

There are also solutions starting out at the top of either mountain and sliding down into the adjacent exterior abyss, for instance (see again Fig. 17.3)

$$\begin{aligned} \tau - \tau_0 &= \mp \frac{2a}{\omega} \int_x^{\infty} \frac{dx'}{(x' - a)(x' + a)} = \pm \frac{1}{\omega} \log \frac{x + a}{x - a} \\ &= \pm \frac{2}{\omega} \operatorname{arccoth} \frac{x}{a}. \end{aligned} \tag{17.33}$$

However, these solutions cannot connect the bottoms of the double well with each other and will not be considered further.

Being in the possession of the classical solutions (17.19) and (17.28) with a finite action, we are now ready to write down the classical contributions to the amplitudes (17.16) and (17.17). According to the semiclassical formula (17.18), they are

$$(a \; L/2 | a \; -L/2) = 1 \times F_\omega(L) \tag{17.34}$$

and

$$(a \; L/2 | -a \; -L/2) = e^{-\mathcal{A}_{\rm cl}/\hbar} \times F_{\rm cl}(L). \tag{17.35}$$

The factor 1 in (17.34) emphasizes the vanishing action of the trivial classical solution (17.19). The exponential $e^{-\mathcal{A}_{\rm cl}/\hbar}$ contains the action of the kink solutions (17.28).

The degeneracy of the solutions in τ_0 is accounted for by the fluctuation factor $F_{\rm cl}(L)$, as will be shown below.

Actually, the classical kink and antikink solutions (17.28) do not occur exactly in (17.35) since they reach the well bottoms at $x = \pm a$ only at infinite Euclidean times $\tau \to \pm\infty$. For the amplitude to be calculated we need solutions for which x is equal to $\pm a$ at large but finite values $\tau = \pm L/2$. Fortunately, the error can be ignored since for large L the kink and antikink solutions approach $\pm a$ exponentially fast. As a consequence the action of a proper solution which would reach $\pm a$ at a finite L differs from the action $\mathcal{A}_{\rm cl}$ only by terms which tend to zero like $e^{-\omega L}$. Since we shall ultimately be interested only in the large-L limit we can neglect such exponentially small deviations.

In the following section we determine the fluctuation factors $F_{\rm cl}$.

17.3 Quadratic Fluctuations

The semiclassical limit includes the effects of the quadratic fluctuations. These are obtained after approximating the potential around each minimum by a harmonic potential and keeping only the lowest term in the expansion (17.3). The fluctuation factor of a pure harmonic oscillator of frequency ω and unit mass has been calculated in Section 2.3 with the result

$$F_\omega(L) = \sqrt{\frac{\omega}{2\pi\hbar \sinh \omega L}} \sim \sqrt{\frac{\omega}{\pi\hbar}} e^{-\omega L/2} + \mathcal{O}(e^{-3\omega L/2}). \tag{17.36}$$

The leading exponential at large L displays the ground state energy $\omega/2$, while the corrections contain all information on the exited states whose energy is $(n + 1/2)\omega$ with $n = 1, 2, 3, \ldots$.

Note that according to the spectral representation of the amplitude (17.15), the factor $\sqrt{\omega/\pi\hbar}$ in (17.36) must be equal to the square of the ground state wave function $\Psi_0(\Delta x_\pm)$ at the potential minimum. This agrees with (17.5).

Consider now the fluctuation factor of a single kink contribution. It is given by the path integral over the fluctuations $y(\tau) \equiv \delta x(\tau)$

$$F_{\rm cl}(L) = \int \mathcal{D}y(\tau) e^{-(1/\hbar)\int_{-L/2}^{L/2} d\tau (1/2)[y'^2 + V''(x_{\rm cl}(\tau))y^2]}, \tag{17.37}$$

where $x_{\rm cl}(\tau)$ is the kink solution, and $y(\tau)$ vanishes at the endpoints:

$$y(L/2) = y(-L/2) = 0. \tag{17.38}$$

Suppose for the moment that $L = \infty$. Then the kink solution is given by (17.28) and we obtain the fluctuation potential

$$\begin{aligned} V''(x_{\rm cl}(\tau)) &= \frac{3}{2}\frac{\omega^2}{a^2} x_{\rm cl}^2(\tau) - \frac{1}{2}\omega^2 = \omega^2 \left(\frac{3}{2} \tanh^2[\omega(\tau - \tau_0)/2] - \frac{1}{2} \right) \\ &= \omega^2 \left(1 - \frac{3}{2} \frac{1}{\cosh^2[\omega(\tau - \tau_0)/2]} \right). \end{aligned} \tag{17.39}$$

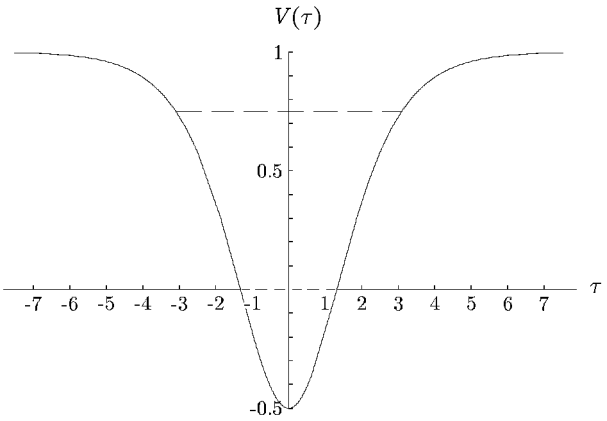

Figure 17.4 Potential (17.41) for quadratic fluctuations around kink solution (17.28) in Schrödinger equation. The dashed lines indicate the bound states at energies 0 and $3\omega^2/4$.

Thus, the quadratic fluctuations are governed by the Euclidean action

$$\mathcal{A}_{\rm fl}^0 = \int_{-L/2}^{L/2} d\tau \frac{1}{2}\left[y'^2 + \omega^2\left(1 - \frac{3}{2}\frac{1}{\cosh^2[\omega(\tau-\tau_0)/2]}\right)y^2\right]. \tag{17.40}$$

The rules for doing a functional integral with a quadratic exponent were explained in Chapter 2. The paths $y(\tau)$ are expanded in terms of eigenfunctions of the differential equation

$$\left[-\frac{d^2}{d\tau^2} + \omega^2\left(1 - \frac{3}{2}\frac{1}{\cosh^2[\omega(\tau-\tau_0)/2]}\right)\right] y_n(\tau) = \lambda_n y_n(\tau), \tag{17.41}$$

with λ_n being the eigenvalues. This is a Schrödinger equation for a particle moving along the τ-axis in an attractive potential well of the Rosen-Morse type [compare
ref(14.135)(14.135) and see Fig. 17.4]:
lab(14.124)
est(14.158)

$$V(\tau) = \omega^2\left(1 - \frac{3}{2}\frac{1}{\cosh^2[\omega(\tau-\tau_0)/2]}\right). \tag{17.42}$$

The eigenfunctions $y_n(\tau)$ satisfy the usual orthonormality condition

$$\int_{-\infty}^{\infty} d\tau y_n(\tau) y_{n'}(\tau) = \delta_{nn'}. \tag{17.43}$$

Given a complete set of these solutions $y_n(\tau)$ with $n = 0, 1, 2, \ldots$, we now perform the *normal-mode expansion*

$$y^{\xi_0,\xi_1,\cdots}(\tau) = \sum_{n=0}^{\infty} \xi_n y_n(\tau). \tag{17.44}$$

After inserting this into (17.40), we perform a partial integration in the kinetic term and the τ-integrals with the help of (17.43), and the Euclidean action of the quadratic fluctuations takes the simple form

$$\mathcal{A} = \frac{1}{2}\sum_{n=0}^{\infty} \lambda_n \xi_n^2. \tag{17.45}$$

With this, the fluctuation factor (17.37) reduces to a product of Gaussian integrals over the normal modes

$$F_{\rm cl}(L) \;=\; \mathcal{N}\prod_{n=0}^{\infty}\left[\int_{-\infty}^{\infty}\frac{d\xi_n}{\sqrt{2\pi\hbar}}\right] e^{-\sum_{n=0}^{\infty}\xi_n^2\lambda_n/2\hbar} = \mathcal{N}\frac{1}{\sqrt{\Pi_n\lambda_n}}. \tag{17.46}$$

The normalization constant $\mathcal{N}$, to be calculated below, accounts for the Jacobian which relates the time-sliced measure to the normal mode measure.

First we shall calculate the eigenvalues λ_n. For this we use the amplitude of the Rosen-Morse potential obtained via the Duru-Kleinert transformation (14.138) in Eq. (14.139). If the potential is written in the form

ref(14.138) lab(x14.160) est(14.161) ref(14.139) lab(8.1443ccca) est(14.162)

$$V(\tau) = \omega^2 - \frac{V_0}{\cosh^2[m(\tau-\tau_0)]}, \tag{17.47}$$

there are bound states for $n = 0, 1, 2, \ldots, n_{\max} < s$, where s is defined by [2]

$$s \equiv \frac{1}{2}\left[-1 + \sqrt{1 + 4\frac{V_0}{m^2}}\right]. \tag{17.48}$$

Their wave functions are, according to (14.141), and (14.143),

ref(14.141) lab(x14.164) est(14.164) ref(14.143) lab(x14.166) est(14.166)

$$\begin{aligned} y_n(\tau) = \sqrt{\frac{m}{n!}}\sqrt{\Gamma(s-n)\Gamma(1+2s-n)}\frac{2^{n-s}}{\Gamma(1+s-n)}\cosh^{n-s}[m(\tau-\tau_0)] \\ \times F(-n, 1+2s-n; s-n+1; \tfrac{1}{2}(1-\tanh[m(\tau-\tau_0)])), \end{aligned} \tag{17.49}$$

where $F(a, b; c; z)$ are the hypergeometric functions (1.453). In terms of s, the parameter V_0 becomes

$$V_0 = m^2 s(s+1). \tag{17.50}$$

The bound-state energies are

$$\lambda_n^2 = \omega^2 - m^2(s-n)^2. \tag{17.51}$$

In the Schrödinger equation (17.41), we have $m = \omega/2,\ V_0 = 3\omega^2/2$, so that $s = 2$ and there are exactly two bound-state solutions. These are

$$y_0(\tau) = -\sqrt{\frac{3\omega}{8}}\frac{1}{\cosh^2[\omega(\tau-\tau_0)/2]} \tag{17.52}$$

and

$$\begin{aligned} y_1(\tau) &= \sqrt{\frac{3\omega}{4}}\frac{1}{\cosh[\omega(\tau-\tau_0)/2]}F(-1,4;2;\tfrac{1}{2}(1-\tanh[\omega(\tau-\tau_0)/2])) \\ &= \sqrt{\frac{3\omega}{4}}\frac{\sinh[\omega(\tau-\tau_0)/2]}{\cosh^2[\omega(\tau-\tau_0)/2]}. \end{aligned} \tag{17.53}$$

The negative sign in (17.52) is a matter of convention, to give $y_1(\tau)$ the same sign as $x_{\rm cl}(\tau-\tau_0)$ in Eq. (17.89) below. The normalization factors can be checked using the formula

$$\int_0^\infty \frac{\sinh^\mu x}{\cosh^\nu x} = \frac{1}{2}B(\frac{\mu+1}{2},\frac{\nu-\mu}{2}), \tag{17.54}$$

with $B(x,y) \equiv \Gamma(x)\Gamma(y)/\Gamma(x+y)$ being the Beta function. The corresponding eigenvalues are

$$\lambda_0 = 0, \quad \lambda_1 = 3\omega^2/4. \tag{17.55}$$

The existence of a zero-eigenvalue mode is a general property of fluctuations around localized classical solutions in a system which is translationally invariant along the τ-axis. It prevents an immediate application of the quadratic approximation, since a zero-eigenvalue mode is not controlled by a Gaussian integral as the others are in Eq. (17.46). This difficulty and its solution will be discussed in Subsection 17.3.1.

In addition to the two bound states, there are continuum wave functions with $\lambda_n \geq \omega^2$. For an energy

$$\lambda_k = \omega^2 + k^2, \tag{17.56}$$

they are given by a linear combination of

$$y_k(\tau) \propto Ae^{ik\tau}F(s+1,-s;1-ik/m;\tfrac{1}{2}(1-\tanh[m(\tau-\tau_0)])) \tag{17.57}$$

and its complex-conjugate (see the end of Subsection 14.4.4). Using the identity for the hypergeometric function[2]

$$\begin{aligned} F(a,b,c;z) &= \frac{\Gamma(c)\Gamma(c-a-b)}{\Gamma(c-a)\Gamma(c-b)}F(a,b;a+b-c+1;1-z) \\ &+ (1-z)^{c-a-b}\frac{\Gamma(c)\Gamma(-c+a+b)}{\Gamma(a)\Gamma(b)}F(c-a,c-b;c-a-b+1;1-z), \end{aligned} \tag{17.58}$$

and $F(a,b;c;0)=1$, we find the asymptotic behavior

$$F \stackrel{\tau\to\infty}{\longrightarrow} 1, \tag{17.59}$$

$$F \stackrel{\tau\to-\infty}{\longrightarrow} \frac{\Gamma(-ik/m)\Gamma(1-ik/m)}{\Gamma(-s-ik/m)\Gamma(s+1-ik/m)} + e^{-2ik\tau}\frac{\Gamma(ik/m)\Gamma(1-ik/m)}{\Gamma(-s)\Gamma(1+s)}. \tag{17.60}$$

[2]M. Abramowitz and I. Stegun, *op. cit.*, formula 15.3.6.

These limits determine the asymptotic behavior of the wave functions (17.57). With an appropriate choice of the normalization factor in (17.57) we fulfill the standard scattering boundary conditions

$$\psi(\tau) \to \begin{cases} e^{ik\tau} + R_k e^{-ik\tau}, & \tau \to -\infty, \\ T_k e^{ik\tau}, & \tau \to \infty. \end{cases} \tag{17.61}$$

These define the transmission and reflection amplitudes. From (17.59) and (17.60) we calculate directly

$$T_k = \frac{\Gamma(-s-ik/m)\Gamma(s+1-ik/m)}{\Gamma(-ik/m)\Gamma(1-ik/m)}, \tag{17.62}$$

$$R_k = \frac{\Gamma(-s-ik/m)\Gamma(s+1-ik/m)}{\Gamma(-s)\Gamma(1+s)}\frac{\Gamma(ik/m)}{\Gamma(-ik/m)} = T_k\frac{\Gamma(ik/m)\Gamma(1-ik/m)}{\Gamma(-s)\Gamma(1+s)}. \tag{17.63}$$

Using the relation $\Gamma(z) = \pi/\sin(\pi z)\Gamma(1-z)$, this can be written as

$$T_k = \frac{\Gamma(s+1-ik/m)}{\Gamma(s+1+ik/m)}\frac{\Gamma(1+ik/m)}{\Gamma(1-ik/m)}\frac{\sin(ik/m)}{\sin(s+ik/m)}, \tag{17.64}$$

$$R_k = T_k\frac{\sin(\pi s)}{\sin(ik/m)}. \tag{17.65}$$

The scattering matrix

$$S_k = \begin{pmatrix} T_k & R_k \\ R_k & T_k \end{pmatrix} \tag{17.66}$$

is unitary since

$$R_k T_k^* + R_k^* T_k = 0, \qquad |T_k|^2 + |R_k|^2 = 1. \tag{17.67}$$

It is diagonal on the state vectors

$$\psi^{\mathrm{e}} = \frac{1}{\sqrt{2}}\begin{pmatrix} 1 \\ 1 \end{pmatrix}, \quad \psi^{\mathrm{o}} = \frac{1}{\sqrt{2}}\begin{pmatrix} 1 \\ -1 \end{pmatrix}, \tag{17.68}$$

which, as we shall prove below, correspond to odd and even partial waves. The respective eigenvalues $\lambda_k^{\mathrm{e,o}} = e^{2i\delta_k^{\mathrm{e,o}}}$ define the phase shifts $\delta_k^{\mathrm{e,o}}$, in terms of which

$$T_k = \frac{1}{2}(e^{2i\delta_k^{\mathrm{e}}} + e^{2i\delta_k^{\mathrm{o}}}), \tag{17.69}$$

$$R_k = \frac{1}{2}(e^{2i\delta_k^{\mathrm{e}}} - e^{2i\delta_k^{\mathrm{o}}}). \tag{17.70}$$

Let us verify the association of the eigenvectors (17.68) with the even and odd partial waves. For this we add to the wave function (17.61) the mirror-reflected solution

$$\psi^{\mathrm{r}}(\tau) \to \begin{cases} T_k e^{-ik\tau}, & \tau \to -\infty, \\ e^{-ik\tau} + R_k e^{ik\tau}, & \tau \to \infty, \end{cases} \tag{17.71}$$

and obtain

$$\psi^{\rm e}(\tau)=\psi(\tau)+\psi^{\rm r}(\tau)\to\left\{\begin{array}{ll} e^{ik\tau}+(R_k+T_k)e^{-ik\tau}, & \tau\to-\infty,\\ e^{-ik\tau}+(R_k+T_k)e^{ik\tau}, & \tau\to\infty.\end{array}\right. \tag{17.72}$$

Inserting (17.69), this can be rewritten as

$$\psi^{\rm e}(\tau)\to\left\{\begin{array}{ll} e^{i\delta_k^{\rm e}}[e^{i(k\tau-\delta_k^{\rm e})}+e^{-i(k\tau-\delta_k^{\rm e})}]=2e^{i\delta_k^{\rm e}}\cos(k|\tau|+\delta_k^{\rm e}), & \tau\to-\infty,\\ e^{i\delta_k^{\rm e}}[e^{-i(k\tau+\delta_k^{\rm e})}+e^{i(k\tau+\delta_k^{\rm e})}]=2e^{i\delta_k^{\rm e}}\cos(k|\tau|+\delta_k^{\rm e}), & \tau\to\infty.\end{array}\right. \tag{17.73}$$

The odd combination, on the other hand, gives

$$\psi^{\rm o}(\tau)=\psi(\tau)-\psi^{\rm r}(\tau)\to\left\{\begin{array}{ll} e^{ik\tau}+(R_k-T_k)e^{-ik\tau}, & \tau\to-\infty,\\ -e^{-ik\tau}-(R_k-T_k)e^{ik\tau}, & \tau\to\infty,\end{array}\right. \tag{17.74}$$

and becomes with (17.69):

$$\psi^{\rm o}(\tau)\to\left\{\begin{array}{ll} e^{i\delta_k^{\rm o}}[e^{i(k\tau-\delta_k^{\rm e})}-e^{-i(k\tau-\delta_k^{\rm o})}]= \ 2ie^{i\delta_k^{\rm e}}\sin(k|\tau|+\delta_k^{\rm o}), & \tau\to-\infty,\\ -e^{i\delta_k^{\rm e}}[e^{-i(k\tau+\delta_k^{\rm o})}-e^{i(k\tau+\delta_k^{\rm e})}]=-2ie^{i\delta_k^{\rm e}}\sin(k|\tau|+\delta_k^{\rm o}), & \tau\to\infty.\end{array}\right. \tag{17.75}$$

From Eqs. (17.69), (17.70) we see that

$$|T_k|^2=\cos^2(\delta_k^{\rm e}-\delta_k^{\rm o}),\qquad |R_k|^2=\sin^2(\delta_k^{\rm e}-\delta_k^{\rm o}), \tag{17.76}$$

and further

$$e^{2i(\delta_k^{\rm e}+\delta_k^{\rm o})}=(T_k+R_k)(T_k-R_k)=T_k^2+\frac{R_kR_k^*T_k}{T_k^*}=T_k^2+(1-T_kT_k^*)\frac{T_k}{T_k^*}=\frac{T_k}{T_k^*}. \tag{17.77}$$

From this we find the explicit equation for the sum of even and odd phase shifts

$$\delta_k^{\rm e}+\delta_k^{\rm o}=\frac{1}{2}\arg\frac{T_k}{T_k^*}=\arg T_k. \tag{17.78}$$

Similarly we derive the equation for the difference of the phase shifts:

$$-i\sin[2(\delta_k^{\rm e}-\delta_k^{\rm o})]=T_kR_k^*-T_k^*R_k=2T_kR_k^*=-2\frac{R_k^*}{T_k^*}|T_k|^2. \tag{17.79}$$

Dividing this by the first equation in (17.76), we obtain

$$-i\tan(\delta_k^{\rm e}-\delta_k^{\rm o})=-\frac{R_k^*}{T_k^*}=-\frac{\sinh(ik/m)}{\sin(\pi s)}, \tag{17.80}$$

and thus

$$\delta_k^{\rm e}-\delta_k^{\rm o}=\arctan\frac{\sin(\pi s)}{\sinh(k/m)}\sin(\pi s). \tag{17.81}$$

For $s =$ integer, the even and odd phase shifts become equal,

$$\delta_k^{\rm e} = \delta_k^{\rm o} \equiv \delta_k, \tag{17.82}$$

so that the reflection amplitude vanishes, and the transmission amplitude reduces to a pure phase factor $T_k = e^{2i\delta_k}$, with the phase shift determined from (17.78) to

$$2\delta_k = -i \log T_k. \tag{17.83}$$

Now the wave functions have the simple asymptotic behavior

$$y_k(\tau) \to e^{i(k\tau \pm \delta_k)}, \quad \tau \to \pm\infty, \tag{17.84}$$

and (17.64) reduces for both even and odd phase shifts to

$$e^{2i\delta_k} = (-1)^s \frac{\Gamma(s+1-ik/m)}{\Gamma(1-ik/m)} \frac{\Gamma(1+ik/m)}{\Gamma(s+1+ik/m)}. \tag{17.85}$$

For the Schrödinger equation (17.41) with $s = 2$, this becomes simply

$$e^{2i\delta_k} = \frac{2-ik/m}{2+ik/m} \frac{1-ik/m}{1+ik/m}, \tag{17.86}$$

and hence

$$\delta_k = \arctan[k/m] + \arctan[k/2m]. \tag{17.87}$$

If we now try to evaluate the product of eigenvalues in (17.46), two difficulties arise:
1) The zero eigenvalue causes the result to be infinite.
2) The continuum states make the evaluation of the product of eigenvalues $\prod_n \sqrt{\lambda_n}$ nontrivial.
These two difficulties will be removed in the following two subsections.

17.3.1 Zero-Eigenvalue Mode

The physical origin of the infinity caused by the zero-eigenvalue solution in the fluctuation integral over ξ_0 in (17.46) lies in the time-translational invariance of the system. This fact supplies the key to removing the infinity. A kink at an imaginary time τ_0 contributes as much to the path integral as a kink at any other time τ_0'. The difference between two adjacent solutions at an infinitesimal temporal distance can be viewed as a small kink fluctuation which does not change the Euclidean action. There is a zero eigenvalue associated with this difference. If there is only a single zero-eigenvalue solution as in the Schrödinger equation (17.41) its wave function must be proportional to the derivative of the kink solution:

$$\begin{aligned} y_0 &= \alpha \left[\frac{x_{\rm cl}(\tau-\tau_0) - x_{\rm cl}(\tau-\tau_1)}{\tau_0 - \tau_1} \right]_{\tau_0 \to \tau_1} = \alpha x_{\rm cl}'(\tau-\tau_0) \\ &= -\alpha \frac{a\omega/2}{\cosh^2[\omega(\tau-\tau_0)/2]}. \end{aligned} \tag{17.88}$$

This coincides indeed with the zero-eigenvalue solution (17.52). The normalization factor α is fixed by the integral

$$\alpha = \left[\int_{-\infty}^{\infty} d\tau x_{\rm cl}'^2\right]^{-1/2}. \tag{17.89}$$

With the help of (17.32) the right-hand side can also be expressed in terms of the kink action:

$$\alpha = \frac{1}{\sqrt{\mathcal{A}_{\rm cl}}}. \tag{17.90}$$

Inserting (17.2) and (17.31), this becomes

$$\alpha = \sqrt{3/2a^2\omega} = \sqrt{3g/\omega^3} \tag{17.91}$$

[the positive square root corresponding to the negative sign in (17.52)]. The zero-eigenvalue mode is associated with a shift of the position of the kink solution from τ_0 to any other place τ_0'. For an infinite length L of the τ-axis, this is the source of the infinity of the integral over ξ_0 in the product (17.46). At a finite L, on the other hand, only a τ-interval of length L is available for displacements. Therefore, the infinite $1/\sqrt{\lambda_0}$ should become proportional to L for large L:

$$\frac{1}{\sqrt{\lambda_0}} = \text{const} \cdot L. \tag{17.92}$$

What is the proportionality constant? We find it by transforming the integration measure (17.46),

$$\mathcal{N}\int_{-\infty}^{\infty}\frac{d\xi_0}{\sqrt{2\pi\hbar}}\prod_{n=1}^{\infty}\left[\int_{-\infty}^{\infty}\frac{d\xi_n}{\sqrt{2\pi\hbar}}\right], \tag{17.93}$$

to a form in which the translational degree of freedom appears explicitly

$$\mathcal{N}\frac{1}{\sqrt{2\pi\hbar}}\int_{-\infty}^{\infty}d\tau_0\prod_{n\neq 0}\int_{-\infty}^{\infty}\left[\frac{d\xi_n}{\sqrt{2\pi\hbar}}\right]\left|\frac{\partial\xi_0}{\partial\tau_0}(\xi_1,\xi_2,\ldots)\right|. \tag{17.94}$$

The Jacobian appearing in the integrand satisfies the identity

$$\int d\tau_0\,\delta(\xi_0)\left|\frac{\partial\xi_0}{\partial\tau_0}\right| = 1. \tag{17.95}$$

Let us calculate this Jacobian using the method developed by Faddeev and Popov [3]. Given an arbitrary fluctuation $y^{\xi_0,\xi_1,\xi_2,\cdots}$, the parameter ξ_0 may be recovered by forming the scalar product with the zero-eigenvalue wave function $y_0(\tau)$:

$$\xi_0 = \int_{-\infty}^{\infty} d\tau y^{\xi_0,\xi_1,\xi_2,\cdots}(\tau)y_0(\tau). \tag{17.96}$$

Moreover, it is easy to see that the fluctuation $y^{\xi_0,\xi_1,\xi_2,\cdots}$ can be replaced by the full path

$$x^{\xi_0,\xi_1,\xi_2,\cdots}(\tau) = x_{\rm cl}(\tau) + y^{\xi_0,\xi_1,\xi_2,\cdots}(\tau), \tag{17.97}$$

so that we can also write

$$\xi_0 = \int_{-\infty}^{\infty} d\tau\, x^{\xi_0,\xi_1,\xi_2,\cdots}(\tau) y_0(\tau). \tag{17.98}$$

This follows from the fact that the additional kink solution $x_{\rm cl}(\tau)$ does not have any overlap with its derivative. Indeed,

$$\begin{aligned} \int_{-\infty}^{\infty} d\tau\, x_{\rm cl}(\tau-\tau_0) y_0(\tau-\tau_0) &\propto \int_{-\infty}^{\infty} d\tau\, x_{\rm cl}(\tau-\tau_0) x'_{\rm cl}(\tau-\tau_0) \\ &\propto \frac{1}{2} x_{\rm cl}^2 \Big|_{-\infty}^{\infty} = 0. \end{aligned} \tag{17.99}$$

With (17.98), the delta function $\delta(\xi_0)$ appearing in (17.95) can be rewritten in the form

$$\delta(\xi_0) = \delta\left(\int_{-\infty}^{\infty} d\tau\, x^{\xi_0,\xi_1,\xi_2,\cdots}(\tau) y_0(\tau) \right). \tag{17.100}$$

To establish the relation between the normal coordinate ξ_0 and the kink position τ_0, we now replace $x^{\xi_0,\xi_1,\xi_2,\cdots}$ by an alternative parametrization of the paths in which the role of the variable ξ_0 is traded against the position of the kink solution, i.e., we rewrite the fluctuating path

$$x^{\xi_0,\xi_1,\xi_2,\cdots}(\tau) = x_{\rm cl}(\tau) + \sum_{n=0}^{\infty} \xi_n y_n(\tau) \tag{17.101}$$

in the form

$$x^{\tau_0,\xi_1,\xi_2,\cdots}(\tau) \equiv x_{\rm cl}(\tau-\tau_0) + \sum_{n=1}^{\infty} \xi_n y_n(\tau-\tau_0). \tag{17.102}$$

By definition the point $\tau_0 = 0$ coincides with $\xi_0 = 0$. Thus, if we insert (17.102) into (17.100) and use this δ-function in the identity (17.95), we find the condition for the Jacobian $\partial\xi_0/\partial\tau_0$:

$$\int_{-\infty}^{\infty} d\tau_0\; \delta\left(\int_{-\infty}^{\infty} d\tau\, x^{\tau_0,\xi_1,\xi_2,\cdots}(\tau) y_0(\tau) \right) \left| \frac{\partial \xi_0}{\partial \tau_0} \right| = 1. \tag{17.103}$$

Since the δ-function has a vanishing argument at $\tau_0 = 0$, we expand the argument in powers of τ_0, keeping only the lowest order. Writing $y_0(\tau) = \alpha x'_{\rm cl}(\tau)$, we obtain

$$\int_{-\infty}^{\infty} d\tau\, x^{\tau_0,\xi_1,\xi_2,\cdots}(\tau) y_0(\tau) = -\alpha\tau_0 \left[\int_{-\infty}^{\infty} d\tau\, x'^2_{\rm cl} + \sum_{n=1}^{\infty} \xi_n \int_{-\infty}^{\infty} d\tau\, x'_{\rm cl}\, y'_n \right] + \mathcal{O}(\tau_0^2). \tag{17.104}$$

Using (17.32) and abbreviating the scalar products in the brackets as

$$r_n \equiv \int_{-\infty}^{\infty} d\tau \, x'_{\rm cl} \, y'_n, \tag{17.105}$$

we may express the right-hand side of (17.104) more succinctly as

$$-\alpha\tau_0 \left[\mathcal{A}_{\rm cl} + \sum_{n=1}^{\infty} \xi_n r_n \right] + \mathcal{O}(\tau_0^2). \tag{17.106}$$

Inserting this into (17.103), and using (17.90), we arrive at the Jacobian

$$\left| \frac{\partial \xi_0}{\partial \tau_0} \right| = {\mathcal{A}_{\rm cl}}^{1/2} \left(1 + {\mathcal{A}_{\rm cl}}^{-1} \sum_{n=1}^{\infty} \xi_n r_n \right). \tag{17.107}$$

As a consequence, the zero-eigenvalue modes contribute to the fluctuation factor (17.46) as follows:

$$\begin{aligned} F_{\rm cl}(L) &= \mathcal{N} \prod_{n=1}^{\infty} \left[\int_{-\infty}^{\infty} \frac{d\xi_n}{\sqrt{2\pi\hbar}} \right] e^{-(1/2\hbar)\sum_{n=1}^{\infty} \xi_n^2 \lambda_n} \int_{-\infty}^{\infty} \frac{d\xi_0}{\sqrt{2\pi\hbar}} e^{-(1/2\hbar)\xi_0^2 \lambda_0} \\ &= \mathcal{N} \prod_{n=1}^{\infty} \left[\int_{-\infty}^{\infty} \frac{d\xi_n}{\sqrt{2\pi\hbar}} e^{-(1/2\hbar)\sum_{n=1}^{\infty} \xi_n^2 \lambda_n} \right] \int_{-\infty}^{\infty} \frac{d\tau_0}{\sqrt{2\pi\hbar}} {\mathcal{A}_{\rm cl}}^{1/2} \left(1 + {\mathcal{A}_{\rm cl}}^{-1} \sum_{n=1}^{\infty} \xi_n r_n \right) \\ &= \mathcal{N} \frac{1}{\sqrt{\prod_{n=1}^{\infty} \lambda_n}} \sqrt{\frac{\mathcal{A}_{\rm cl}}{2\pi\hbar}} \int_{-\infty}^{\infty} d\tau_0. \end{aligned} \tag{17.108}$$

The linear terms in the large parentheses disappear at the level of quadratic fluctuations since they are odd in ξ. Thus we may use for *quadratic fluctuations* the simple *mnemonic rule*

$$-\frac{\partial \xi_0}{\partial \tau_0} = \frac{\partial x(\tau)/\partial \tau_0}{\partial x(\tau)/\partial \xi_0} = \frac{\dot{x}_{\rm cl}(\tau) + \ldots}{\alpha \dot{x}_{\rm cl}(\tau)} = \frac{1}{\alpha} + \ldots = \sqrt{\mathcal{A}_{\rm cl}} + \ldots, \tag{17.109}$$

where $\ldots$ stands for the irrelevant linear terms in ξ_n inside the integral (17.108).

For higher-order fluctuations, the linear terms in the large parentheses cannot be ignored. They contribute an effective Euclidean action

$$\mathcal{A}_{\rm e}^{\rm eff} = -\hbar \log \left[1 + {\mathcal{A}_{\rm cl}}^{-1} \sum_{n=1}^{\infty} \xi_n r_n \right] = -\hbar \log \left[1 + \mathcal{A}_{\rm cl}^{-1} \int d\tau \, x'_{\rm cl}(\tau) y'(\tau) \right], \tag{17.110}$$

which will be needed for calculations in Section 17.8.

The integral over τ_0 is now an appropriate place to impose the finiteness of the time interval $\tau \in (-L/2, L/2)$, namely

$$\int_{-L/2}^{L/2} d\tau_0 = L. \tag{17.111}$$

A comparison of (17.108) with (17.46) shows that the correct evaluation of the formally diverging zero-eigenvalue contribution $1/\sqrt{\lambda_0}$ is equivalent to the following replacement:

$$\frac{1}{\sqrt{\lambda_0}} \equiv \int \frac{d\xi_0}{\sqrt{2\pi\hbar}} e^{-(1/2\hbar)\lambda_0 \xi_0^2} \longrightarrow \sqrt{\frac{\mathcal{A}_{\rm cl}}{2\pi\hbar}} \int_{-L/2}^{L/2} d\tau_0 = \sqrt{\frac{\mathcal{A}_{\rm cl}}{2\pi\hbar}} \, L. \tag{17.112}$$

17.3.2 Continuum Part of Fluctuation Factor

We now turn to the second problem, the calculation of the product of the continuum eigenvalues in (17.46). To avoid carrying around the overall normalization factor $\mathcal{N}$ it is convenient to factor out the quadratic fluctuations (17.36) in the absence of a kink solution. Let λ_n^0 be the associated eigenvalues. Their fluctuation potential $V''(x_{\rm cl}(\tau)) = \omega^2 x^2$ is harmonic [compare (17.39)] with a fluctuation factor known from (2.171). Comparing this with the expression (17.46) without a kink, we obtain for the normalization factor the equation

$$\mathcal{N}\frac{1}{\sqrt{\prod_n \lambda_n^0}} = F_\omega(L) = \sqrt{\frac{\omega}{2\pi\hbar \sinh \omega L}} \sim \sqrt{\frac{\omega}{\pi\hbar}} e^{-\omega L/2}. \tag{17.113}$$

Pulling this factor out of the product on the right-hand side of (17.46), we are left with a ratio of eigenvalue products:

$$F_{\rm cl}(L) = \mathcal{N}\frac{1}{\sqrt{\prod_n \lambda_n}} = \mathcal{N}\frac{1}{\sqrt{\prod_n \lambda_n^0}}\sqrt{\frac{\prod_n \lambda_n^0}{\prod_n \lambda_n}} = F_\omega(L)\sqrt{\frac{\prod_n \lambda_n^0}{\prod_n \lambda_n}}. \tag{17.114}$$

As long as L is finite, the continuum wave functions are all discrete. Let $\partial n/\partial k$ denote their density of states per momentum interval. Then the ratio of the continuum eigenvalues can be written for large L as

$$\sqrt{\frac{\prod_n \lambda_n^0}{\prod_n \lambda_n}}\bigg|_{\rm cont} = \exp\left[-\frac{1}{2}\int_0^\infty dk \left(\frac{\partial n}{\partial k} - \frac{\partial n}{\partial k}\Big|_0\right)\log \lambda_n\right]. \tag{17.115}$$

The density of states, in turn, may be extracted from the phase shifts (17.85). For this we observe that for a very large L where boundary conditions are a matter of choice, we may impose the periodic boundary condition

$$y(\tau + L) = y(\tau). \tag{17.116}$$

Together with the asymptotic forms (17.84), this implies

$$e^{i(kL/2+\delta_k)} = e^{-i(kL/2+\delta_k)}, \tag{17.117}$$

which quantizes the wave vectors k to discrete values satisfying

$$kL + 2\delta_k = 2\pi n. \tag{17.118}$$

The derivative with respect to k yields the density of states

$$\frac{\partial n}{\partial k} = \frac{L}{2\pi} + \frac{1}{\pi}\frac{d\delta_k}{dk}. \tag{17.119}$$

Since the phase shifts vanish in the absence of a kink solution, this implies

$$\frac{\partial n}{\partial k}\Big|_0 = \frac{L}{2\pi}, \tag{17.120}$$

and the general formula (17.115) becomes simply

$$\sqrt{\frac{\prod_n \lambda_n^0}{\prod_n \lambda_n}}\bigg|_{\rm cont} = \exp\left[-\frac{1}{2\pi}\int_0^\infty dk \frac{d\delta_k}{dk}\log(\omega^2+k^2)\right]. \tag{17.121}$$

To calculate the integral for our specific fluctuation problem (17.41), we use the expression (17.85) to find the derivative of the phase shift for any integer value of s:

$$\frac{d\delta_k}{dk} = -\frac{1}{m}\left[\frac{2}{4+(k/m)^2}+\ldots+\frac{s}{s^2+(k/m)^2}\right]. \tag{17.122}$$

For $s=2$, the exponent in (17.121) becomes

$$\frac{1}{2\pi}\int_{-\infty}^\infty dx\left(\frac{1}{1+x^2}+\frac{2}{4+x^2}\right)\log\left[\omega^2(1+x^2m^2/\omega^2)\right]. \tag{17.123}$$

The ω^2-term in the logarithm can be separated from this using Levinson's theorem [1]. It states that the integral $\int_0^\infty dk(\partial n/\partial k - \partial n/\partial k|_0)$ is equal to the number of bound states:

$$\int_0^\infty dk\left(\frac{\partial n}{\partial k}-\frac{\partial n}{\partial k}\Big|_0\right) = \frac{1}{\pi}\int_0^\infty dk\frac{d\delta_k}{dk} = s. \tag{17.124}$$

This relation is obviously fulfilled by (17.122). It is a consequence of the fact that a potential with s bound states has s states less in the continuum than a free system. Using this property, the integral (17.123) can be rewritten as

$$\log\omega^2 + \int_{-\infty}^\infty \frac{dx}{2\pi}\left(\frac{1}{1+x^2}+\frac{2}{4+x^2}\right)\log(1+x^2m^2/\omega^2). \tag{17.125}$$

The rescaled integral is calculated using the formula

$$\int_{-\infty}^\infty \frac{dx}{2\pi}\frac{\log(1+p^2x^2)}{r^2+s^2x^2} = \frac{1}{rs}\log\left(1+p\frac{r}{s}\right). \tag{17.126}$$

The result is

$$\log\omega^2 + \log\left(1+\frac{m}{\omega}1\right)+\log\left(1+\frac{m}{\omega}2\right). \tag{17.127}$$

When inserted into the exponent of (17.121), it yields

$$\sqrt{\frac{\prod_n \lambda_n^0}{\prod_n \lambda_n}}\bigg|_{\rm cont} = \omega^2\left(1+\frac{m}{\omega}\right)\left(1+\frac{m}{\omega}2\right). \tag{17.128}$$

In our case with $m=\omega/2$, this reduces to $3\omega^2$. Including the bound-state eigenvalue λ_1 of Eq. (17.55) in the denominator, this amounts to

$$\sqrt{\frac{\prod_n \lambda_n^0}{\prod_n' \lambda_n}} = \frac{1}{\sqrt{3\omega^2/4}}3\omega^2 = \sqrt{12}\omega \equiv K'. \tag{17.129}$$

Multiplying this with the zero-eigenvalue contribution as evaluated in Eq. (17.108), we arrive at the final result for the fluctuation factor in the presence of a kink or an antikink solution:

$$F_{\rm cl}(L) = F_\omega(L) K L, \tag{17.130}$$

with

$$K = \frac{1}{\sqrt{\lambda_0} L} K' = \sqrt{\frac{\mathcal{A}_{\rm cl}}{2\pi\hbar}} \sqrt{12}\omega. \tag{17.131}$$

17.4 General Formula for Eigenvalue Ratios

The above-calculated ratio of eigenvalue products

$$\sqrt{\frac{\prod_n \lambda_n^0}{\prod_n \lambda_n}}\bigg|_{\rm cont} \tag{17.132}$$

of the Rosen-Morse Schrödinger equation appears in many applications with different potential strength parameters s. It is therefore useful to derive a formula for this ratio which is valid for any s. The eigenvalue equation reads

$$\left[-\frac{d^2}{d\tau^2} + \omega^2 - \frac{m^2 s(s+1)}{\cosh^2 m(\tau-\tau_0)}\right] y_n(\tau) = \lambda_n y_n(\tau). \tag{17.133}$$

First we consider the case of an arbitrary integer value of s. Following the previous discussion, the ratio of eigenvalue products is found to be

$$\begin{aligned} \sqrt{\frac{\prod_n \lambda_n^0}{\prod_n \lambda_n}}\bigg|_{\rm cont} &= \exp\left[-\frac{1}{2\pi}\int_0^\infty dk \frac{d\delta_k}{dk} \log(\omega^2+k^2)\right] \qquad (17.134)\\ &= \exp\left\{-\frac{1}{2\pi}\int_0^\infty d(k/m) \sum_{n=1}^{s} \frac{n}{n^2+(k/m)^2} \log[\omega^2 + (k/m)^2 m^2]\right\}. \end{aligned}$$

The ω^2-term in the logarithm is eliminated by the generalization of (17.124) to any integer s:

$$\frac{1}{\pi}\int_{-\infty}^{\infty} d(k/m) \sum_{n=1}^{s} \frac{n}{n^2+(k/m)^2} = s. \tag{17.135}$$

Hence

$$\sqrt{\frac{\prod_n \lambda_n^0}{\prod_n \lambda_n}}\bigg|_{\rm cont} = \omega^s \exp\left[\frac{1}{2\pi}\int_{-\infty}^{\infty} dx \sum_{n=1}^{s} \frac{n}{n^2+x^2} \log(1 + x^2 m^2/\omega^2)\right]. \tag{17.136}$$

The integrals can be done using formula (17.126), and we obtain

$$\sqrt{\frac{\prod_n \lambda_n^0}{\prod_n \lambda_n}}\bigg|_{\rm cont} = \omega^s \prod_{n=1}^{s} \left(1 + \frac{m}{\omega} n\right). \tag{17.137}$$

For $s = 2$, and $m = \omega/2$, this reduces to the previous result (17.128).

Only a little more work is required to find the ratio of all discrete and continuous eigenvalue products for a noninteger value of s. Introduce a new parameter z, let s be a parameter smaller than 1 so that there are no bound states, and consider the fluctuation equation

$$\left[-\frac{d^2}{d\tau^2} + m^2\left(z - \frac{s(s+1)}{\cosh^2 m(\tau-\tau_0)}\right)\right] y_n(\tau) = \lambda_n y_n(\tau). \tag{17.138}$$

The general Schrödinger operator under consideration (17.133) corresponds to $z = \omega^2/m^2$. Since there are no bound states by assumption, the first line in formula (17.134) now gives the ratio of *all* eigenvalues:

$$\sqrt{\frac{\prod_n \lambda_n^0}{\prod_n \lambda_n}} = \exp\left[-\frac{1}{2\pi}\int_{-\infty}^{\infty} dk \frac{d\delta_k}{dk}\log(m^2 z + k^2)\right]. \tag{17.139}$$

Here δ_k is equal to the average of even and odd phase shifts $(\delta_k^{\mathrm{e}} + \delta_k^{\mathrm{o}})/2$. For the same reason, we can replace $\log(m^2 z + k^2)$ by $\log(z + k^2/m^2)$ without error [using the generalization of (17.124)]. After substituting $k^2 \to \omega^2\epsilon$, we find

$$\sqrt{\frac{\Pi_n \lambda_n^0}{\Pi_n \lambda_n}} = \exp\left[-\frac{1}{2\pi}\int_C d\epsilon \frac{d\delta\omega\sqrt{\epsilon}}{d\epsilon}\log(z+\epsilon)\right], \tag{17.140}$$

where the contour of integration C encircles the right-hand cut clockwise in the ϵ-plane. A partial integration brings this to

$$\exp\left(\frac{1}{2\pi}\int_C d\epsilon\, \delta_{m\sqrt{\epsilon}} \frac{1}{z+\epsilon}\right). \tag{17.141}$$

For $z < 0$, the contour of integration can be deformed to encircle the only pole at $\epsilon = -z$ counterclockwise, yielding

$$\sqrt{\frac{\prod_n \lambda_n^0}{\prod_n \lambda_n}} = \exp[i\delta_{m\sqrt{-z}}]. \tag{17.142}$$

Inserting for δ_k the average of even and odd phase shifts from (17.78), we obtain

$$\sqrt{\frac{\prod_n \lambda_n^0}{\prod_n \lambda_n}} = \left[\frac{\Gamma(\sqrt{z}-s)\Gamma(\sqrt{z}+s+1)}{\Gamma(\sqrt{z})\Gamma(\sqrt{z}+1)}\right]^{1/2}. \tag{17.143}$$

In the fluctuation equation (17.41), the parameters m^2 and $\omega^2 = zm^2$ are such as to create a zero eigenvalue at $n = 0$ according to formula (17.51). Then $z = s^2$. In the neighborhood of this z-value, the eigenvalue

$$\lambda_0 = m^2[z - s^2] \tag{17.144}$$

is a would-be zero eigenvalue. Dividing it out of the product (17.143), we obtain an equation which remains valid in the limit $z \to s^2$:

$$\sqrt{\frac{\prod_n \lambda_n^0}{\prod_n' \lambda_n}} = m \left[(\sqrt{z}+s) \frac{\Gamma(\sqrt{z}-s+1)\Gamma(\sqrt{z}+s+1)}{\Gamma(\sqrt{z})\Gamma(\sqrt{z}+1)} \right]^{1/2}. \tag{17.145}$$

This can be continued analytically to arbitrary z and s, as long as z remains sufficiently close to $s=2$. For $s=2$ and $z=4$ (corresponding to $m=\omega/2$) we recover the earlier result (17.129):

$$\sqrt{\frac{\prod_n \lambda_n^0}{\prod_n' \lambda_n}} = \sqrt{12}\omega. \tag{17.146}$$

17.5 Fluctuation Determinant from Classical Solution

The above evaluations of the fluctuation determinant require the complete knowledge of the bound and continuum spectrum of the fluctuation equation. Fortunately, there exists a way to find the determinant which needs much less information, requiring only the knowledge of the large-τ behavior of the classical solution and the value of its action. The basis for this derivation is the Gelfand-Yaglom formula derived in Section 2.4. According to it, the fluctuation determinant of a differential operator

$$\hat{\mathcal{O}} = -\frac{d^2}{d\tau^2} + \omega^2 - \frac{m^2 s(s+1)}{\cosh^2[m(\tau-\tau_0)]} \tag{17.147}$$

is given by the value of the zero-eigenvalue solution $D(\tau)$ at the final τ value $\tau = L/2$

$$\det \hat{\mathcal{O}} = \mathcal{N} D(L/2), \tag{17.148}$$

provided that it was chosen to satisfy the initial conditions at $\tau = -L/2$:

$$D(-L/2) = 0, \quad \dot{D}(-L/2) = 1. \tag{17.149}$$

The normalization factor $\mathcal{N}$ is irrelevant when considering ratios of fluctuation determinants, as we do in the problem at hand.[3] To satisfy the boundary conditions (17.149), we need two linearly independent solutions of zero eigenvalue. One is known from the invariance under time translations. It is proportional to the time derivative of the classical solution [see (17.88)]:

$$y_0(\tau) = \alpha x_{\rm cl}'(\tau). \tag{17.150}$$

[3] If the determinant is calculated for the time-sliced operator $\hat{\mathcal{O}}$ with $d/d\tau$ replaced by the difference operator ∇_τ, the normalization is $\mathcal{N} = 1/\epsilon$ where ϵ is the thickness of the time slices. See Chapter 2.

In the above fluctuation problem (17.41) with $s = 2$ and $m = \omega/2$, the classical solution is $x_{\rm cl}(\tau) = \operatorname{arctanh}[\omega(\tau - \tau_0)/2]$. It has the asymptotic behavior

$$y_0(\tau) \to \frac{\omega}{2} e^{-\omega|\tau|} \quad \text{for} \quad \tau \to \pm\infty, \tag{17.151}$$

with a symmetric exponential falloff in both directions of the τ-axis. In the sequel it will be convenient to work with zero-eigenvalue solutions without the prefactor $\omega/2$, which behave asymptotically like a pure exponential. These will be denoted by $\xi(\tau)$ and $\eta(\tau)$, the solution $\xi(\tau)$ being proportional to y_0, i.e.,

$$\xi(\tau) \to e^{-\omega|\tau|} \quad \text{for} \quad \tau \to \pm\infty. \tag{17.152}$$

The second independent solution can be found from d'Alembert's formula (2.236). Its explicit form is not required; only its asymptotic behavior is relevant. Assuming the Lagrangian to be invariant under time reversal, which is usually the case, this asymptotic behavior is found via the following argument: Since $\phi_0^{(2)}(\tau)$ is linearly independent of $\phi_0^{(1)}(\tau)$, we can be sure that it has asymptotically the opposite exponential behavior (i.e., it grows with τ) and the opposite symmetry under time reversal (i.e., it is antisymmetric). Thus η must behave as follows:

$$\eta(\tau) \to \pm e^{\omega|\tau|} \quad \text{for} \quad \tau \to \pm\infty. \tag{17.153}$$

We now form the linear combination which satisfies the boundary conditions (17.149) for large negative $\tau = -L/2$:

$$D(\tau) = \frac{1}{W}\left[\xi(-L/2)\eta(\tau) - \eta(-L/2)\xi(\tau)\right], \tag{17.154}$$

where

$$W \equiv W[\xi(\tau)\eta(\tau)] = \xi(\tau)\dot{\eta}(\tau) - \eta(\tau)\dot{\xi}(\tau) \tag{17.155}$$

is the *Wronskian* of the two solutions. It is independent of τ and can be evaluated from the asymptotic behavior as

$$W = 2\omega. \tag{17.156}$$

Inserting (17.152) and (17.153) into (17.154), we find the solution

$$D(\tau) = \frac{1}{W}\left[e^{-\omega L/2}\eta(\tau) + e^{\omega L/2}\xi(\tau)\right]. \tag{17.157}$$

Even without knowing the solutions $\phi_0^{(1)}(\tau)$, $\phi_0^{(2)}(\tau)$ at a finite τ, the fluctuation determinant at large $\tau = L/2$ can be written down:

$$D(L/2) = \frac{2}{W} = \frac{1}{\omega}. \tag{17.158}$$

For fluctuations around the constant classical solution, the zero-eigenvalue solution with the boundary conditions (17.149) is

$$D^{(0)}(\tau) = \frac{1}{\omega}\sinh[\omega(\tau + L/2)]. \tag{17.159}$$

It behaves for large $\tau = L$ like

$$D^{(0)}(L/2) \to \frac{1}{2\omega}e^{\omega L} \quad \text{for large } L. \tag{17.160}$$

The ratio is therefore

$$\frac{D^{(0)}(L/2)}{D(L/2)} \to \frac{1}{2}e^{\omega L} \qquad \text{for large } L. \tag{17.161}$$

This exponentially large number is a signal for the presence of a would-be zero eigenvalue in $D(L/2)$. Since the τ-interval $(-L/2, L/2)$ is finite, there exists no exactly vanishing eigenvalue. In the finite interval, the derivative (17.150) of the kink solution does not quite satisfy the Dirichlet boundary condition. If the vanishing at the endpoints was properly enforced, the particle distribution would have to be compressed somewhat, and this would shift the energy slightly upwards. The shift is exponentially small for large L, so that the would-be zero eigenvalue has an exponentially small eigenvalue $\lambda_0 \propto e^{-\omega L}$. A finite result for $L \to \infty$ is obtained by removing this mode from the ratio (17.161) and considering the limit

$$\frac{\prod_n {\lambda_n}^0}{\prod'_n \lambda_n} = \lim_{L\to\infty} \frac{D^{(0)}(L/2)}{D(L/2)}\lambda_0. \tag{17.162}$$

The leading $e^{-\omega L}$-behavior of the would-be zero eigenvalue can be found perturbatively using as before only the asymptotic behavior of the two independent solutions. To lowest order in perturbation theory, an eigenfunction satisfying the Dirichlet boundary condition at finite L is obtained from an eigenfunction ϕ_0 which vanishes at $\tau = -L/2$ by the formula

$$\phi_0^L(\tau) = \phi_0(\tau) + \frac{\lambda_0}{W}\int_{-L/2}^{\tau} d\tau' \, [\xi(\tau)\eta(\tau') - \eta(\tau)\xi(\tau')]\,\phi_0(\tau'). \tag{17.163}$$

The limits of integration ensure that $\phi_0^L(\tau)$ vanishes at $\tau = -L/2$. The eigenvalue λ_0 is determined by enforcing the vanishing also at $\tau = L/2$. Taking for $\phi_0(\tau)$ the zero-eigenvalue solution $D(\tau)$

$$\lambda_0 = -D(L/2)W\left[\xi(L/2)\int_{-L/2}^{L/2} d\tau\,\eta(\tau)D(\tau) - \eta(L/2)\int_{-L/2}^{L/2} d\tau\,\xi(\tau)D(\tau)\right]^{-1}. \tag{17.164}$$

Inserting (17.154) and using the orthogonality of $\xi(\tau)$ and $\eta(\tau)$ (following from the fact that the first is symmetric and the second antisymmetric), this becomes

$$\lambda_0 = -D(L/2)W^2\left[\xi(-L/2)\xi(L/2)\int_{-L/2}^{L/2} d\tau\,\eta^2(\tau) + \eta(-L/2)\eta(L/2)\int_{-L/2}^{L/2} d\tau\,\xi^2(\tau)\right]^{-1}. \tag{17.165}$$

Invoking once more the symmetry of $\xi(\tau)$ and $\eta(\tau)$ and the asymptotic behavior (17.152) and (17.153), we obtain

$$\lambda_0 = -D(L/2)W^2 \left[e^{-\omega L} \int_{-L/2}^{L/2} d\tau\, \eta^2(\tau) - e^{\omega L} \int_{-L/2}^{L/2} d\tau\, \xi^2(\tau) \right]^{-1}. \qquad (17.166)$$

The first integral diverges like $e^{\omega L}$; the second is finite. The prefactor makes the second integral much larger than the first, so that we find for large L the would-be zero eigenvalue

$$\lambda_0 = D(L/2)e^{-\omega L} \frac{W^2}{\int_{-\infty}^{\infty} d\tau\, \xi^2(\tau)}. \qquad (17.167)$$

This eigenvalue is exponentially small and positive, as expected. Inserting it into (17.162) and using (17.156) and (17.160), we find the eigenvalue ratio

$$\frac{\prod_n \lambda_n^0}{\prod_n' \lambda_n} = \lim_{L\to\infty} 2\omega \frac{1}{\int_{-\infty}^{\infty} d\tau\, \xi^2(\tau)}. \qquad (17.168)$$

The determinant $D(L/2)$ has disappeared and the only nontrivial quantity to be evaluated is the normalization integral over the translational eigenfunction $\xi(\tau)$.

The normalization integral requires the knowledge of the full τ-behavior of the zero-eigenvalue solution $\phi_0^{(1)}(\tau)$; the asymptotic behavior used up to this point is insufficient. Fortunately, the classical solution $x_{\rm cl}(\tau)$ also supplies this information. The normalized solution is $y_0 = \alpha x'_{\rm cl}(\tau)$ behaving asymptotically like $2a\alpha\omega e^{-\omega\tau}$. Imposing the normalization convention (17.152) for $\phi_0^{(1)}(\tau)$, we identify

$$\xi(\tau) = \frac{1}{2a\omega\alpha} \alpha x'_{\rm cl}(\tau). \qquad (17.169)$$

Using the relation (17.32), the normalization integral is simply

$$\int_{-\infty}^{\infty} d\tau\, \xi(\tau)^2 = \frac{\mathcal{A}_{\rm cl}}{4a^2\omega^2}. \qquad (17.170)$$

With it the eigenvalue ratio (17.168) becomes

$$\frac{\prod_n \lambda_n^0}{\prod_n' \lambda_n} = 2\omega \frac{4a^2\omega}{\mathcal{A}_{\rm cl}}. \qquad (17.171)$$

By inserting the value of the classical action $\mathcal{A}_{\rm cl} = 2a^2\omega/3$ from (17.31), we obtain

$$\frac{\prod_n \lambda_n^0}{\prod_n' \lambda_n} = 12\omega^2, \qquad (17.172)$$

just as in (17.146) and (17.129).

It is remarkable that the calculation of the ratio of the fluctuation determinants with this method requires only the knowledge of the classical solution $x_{\rm cl}(\tau)$.

17.6 Wave Functions of Double-Well

The semiclassical result for the amplitudes

$$(a\ L/2|a\ -L/2), \quad (a\ L/2|-a\ -L/2), \tag{17.173}$$

with the endpoints situated at the bottoms of the potential wells can easily be extended to variable endpoints $x_b \neq a, x_a \neq \pm a$, as long as these are situated near the bottoms. The extended amplitudes lead to approximate particle wave functions for the lowest two states. The extension is trivial for the formula (17.34) without a kink solution. We simply multiply the fluctuation factor by the exponential $\exp(-\mathcal{A}_{\rm cl}/\hbar)$ containing the classical action of the path from x_a to x_b. If x_a and x_b are both near one of the bottoms of the well, the entire classical orbit remains near this bottom. If the distance of the orbit from the bottom is less than $1/a\sqrt{\omega}$, the potential can be approximated by the harmonic potential $\omega^2 x^2$. Thus near the bottom at $x = a$, we have the simple approximation to the action

$$\mathcal{A}_{\rm cl} \approx \frac{\omega}{2\hbar \sinh \omega L} \left\{ [(x_a - a)^2 + (x_b - a)^2] \cosh \omega L - 2(x_b - a)(x_a - a) \right\}. \tag{17.174}$$

For a very long Euclidean time L, this tends to

$$\mathcal{A}_{\rm cl} \approx \frac{\omega}{2\hbar}[(x_b - a)^2 + (x_a - a)^2]. \tag{17.175}$$

The amplitude (17.34) can therefore be generalized to

$$(x_b\ L/2|x_a\ L/2) \approx \sqrt{\frac{\omega}{\pi\hbar}} e^{-(\omega/2\hbar)[(x_b-a)^2+(x_a-a)^2]} e^{-\omega L/2\hbar}.$$

This can also be written in terms of the bound-state wave functions (17.5) for $n = 0$ as

$$(x_b\ L/2|x_a\ L/2) \approx \psi_0(x_b - a)\psi_0(x_a - a)e^{-\omega L/2\hbar}. \tag{17.176}$$

For the amplitude (17.35) with the path running from one potential valley to the other, the construction is more subtle. The approximate solution is obtained by combining a harmonic classical path running from $(x_a, -L/2)$ to $(a, -L/4)$, a kink solution running from $(a, -L/4)$ to $(a, L/4)$, and a third harmonic classical path running from $(a, L/4)$ to $(x_b, L/2)$. This yields the amplitude

$$\sqrt{\frac{\omega}{\pi\hbar}} e^{-(\omega/2\hbar)(x_b-a)^2} K L e^{-\mathcal{A}_{\rm cl}/\hbar} e^{-(\omega/2\hbar)(x_a-a)^2}. \tag{17.177}$$

Note that by patching the three pieces together, it is impossible to obtain a true classical solution. For this we would have to solve the equations of motion containing a kink with the modified boundary conditions $x(-L/2) = x_a,\ x(L/2) = x_b$. From the exponential convergence of $x(\tau) \to \pm a$ (like $e^{-\omega L}$) it is, however, obvious that the

true classical action differs from the action of the patched path only by exponentially small terms.

As before, the prefactor in (17.177) can be attributed to the ground state wave functions $\psi_0(x)$, and we find the amplitude for x_b close to $-a$ and x_a close to a:

$$(x_b\ L/2|x_a\ -L/2) \approx \psi_0(x_b+a)\psi_0(x_a-a)KLe^{-\mathcal{A}_{\rm cl}/\hbar}e^{-\omega L/2\hbar}. \qquad (17.178)$$

17.7 Gas of Kinks and Antikinks and Level Splitting Formula

The above semiclassical treatment is correct to leading order in $e^{-\omega L}$. This accuracy is not sufficient to calculate the degree of level splitting between the two lowest states of the double well caused by tunneling. Further semiclassical contributions to the path integral must be included. These can be found without further effort. For very large L, it is quite easy to accommodate many kinks and antikinks along the τ-axis without a significant deviation of the path from the equation of motion. Due to the fast approach to the potential bottoms $x = \pm a$ near each kink or antikink solution, an approximate solution can be constructed by smoothly combining a number of individual solutions as long as they are widely separated from each other. The deviations from a true classical solution are all exponentially small if the separation distance $\Delta\tau$ on the τ-axis is much larger than the size of an individual kink (i.e., $\Delta\tau \gg 1/\omega$). The combined solution may be thought of as a very dilute gas of kinks and antikinks on the τ-axis. This situation is referred to as the *dilute-gas limit*. Consider such an "almost-classical solution" consisting of N kink-antikink solutions $x_{\rm cl}(\tau) = \pm a\tanh[\omega(\tau-\tau_i)/2]$ in alternating order positioned at, say, $\tau_1 \gg \tau_2 \gg \tau_3 \gg \ldots \gg \tau_N$ and smoothly connected at some intermediate points $\bar\tau_1, \ldots, \bar\tau_{N-1}$. In the dilute-gas approximation, the combined action is given by the sum of the individual actions. For the amplitude (17.34) in which the paths connect the same potential valleys, the number of kinks must be equal to the number of antikinks. The action combined is then an even multiple of the single kink action:

$$\mathcal{A}_{2n} \approx 2n\mathcal{A}_{\rm cl}. \qquad (17.179)$$

For the amplitude (17.35), where the total number is odd, the combined action is

$$\mathcal{A}_{2n+1} \approx (2n+1)\mathcal{A}_{\rm cl}. \qquad (17.180)$$

As the kinks and antikinks are localized objects of size $2/\omega$, it does not matter how they are distributed on the large-τ interval $[-L/2, L/2]$, as long as their distances are large compared with their size. In the dilute-gas limit, we can neglect the sizes. In the path integral, the translational degree of freedom of widely spaced N kinks and antikinks leads, via the zero-eigenvalue modes, to the multiple integral

$$\int_{-L/2}^{L/2} d\tau_N \int_{-L/2}^{\tau_N} d\tau_{N-1} \ldots \int_{-L/2}^{\tau_1} d\tau_1 = \frac{L^N}{N!}. \qquad (17.181)$$

The Jacobian associated with these N integrals is [see (17.112)]

$$\sqrt{\frac{\mathcal{A}_{\rm cl}}{2\pi\hbar}}^{N}. \tag{17.182}$$

The fluctuations around the combined solution yield a product of the individual fluctuation factors. For a given set of connection points we have

$$\frac{1}{\sqrt{\Pi_n' \lambda_n}\Big|_{\bar{L}_N}} \frac{1}{\sqrt{\Pi_n' \lambda_n}\Big|_{\bar{L}_{N-1}}} \times \ldots \times \frac{1}{\sqrt{\Pi_n' \lambda_n}\Big|_{\bar{L}_1}}, \tag{17.183}$$

where $\bar{L}_i \equiv \bar{\tau}_i - \bar{\tau}_{i-1}$ are the patches on the τ-axis in which the individual solutions are exact. Their total sum is

$$L = \sum_{i=1}^{N} \bar{L}_i. \tag{17.184}$$

We now include the effect of the fluctuations at the intermediate times $\bar{\tau}_i$ where the individual solutions are connected. Remembering the amplitudes (17.176), we see that the fluctuation factor for arbitrary endpoints x_i, x_{i-1} near the bottom of the potential valley must be multiplied at each end with a wave function ratio $\psi_0(x \pm a)/\psi_0(0)$. Thus we have to replace

$$\frac{1}{\sqrt{\Pi_n \lambda_n}} \to \frac{\psi_0(x_i \pm a)}{\psi_0(0)} \frac{1}{\sqrt{\Pi_n \lambda_n}} \frac{\psi_0^\dagger(x_{i-1} \pm a)}{\psi_0^\dagger(0)}. \tag{17.185}$$

The adjacent x_i-values of all fluctuation factors are set equal and integrated out, giving

$$\begin{aligned}\frac{1}{\sqrt{\Pi_n \lambda_n}}\Big|_L = \int dx_N \cdots dx_1 \frac{1}{\sqrt{\Pi_n \lambda_n}}\Big|_{L_N} \frac{\psi_0(x_{N-1}-a)\psi_0^\dagger(x_{N-1}-a)}{|\psi_0(0)|^2} \frac{1}{\sqrt{\Pi_n \lambda_n}}\Big|_{L_{N-1}} \\ \times \ldots \times \frac{\psi_0(x_1-a)\psi_0^\dagger(x_1-a)}{|\psi_0(0)|^2} \frac{1}{\sqrt{\Pi_n \lambda_n}}\Big|_{L_1}.\end{aligned} \tag{17.186}$$

Due to the unit normalization of the ground state wave functions, the integrals are trivial. Only the $|\psi_0(0)|^2$-denominators survive. They yield a factor

$$\frac{1}{|\psi_0(0)|^{2(N-1)}} = \sqrt{\frac{\omega}{\pi\hbar}}^{-(N-1)}. \tag{17.187}$$

It is convenient to multiply and divide the result by the square root of the product of eigenvalues of the harmonic kink-free fluctuations, whose total fluctuation factor is known to be

$$\frac{1}{\sqrt{\Pi_n \lambda_n^0}|_L} = \sqrt{\frac{\omega}{\pi\hbar}} e^{-\omega L/2\hbar}. \tag{17.188}$$

Then we obtain the total corrected fluctuation factor

$$\sqrt{\frac{\omega}{\pi\hbar}}^{-(N-2)} e^{-\omega L/2\hbar} \sqrt{\prod_n \lambda_n^0}\Big|_L \frac{1}{\sqrt{\Pi_n' \lambda_n}\Big|_{L_1}} \frac{1}{\sqrt{\Pi_n' \lambda_n}\Big|_{L_2}} \times \ldots \times \frac{1}{\sqrt{\Pi_n' \lambda_n}\Big|_{L_N}}. \quad (17.189)$$

We now observe that the harmonic fluctuation factor (17.188) for the entire interval $\sqrt{\prod_n \lambda_n^0}|_L = \sqrt{\omega/\pi\hbar}\exp(-\omega L/2\hbar)$ can be factorized into a product of such factors for each interval $\bar{\tau}_i, \bar{\tau}_{i-1}$ as follows:

$$\sqrt{\prod_n \lambda_n^0}\Big|_L = \sqrt{\frac{\omega}{\pi\hbar}}^{-(N-1)} \sqrt{\prod_n \lambda_n^0}\Big|_{L_1} \cdots \sqrt{\prod_n \lambda_n^0}\Big|_{L_N}. \quad (17.190)$$

The total corrected fluctuation factor can therefore be rewritten as

$$\sqrt{\frac{\omega}{\pi\hbar}} e^{-\omega L/2\hbar} \sqrt{\frac{\prod_n \lambda_n^0}{\Pi_n' \lambda_n}}\Big|_{L_1} \times \ldots \times \sqrt{\frac{\prod_n \lambda_n^0}{\Pi_n' \lambda_n}}\Big|_{L_N}. \quad (17.191)$$

Each eigenvalue ratio gives the L_i-independent result

$$K' = \sqrt{\frac{\prod_n \lambda_n^0}{\Pi_n' \lambda_n}}\Big|_{L_i}, \quad (17.192)$$

with K' of Eq. (17.131). Expressing K' in terms of K via

$$K' = \sqrt{\frac{\mathcal{A}_{\rm cl}}{2\pi\hbar}}^{-1} K, \quad (17.193)$$

the factors $\sqrt{\mathcal{A}_{\rm cl}/2\pi\hbar}^{-1}$ remove the Jacobian factors (17.182) arising from the positional integrals (17.181). Altogether, the total fluctuation factor of N kink-antikink solutions with all possible distributions on the τ-axis is

$$\sqrt{\frac{\omega}{\pi\hbar}} e^{-\omega L/2\hbar} \frac{L^N}{N!} K^N e^{-N\mathcal{A}_{\rm cl}/\hbar}. \quad (17.194)$$

Summing over all even and odd kink-antikink configurations, we thus obtain

$$(a\ L/2| \pm a\ -L/2) = \sqrt{\frac{\omega}{\pi\hbar}} e^{-\omega L/2\hbar} \sum_{\substack{\text{even}\\ \text{odd}}} \frac{1}{N!} (KLe^{-\mathcal{A}_{\rm cl}/\hbar})^N. \quad (17.195)$$

This can be summed up to

$$(a\ L/2| \pm a\ -L/2) = \sqrt{\frac{\omega}{\pi\hbar}} e^{-\omega L/2\hbar} \times \frac{1}{2}\left[\exp\left(KLe^{-\mathcal{A}_{\rm cl}/\hbar}\right) \pm \exp\left(-KLe^{-\mathcal{A}_{\rm cl}/\hbar}\right)\right]. \quad (17.196)$$

As in the previous section, we generalize this result to positions x_b, x_a near the potential minima (with a maximal distance of the order of $\sqrt{\hbar/\omega}$). Using the classical action (17.175) and expressing it in terms of ground state wave functions, we can now add the contribution of the amplitudes for all possible configurations, arriving at

$$\begin{aligned}(x_b\ L/2|x_a\ -L/2) &= e^{-\omega L/2\hbar} \\ &\times \Big\{\psi_0(x_b-a)\psi_0(x_a-a)\frac{1}{2}\left[\exp(Ke^{-\mathcal{A}_{\rm cl}/\hbar}L)+\exp(-Ke^{-\mathcal{A}_{\rm cl}/\hbar}L)\right] \\ &+\psi_0(x_b-a)\psi_0(x_a-a)\frac{1}{2}\left[\exp(Ke^{-\mathcal{A}_{\rm cl}/\hbar}L)-\exp(-Ke^{-\mathcal{A}_{\rm cl}/\hbar}L)\right] \\ &+(x_b\to -x_b)+(x_a\to -x_a)+(x_b\to -x_b, x_a\to -x_a)\Big\}.\end{aligned} \tag{17.197}$$

The right-hand side is recombined to

$$\begin{aligned}&\frac{1}{\sqrt{2}}[\psi_0(x_b-a)+\psi_0(x_b+a)]\times\frac{1}{\sqrt{2}}[\psi_0(x_a-a)+\psi_0(x_a+a)] \\ &\qquad\times\exp\left[-\left(\frac{\omega}{2}-Ke^{-\mathcal{A}_{\rm cl}/\hbar}\right)L\right] \\ &+\frac{1}{\sqrt{2}}[\psi_0(x_b-a)-\psi_0(x_b+a)]\times\frac{1}{\sqrt{2}}[\psi_0(x_a-a)-\psi_0(x_a+a)] \\ &\qquad\times\exp\left[-\left(\frac{\omega}{2}+Ke^{-\mathcal{A}_{\rm cl}/\hbar}\right)L\right].\end{aligned} \tag{17.198}$$

Here we identify the ground state wave function as the symmetric combination of the ground state wave functions of the individual wells

$$\Psi_0(x)=\frac{1}{\sqrt{2}}[\psi_0(x-a)+\psi_0(x+a)]. \tag{17.199}$$

Its energy is

$$\mathcal{E}^{(0)}=E^{(0)}-\frac{\Delta E^{(0)}}{2}=\left(\omega/2-Ke^{-\ A_{\rm cl}/\hbar}\right)\hbar. \tag{17.200}$$

The first excited state has the antisymmetric wave function

$$\Psi_1(x)=\frac{1}{\sqrt{2}}[\psi_0(x-a)-\psi_0(x+a)] \tag{17.201}$$

and the slightly higher energy

$$\mathcal{E}^{(1)}=E^{(0)}+\frac{\Delta E^{(0)}}{2}=\left(\omega/2+Ke^{-\mathcal{A}_{\rm cl}/\hbar}\right)\hbar. \tag{17.202}$$

The level splitting is therefore

$$\Delta E=2K\hbar e^{-\mathcal{A}_{\rm cl}/\hbar}. \tag{17.203}$$

Inserting K from (17.131), we obtain the formula

$$\Delta E = 4\sqrt{3}\sqrt{\frac{\mathcal{A}_{\rm cl}}{2\pi\hbar}}\hbar\omega e^{-\mathcal{A}_{\rm cl}/\hbar}, \tag{17.204}$$

with $\mathcal{A}_{\rm cl} = (2/3)a^2\omega$. When expressing the action in terms of the height of the potential barrier $V_{\rm max} = a^2\omega^2/8 = 3\omega\mathcal{A}_{\rm cl}/16$, the formula reads

$$\Delta E = 4\sqrt{3}\sqrt{\frac{8V_{\rm max}}{3\pi\omega\hbar}}\hbar\omega e^{-16V_{\rm max}/3\hbar\omega}. \tag{17.205}$$

The level splitting decreases exponentially with increasing barrier height. Note that $V_{\rm max}$ is related to the coupling constant of the x^4-interaction by $V_{\rm max} = \omega^4/16g$.

To ensure the consistency of the approximation we have to check that the assumption of a low density gas of kinks and antikinks is self-consistent. When looking at the series (17.195) for the exponential (17.196), we see that the average number of contributing terms is given by

$$\bar{N} \approx KLe^{-\mathcal{A}_{\rm cl}/\hbar} = \frac{\Delta E}{2\hbar}L. \tag{17.206}$$

The associated average separation between kinks and antikinks is

$$\Delta L \equiv 2\hbar/\Delta E. \tag{17.207}$$

If we compare this with their size $2/\omega$, we find the ratio

$$\frac{\text{distance}}{\text{size}} \approx \frac{\hbar\omega}{\Delta E}. \tag{17.208}$$

For increasing barrier height, the level splitting decreases and the dilution increases exponentially. Thus the dilute-gas approximation becomes exact in the limit of infinite barrier height.

17.8 Fluctuation Correction to Level Splitting

ref(5.78) lab(5.56) est(5.77)

Let us calculate the first fluctuation correction to the level splitting formula (17.204). For this we write the potential (17.1) as in (5.78):

$$V(x) = -\frac{\omega^2}{4}x^2 + \frac{g}{4}x^4 + \frac{1}{4g}, \tag{17.209}$$

with the interaction strength

$$g \equiv \frac{\omega^2}{2a^2}. \tag{17.210}$$

Expanding the action around the classical solution, we obtain the action of the fluctuations $y(\tau) = x(\tau) - x_{\rm cl}(\tau)$. Its quadratic part was given in Eq. (17.40) which we write as

$$\mathcal{A}^0_{\rm fl} = \frac{1}{2}\int d\tau d\tau'\, y(\tau)\mathcal{O}_\omega(\tau,\tau')y(\tau'), \tag{17.211}$$

with the functional matrix

$$\mathcal{O}_\omega(\tau,\tau') \equiv \left[-\frac{d^2}{d\tau^2}+\omega^2\left(1-\frac{3}{2}\frac{1}{\cosh^2[\omega(\tau-\tau_0)/2]}\right)\right]' \delta(\tau-\tau') \tag{17.212}$$

ref(14.136) associated with the Schrödinger operator for a particle in a Rosen-Morse potential (14.136). The lab(14.125) prime indicates the absence of the zero eigenvalue in the spectral decomposition of $\mathcal{O}_\omega(\tau,\tau')$. Since est(14.159) the associated mode does not perform Gaussian fluctuations, it must be removed from $y(\tau)$ and treated separately. At the semiclassical level, this was done in Subsection 17.3.1, and the zero eigenvalue appeared in the level splitting formula (17.204) as a factor (17.112). The removal gave rise to an additional effective interaction (17.110):

$$\mathcal{A}_{\rm e}^{\rm eff} = -\hbar\log\left[1+\mathcal{A}_{\rm cl}^{-1}\int d\tau\, x'_{\rm cl}(\tau)y'(\tau)\right]. \tag{17.213}$$

With (17.88)–(17.91), this can be rewritten after a partial integration as

$$\mathcal{A}_{\rm e}^{\rm eff} \;=\; -\hbar\log\left[1-\sqrt{\frac{3g}{\omega^3}}\int d\tau\, y_0'(\tau)y(\tau)\right]. \tag{17.214}$$

The interaction between the fluctuations is

$$\mathcal{A}_{\rm fl}^{\rm int} = \frac{g}{4}\int d\tau\,\left[y^4(\tau)+4x_{\rm cl}(\tau)y^3(\tau)\right]. \tag{17.215}$$

In the path integral, we now perform a Taylor series expansion of the exponential $e^{-(\mathcal{A}_{\rm fl}^{\rm int}+\mathcal{A}_e^{\rm eff})/\hbar}$ in powers of the coupling strength g. A perturbative evaluation of the correlation functions of the fluctuations $y(\tau)$ according to the rules of Section 3.20 produces a correction factor to the path integral

$$C = \left[1-(I_1+I_2+I_3)\frac{g\hbar}{\omega^3}+\mathcal{O}(g^2)\right], \tag{17.216}$$

where I_1, I_2, and I_3 are the dimensionless integrals running over the entire τ-axis:

$$\begin{aligned}
I_1 &= \frac{\omega^3}{4\hbar^2}\int d\tau\,\langle y^4(\tau)\rangle_{\mathcal{O}_\omega},\\
I_2 &= -\frac{\omega^3 g}{2\hbar^3}\int d\tau d\tau'\, x_{\rm cl}(\tau)\langle y^3(\tau)y^3(\tau')\rangle_{\mathcal{O}_\omega}x_{\rm cl}(\tau'),\\
I_3 &= -\frac{\omega^3}{\hbar^2}\sqrt{\frac{3g}{\omega^3}}\int d\tau d\tau'\, y_0'(\tau)\langle y(\tau)y^3(\tau')\rangle_{\mathcal{O}_\omega}x_{\rm cl}(\tau').
\end{aligned} \tag{17.217}$$

In order to check the dimensions we observe that the classical solution (17.28) can be written with (17.210) as $x_{\rm cl}(\tau)=\sqrt{\omega^2/2g}\tanh[\omega(\tau-\tau_0)/2]$, while $y(\tau)$ and τ have the dimensions $\sqrt{\hbar/\omega}$ and $1/\omega$, respectively. The Dirac brackets $\langle\ldots\rangle_{\mathcal{O}_\omega}$ denote the expectation with respect to the quadratic fluctuations controlled by the action (17.211). Due to the absence of a zero eigenvalue, the fluctuations are harmonic. The expectation values of the various powers of $y(\tau)$ can therefore be expanded according to the Wick rule of Section 3.17 into a sum of pair contractions involving products of Green functions

$$G'_{\mathcal{O}_\omega}(\tau,\tau') \;=\; \langle y(\tau)y(\tau')\rangle_{\mathcal{O}_\omega} = \hbar\mathcal{O}_\omega^{-1}(\tau,\tau'), \tag{17.218}$$

where $\mathcal{O}_\omega^{-1}(\tau,\tau')$ denotes the inverse of the functional matrix (17.212).

The first term in (17.217) gives rise to three Wick contractions and becomes

$$I_1 = \frac{3\omega^3}{4\hbar^2}\int d\tau\, G'^2_{\mathcal{O}_\omega}(\tau,\tau). \tag{17.219}$$

The integrand contains an asymptotically constant term which produces a linear divergence for large L. This divergence is subtracted out as follows:

$$I_1 = L\frac{3\omega}{16} + \frac{3\omega^3}{4\hbar^2}\int d\tau\,\left[G'^2_{\mathcal{O}_\omega}(\tau,\tau) - \frac{\hbar^2}{4\omega^2}\right]. \tag{17.220}$$

The first term is part of the first-order fluctuation correction *without* the classical solution, i.e., it contributes to the constant background energy of the classical solution. It is obtained by replacing

$$G'^2_{\mathcal{O}_\omega}(\tau,\tau') \to \hbar G_\omega(\tau-\tau') = \frac{\hbar}{2\omega}e^{-\omega|\tau-\tau'|} \tag{17.221}$$

[recall (3.304) and (3.249)]. In the amplitudes (17.195), the background energy changes only the exponential prefactor $e^{-\omega L/2\hbar}$ to $e^{-(1+3g\hbar/16\omega^3)\omega L/2\hbar}$ and does not contribute to the level splitting. The level splitting formula receives a correction factor

$$C' = \left[1 - c_1\frac{g\hbar}{\omega^3} + \ldots\right] = \left[1 - (I'_1 + I'_2 + I'_3)\frac{g\hbar}{\omega^3} + \mathcal{O}(g^2)\right], \tag{17.222}$$

in which all contributions proportional to L are removed. Thus I_1 is replaced by its subtracted part $I'_1 \equiv I_1 - L3\omega/16$.

The integral I_2 has 15 Wick contractions which decompose into two classes:

$$\begin{aligned} I_2 \;\equiv\; I_{21} + I_{22} &= -\frac{g\omega^3}{2\hbar^3}\int d\tau d\tau' \\ &\times\; x_{\rm cl}(\tau)\left[6G'^3_{\mathcal{O}_\omega}(\tau,\tau') + 9G'_{\mathcal{O}_\omega}(\tau,\tau)G'_{\mathcal{O}_\omega}(\tau,\tau')G'_{\mathcal{O}_\omega}(\tau',\tau')\right]x_{\rm cl}(\tau'). \end{aligned} \tag{17.223}$$

Each of the two subintegrals I_{21} and I_{22} contains a divergence with L which can again be found via the replacement (17.221). The subtracted integrals in (17.222) are $I'_{21} = I_{21} + \omega L/8$ and $I'_{22} = I_{22} + 3\omega L/16$. Thus, altogether, the exponential prefactor $e^{-\omega L/2\hbar}$ in the amplitudes (17.195) is changed to $e^{-[1/2+(3/16-1/8-9/16)g\hbar/\omega^3)\omega L/2\hbar} = e^{-(1/2-g\hbar/2\omega^3)\omega L/2\hbar}$, in agreement with (5.258). To compare the two expressions, we have to set $\omega = \sqrt{2}$ since the present ω is the frequency at the bottom of the potential wells whereas the ω in Chapter 5 [which is set equal to 1 in (5.258)] parametrized the negative curvature at $x = 0$.

The Wick contractions of the third term lead to the finite integral

$$I_3 = I'_3 = -3\frac{\omega^3}{\hbar^2}\sqrt{\frac{3g}{\omega^3}}\int d\tau d\tau'\, y'_0(\tau)G'_{\mathcal{O}_\omega}(\tau,\tau')G'_{\mathcal{O}_\omega}(\tau',\tau')x_{\rm cl}(\tau'). \tag{17.224}$$

The correction factor (17.216) can be pictured by means of Feynman diagrams as

$C = 1 - 3$ 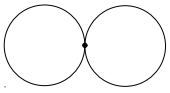 $+\,\frac{1}{2!}\Big(6$ 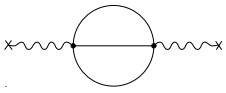 $+\,9$ 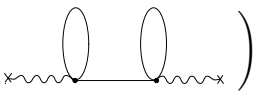 $\Big)$

$+\;3$ 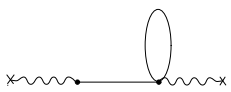 $+\,\mathcal{O}(g^2),$ (17.225)

where the vertices and lines represent the analytic expressions shown in Fig. 17.5.

For the evaluation of the integrals we need an explicit expression for $G'_{\mathcal{O}_\omega}(\tau,\tau')$. This is easily found from the results of Section 14.4.4. In Eq. (14.139), we gave the fixed-energy amplitude $(x_b|x_a)_{E_{\mathcal{RM}},E_{\mathcal{PT}}}$ solving the Schrödinger equation

ref(14.139)
lab(8.1443eq1)
est(14.162)

$$\left(-\frac{\hbar^2}{2\mu}\frac{d^2}{dx^2} - E_{\mathcal{RM}} + \frac{\hbar^2}{2\mu} - \frac{E_{\mathcal{PT}}}{\cosh^2 x}\right)(x_b|x_a)_{E_{\mathcal{RM}},E_{\mathcal{PT}}} = -i\hbar\delta(x_b - x_a). \tag{17.226}$$

Inserting $E_{\mathcal{PT}} = (\hbar^2/2\mu)s(s+1)$, the amplitude reads for $x_b > x_a$

$$(x_b|x_a)_{E_{\mathcal{RM}},E_{\mathcal{PT}}} = \frac{-i\mu}{\hbar}\Gamma(m(E_{\mathcal{RM}})-s)\Gamma(s+m(E_{\mathcal{RM}})+1) \times P_s^{-m(E_{\mathcal{RM}})}(\tanh x_b)P_s^{-m(E_{\mathcal{RM}})}(-\tanh x_a), \tag{17.227}$$

with

$$m(E_{\mathcal{RM}}) = \sqrt{1-2\mu E_{\mathcal{RM}}/\hbar^2}. \tag{17.228}$$

After a variable change $x = \omega\tau/2$ and $\hbar^2/\mu = \omega^2/2$, we set $s = 2$ and insert the energy $E_{\mathcal{RM}} = -3\omega^2/4$. Then the operator in Eq. (17.226) coincides with $\mathcal{O}_\omega(\tau,\tau')$ of Eq. (17.212), and we obtain the desired Green function for $\tau > \tau'$

$$G_{\mathcal{O}_\omega}(\tau,\tau') = \frac{\hbar}{\omega}\Gamma(m-2)\Gamma(m+3)\,P_2^{-m}(\tanh\frac{\omega\tau}{2})\,P_2^{-m}(-\tanh\frac{\omega\tau'}{2}), \tag{17.229}$$

with $m = 2$. Due to translational invariance along the τ-axis, this Green function has a pole at $E_{\mathcal{RM}} = -3\omega^2/4$ which must be removed before going to this energy. The result is the subtracted Green function $G'_{\mathcal{O}_\omega}(\tau,\tau')$ which we need for the perturbation expansion. The subtraction procedure is most easily performed using the formula $G'_{\mathcal{O}_\omega} = (d/dE_{\mathcal{RM}})E_{\mathcal{RM}}G_{\mathcal{O}_\omega}|_{E_{\mathcal{RM}}=-3\omega^2/4}$. In terms of the parameter m, this amounts to

$$G'_{\mathcal{O}_\omega}(\tau,\tau') = \frac{1}{2m}\frac{d}{dm}(m^2-4)G_{\mathcal{O}_\omega}(\tau,\tau')\Big|_{m=2}. \tag{17.230}$$

Inserting into (17.227) the Legendre polynomials from (14.143),

ref(14.143)
lab(x14.166)
est(14.166)

$$P_2^{-m}(z) \;=\; \frac{1}{\Gamma(1+m)}\left(\frac{1+z}{1-z}\right)^{-m/2}\left[1-\frac{3}{1+m}(1-z)+\frac{3}{(1+m)(2+m)}(1-z)^2\right], \tag{17.231}$$

the Green function (17.230) can be written as

$$G'_{\mathcal{O}_\omega}(\tau,\tau') = \hbar[Y_0(\tau_>)y_0(\tau_<) + y_0(-\tau_>)Y_0(-\tau_<)], \tag{17.232}$$

where $\tau_>$ and $\tau_<$ are the greater and the smaller of the two times τ and τ', respectively, and $y_0(\tau), Y_0(\tau)$ are the wave functions

$$y_0(\tau) = -2\sqrt{6\omega}P_2^{-2}\left(-\tanh\frac{\omega\tau}{2}\right) = -\sqrt{\frac{3\omega}{8}}\frac{1}{\cosh^2\frac{\omega\tau}{2}}, \tag{17.233}$$

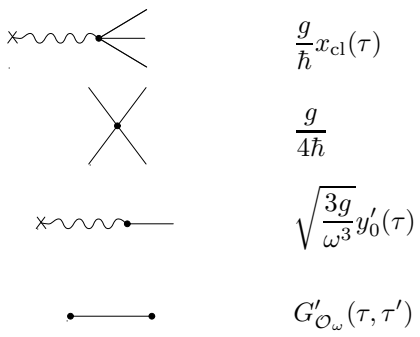

Figure 17.5 Vertices and lines of Feynman diagrams for correction factor C in Eq. (17.225).

$$Y_0(\tau) = \frac{1}{2\sqrt{6\omega}} \frac{1}{2\omega m} \left\{ \frac{1}{2} \left[\frac{d}{dm}(m^2-4)\Gamma(m-2)\Gamma(m+3) \right] P_2^{-m}\left(\tanh\frac{\omega\tau}{2}\right) \right.$$
$$\left. + \left[(m^2-4)\Gamma(m-2)\Gamma(m+3)\right] \frac{d}{dm} P_2^{-m}\left(\tanh\frac{\omega\tau}{2}\right) \right\}\Bigg|_{m=2}. \quad (17.234)$$

From (17.231) we see that

$$\frac{d}{dm} P_2^{-m}\left(\tanh\frac{\omega\tau}{2}\right)\Big|_{m=2} = \frac{\sqrt{6}}{144} y_0(\tau)[6(3-2\gamma+\omega\tau) - e^{-\omega\tau}(8+e^{-\omega\tau})], \quad (17.235)$$

where $\gamma \approx 0.5773156649$ is the Euler-Mascheroni constant (2.469). Hence

$$Y_0(\tau) = \frac{1}{12\omega^2} y_0(\tau)[e^{-\omega\tau}(e^{-\omega\tau}+8) - 2(2+3\omega\tau)]. \quad (17.236)$$

For $\tau = \tau'$, the Green function is

$$G'_{\mathcal{O}_\omega}(\tau,\tau) = \frac{\hbar}{2\omega} \frac{1}{\cosh^4\frac{\omega\tau}{2}} \left(\cosh^4\frac{\omega\tau}{2} + \cosh^2\frac{\omega\tau}{2} - \frac{11}{8} \right). \quad (17.237)$$

Note that an application of the Schrödinger operator (17.212) to the wave functions $Y_0(\tau)$ and $y_0(\tau)$ produces $-y_0(\tau)$ and 0, respectively. These properties can be used to construct the Green function $G'_{\mathcal{O}_\omega}(\tau,\tau')$ by a slight modification of the Wronski method of Chapter 3. Instead of the differential equation $\mathcal{O}_\omega G(\tau,\tau') = \hbar\delta(\tau-\tau')$, we must solve the projected equation

$$\mathcal{O}'_\omega G'_{\mathcal{O}_\omega}(\tau,\tau') = \hbar[\delta(\tau-\tau') - y_0(\tau)y_0(\tau')], \quad (17.238)$$

where the right-hand side is the completeness relation without the zero-eigenvalue solution:

$$\sum_{n\neq 0} y_n(\tau)y_n(\tau') = \delta(\tau-\tau') - y_0(\tau)y_0(\tau'). \quad (17.239)$$

The solution of the projected equation (17.238) is precisely given by the combination (17.232) of the solutions $Y_0(\tau)$ and $y_0(\tau)$ with the above-stated properties.

The evaluation of the Feynman integrals I_1, I_{21}, I_{22}, I_3 is somewhat tedious and is therefore described in Appendix 17A. The result is

$$I'_1 = \frac{97}{560}, \quad I'_{21} = \frac{53}{420}, \quad I'_{22} = \frac{117}{560}, \quad I_3 = \frac{49}{20}. \quad (17.240)$$

These constants yield for the correction factor (17.222)

$$C' = \left[1 - \frac{71}{24}\frac{g\hbar}{\omega^3} + \mathcal{O}(g^2)\right], \quad (17.241)$$

modifying the level splitting formula (17.204) for the ground state energy to

$$\Delta E^{(0)} = 4\sqrt{3}\sqrt{\frac{\omega^3/3g}{2\pi\hbar}}\hbar\omega e^{-\omega^3/3g\hbar - 71g\hbar/24\omega^3 + \cdots}. \quad (17.242)$$

This expression can be compared with the known energy eigenvalues of the lowest two double-well states. In Section 5.15, we have calculated the variational approximation $W_3(x_0)$ to the effective classical potential of the double well and obtained for small g an energy (see Fig. 5.24) which did not yet incorporate the effects of tunneling. We now add to this the level shifts $\pm\Delta E^{(0)}/2$ from Eq. (17.242) and obtain the curves also shown in Fig. 5.24. They agree reasonably well with the Schrödinger energies.

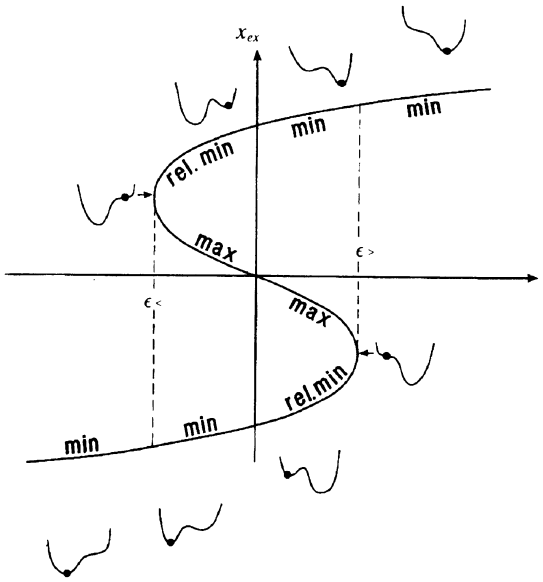

Figure 17.6 Positions of extrema $x_{\rm ex}$ in asymmetric double-well potential, plotted as function of asymmetry parameter ϵ. If rotated by 90^0, the plot shows the typical cubic shape. Between $\epsilon_>$ and $\epsilon_<$, there are two minima and one central maximum. The branches denoted by "min" are absolute minima; those denoted by "rel min" are relative minima.

17.9 Tunneling and Decay

The previous discussion of level splitting leads us naturally to another important tunneling phenomenon of quantum theory: the decay of metastable states. Suppose that the potential is not completely symmetric. For definiteness, let us add to $V(x)$ of Eq. (17.1) a linear term which breaks the symmetry $x \to -x$:

$$\Delta V = -\epsilon \frac{x-a}{2a}. \tag{17.243}$$

For small $\epsilon > 0$, this slightly depresses the left minimum at $x = -a$. The positions of the extrema are found from the cubic equation

$$V'(x_{\rm ex}) = \frac{\omega^2 a}{2}\left[\left(\frac{x_{\rm ex}}{a}\right)^3 - \frac{x_{\rm ex}}{a} - \frac{\epsilon}{\omega^2 a^2}\right] = 0. \tag{17.244}$$

They are shown in Fig. 17.6. For large ϵ, there is only one extremum, and this is always a minimum. In the region where $x_{\rm ex}$ has three solutions, say x_-, x_0, x_+, the branches denoted by "rel min." in Fig. 17.6 correspond to relative minima which lie higher than the absolute minimum. The central branch corresponds to a maximum. As ϵ decreases from large positive to large negative values, a classical particle at rest at the minimum follows the upper branch of the curve and drops to the lower branch as ϵ becomes smaller than $\epsilon_<$. Quantum-mechanically, however, there is tunneling

to the lower state before $\epsilon_<$. Tunneling sets in as soon as ϵ becomes negative, i.e., as soon as the initial minimum at x_+ comes to lie higher than the other minimum at x_-. The state whose wave packet is localized initially around x_+ decays into the lower minimum around x_-. After some finite time, the wave packet is concentrated around x_-.

A state with a finite lifetime is described analytically by an energy which lies in the lower half of the complex energy plane, i.e., which carries a negative imaginary part $E^{\rm im}$. The imaginary part gives half the decay rate $\Gamma/2\hbar$. This follows directly from the temporal behavior of a wave function with an energy $E = E^{\rm re} + iE^{\rm im}$ which is given by

$$\psi(\mathbf{x})e^{-iEt/\hbar} = \psi(\mathbf{x})e^{-iE^{\rm re}t/\hbar}e^{E^{\rm im}t/\hbar} = \psi(\mathbf{x})e^{-iE^{\rm re}t/\hbar}e^{-\Gamma t/2\hbar}. \tag{17.245}$$

The last factor leads to an exponential decay of the norm of the state

$$\int d^3x|\psi(\mathbf{x})|^2 = e^{-\Gamma t/\hbar}, \tag{17.246}$$

which shows that $\hbar/\Gamma$ is the lifetime of the state. A positive sign of the imaginary part of the energy is ruled out since it would imply the state to have an exponentially growing norm.

We are now going to calculate Γ for the lowest state.[4] If ϵ has a small negative value, the initial probability is concentrated in the potential valley around the right-hand minimum $x = x_+ \approx a$. We assume the potential barrier to be high compared to the ground state energy. Then a semiclassical treatment is adequate. In this approximation we evaluate the amplitude

$$(x_+t_b|x_+t_a).$$

It contains the desired information on the lifetime of the lowest state by behaving, for large $t_b - t_a$, as

$$(x_+t_b|x_+t_a) \sim \psi_0(0)\psi_0(0)e^{-iE^{\rm re}(t_b-t_a)/\hbar}e^{-\Gamma(t_b-t_a)/2\hbar}.$$

As before, it is convenient to work with the Euclidean amplitude with $\tau_a = -L/2$ and $\tau_b = L/2$,

$$(x_+\ L/2|x_+ - L/2), \tag{17.247}$$

which behaves for large L as

$$(x_+\ L/2|x_+ - L/2) \sim \psi_0(0)\psi_0(0)e^{-E^{\rm re}L/\hbar}e^{i\Gamma L/2\hbar}. \tag{17.248}$$

The classical approximation to this amplitude is dominated by the path solving the imaginary-time equation of motion which corresponds to a real-time motion in the reversed potential $-V(x)$ (see Fig. 17.7). The particle starts out at $x = x_+$ for

[4] Due to the finite lifetime this state is not stationary. For sufficiently long lifetimes, however, it is approximately stationary for a finite time.

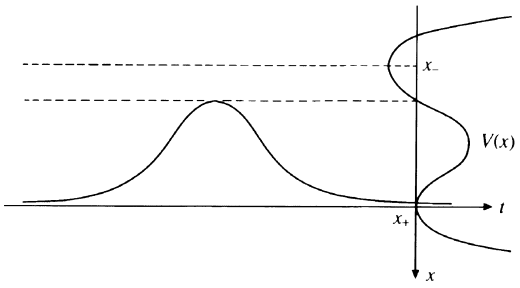

Figure 17.7 Classical bubble solution in reversed asymmetric quartic potential for $\epsilon < 0$, starting out at the potential maximum at x_+, crossing the valley, and returning to the maximum.

$\tau = -L/2$, traverses the minimum of $-V(x)$ at some finite value $\tau = \tau_0$, and comes back to x_+ at $\tau = L/2$. This solution is sometimes called a *bounce* solution, because of its returning to the initial point.

There exists an important application of the tunneling theory to the vaporization process of overheated water, to be discussed in Section 17.11. There the same type of solutions plays the role of *critical bubbles* triggering the phase transition. Since bounce solutions were first discussed in this context [4], we shall call them *bubble solutions* or critical bubbles.

We now proceed as in the previous section, i.e., we calculate
a) the classical action of a bubble solution,
b) the quadratic fluctuations around a bubble solution,
c) the sum over infinitely many bubble solutions.

By following these three steps naively, we obtain the amplitude

$$(x_+ \; L/2|x_+ - L/2) = \sqrt{\frac{\omega}{\pi\hbar}} e^{-\omega L/2\hbar} \exp\left[\sqrt{\mathcal{A}_{\rm cl}/2\pi\hbar} K' L e^{-\mathcal{A}_{\rm cl}/\hbar}\right]. \qquad (17.249)$$

Here $\mathcal{A}_{\rm cl}$ is the action of the bubble solution and K' collects the fluctuations of all nonzero-eigenvalue modes in the presence of the bubble solution as in (17.192):

$$K' = \sqrt{\left.\frac{\prod_n^0 \lambda_n}{\prod_n' \lambda_n}\right|_L}. \qquad (17.250)$$

The translational invariance makes the imaginary part in the exponent proportional to the total length L of the τ-axis.

From the large-L behavior of the amplitude (17.249) we obtain the ground state energy

$$E^{(0)} = \left(\frac{\omega}{2} - \sqrt{\frac{\mathcal{A}_{\rm cl}}{2\pi\hbar}} K' e^{-\mathcal{A}_{\rm cl}/\hbar}\right). \qquad (17.251)$$

In order to deduce the finite lifetime of the state from this formula we note that, just like the kink solution, the bubble solution has a zero-eigenvalue fluctuation

associated with the time translation invariance of the system. As before, its wave function is given by the time derivative of the bubble solution

$$y_0(\tau) = \frac{1}{\sqrt{\mathcal{A}_{\rm cl}}} x'_{\rm cl}(\tau). \tag{17.252}$$

In contrast to the kink solution, however, the bubble solution returns to the initial position, implying that $x_{\rm cl}(\tau)$ has a maximum. Thus, the zero-eigenvalue mode $\propto x'_{\rm cl}(\tau)$ contains a sign change (see Fig. 17.7). In wave mechanics, such a place is called a *node* of the wave function. A wave function with a node cannot be the ground state of the Schrödinger equation governing the fluctuations

$$\left[-\frac{d^2}{d\tau^2} + V''(x_{\rm cl}(\tau))\right] y_n(\tau) = \lambda_n y_n(\tau). \tag{17.253}$$

A symmetric wave function without a node must exist, which will have a lower energy than the zero-eigenvalue mode, i.e., it will have a negative eigenvalue $\lambda_{-1} < 0$. The associated wave function is denoted by $y_{-1}(\tau)$. It corresponds to a size fluctuation of the bubble solution. The nodeless wave function $y_{-1}(\tau)$ is the ground state. There can be no further negative-eigenvalue solution [5].

It is instructive to trace the origin of the negative sign within the efficient calculation method of the fluctuation determinant in Section 17.5. In contrast to the instanton treated there, the bubble solution has opposite symmetry, with an antisymmetric translational mode $x'_{\rm cl}(\tau)$. From this we may construct again two linearly independent solutions to find the determinant $D(\tau)$ to be used in Eq. (17.154).

The negative eigenvalue λ_{-1} enters in the calculation of the functional integral (17.46) via a fluctuation integral

$$\int \frac{d\xi_1}{\sqrt{2\pi\hbar}} e^{-(1/2\hbar)\xi_1^2 \lambda_{-1}}. \tag{17.254}$$

This integral diverges. The harmonic fluctuations of the integration variable take place around a maximum; they are unstable. At first sight one might hope to obtain a correct result by a naive analytic continuation doing first the integral for $\lambda_{-1} > 0$, where it gives

$$\int \frac{d\xi_{-1}}{\sqrt{2\pi\hbar}} e^{-(1/2\hbar)\xi_{-1}^2 \lambda_{-1}} = \frac{1}{\sqrt{\lambda_{-1}}}, \tag{17.255}$$

and then continuing the right-hand side analytically to negative λ_{-1}. The result would be

$$\int \frac{d\xi_{-1}}{\sqrt{2\pi\hbar}} e^{-(1/2\hbar)\xi_{-1}^2 \lambda_{-1}} = \pm \frac{i}{\sqrt{|\lambda_{-1}|}}. \tag{17.256}$$

From (17.250) and (17.251) we then might expect the formula for the decay rate to be

$$\frac{1}{\hbar}\Gamma = -2i \sqrt{\frac{\mathcal{A}_{\rm cl}}{2\pi\hbar}} K' e^{-\mathcal{A}_{\rm cl}/\hbar} \quad \text{(wrong)}, \tag{17.257}$$

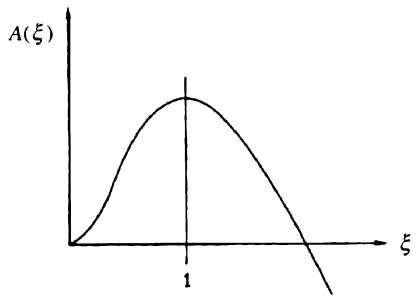

Figure 17.8 Action of deformed bubble solution as function of deformation parameter ξ. The maximum at $\xi = 1$ represents the critical bubble.

with

$$K' = i|K'| = \sqrt{\frac{\prod_n^0 \lambda_n}{\prod_{n\neq 0,-1}\lambda_n}\bigg|_L} \frac{i}{\sqrt{|\lambda_{-1}|}}. \tag{17.258}$$

However, this naive manipulation does not quite give the correct result. As we shall see immediately, the error consists in a missing factor 1/2 which has a simple physical explanation. A more careful analytic continuation is necessary to find this factor [4]. As a function of ξ, it behaves as shown in Fig. 17.8.

For a proper analytic continuation, consider a continuous sequence of paths in the functional space and parametrize it by some variable ξ. Let the trivial path

$$x(\tau) \equiv x_+ \tag{17.259}$$

correspond to $\xi = 0$, and the bubble solution

$$x(\tau) = x_{\rm cl}(\tau) \tag{17.260}$$

to $\xi = 1$. The action of the trivial path is zero, that of the bubble solution is $\mathcal{A} = \mathcal{A}_{\rm cl}$. As the parameter ξ increases to values > 1, the bubble solution is deformed with a growing portion of the curve moving down towards the bottom of the lower potential valley (see Fig. 17.9). This lowers the action more and more.

There is a maximum at the bubble solution $\xi = 1$. The negative eigenvalue $\lambda_{-1} < 0$ of the fluctuation equation (17.253) is proportional to the negative curvature at the maximum. Since there exists only a single negative eigenvalue, the fluctuation determinant of the remaining modes is positive. It does not influence the process of analytic continuation. Thus we may study the analytic continuation within a simple model integral designed to have the qualitative behavior described above:

$$Z = \int_0^\infty \frac{d\xi}{\sqrt{2\pi}} e^{\lambda(\xi^2+\alpha\xi^3)}. \tag{17.261}$$

The parameter λ stands for the negative eigenvalue λ_{-1}, whereas α is an auxiliary parameter to help perform the analytic continuation. For $\alpha > 0$, the integral is

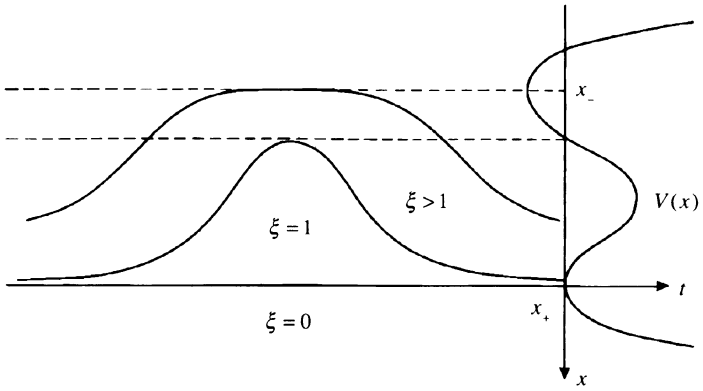

Figure 17.9 Sequence of paths as function of parameter ξ, starting out at $\xi = 0$, with a constant solution in the metastable valley $x(\tau) \equiv x \equiv x_+$, reaching the extremal bubble solution $x(\tau) \equiv x_{\rm cl}(\tau)$ for $\xi = 1$, and sliding more and more down towards the stable minimum for $1 < \xi \to \infty$.

stable and well defined. For $\alpha < 0$, the "Euclidean action" in the exponent $\mathcal{A} = -\lambda(\xi^2 + \alpha\xi^3)$ has a maximum at

$$\xi_m = -\frac{2}{3\alpha}. \tag{17.262}$$

Near the maximum, it has the expansion

$$\mathcal{A} = -\lambda\left[\frac{4}{27\alpha^2} - (\xi - \xi_m)^2 + \ldots\right]. \tag{17.263}$$

The second term possesses a negative curvature λ which represents the negative eigenvalue λ_{-1}. The parameter α^2 plays the role of $\hbar/(-\lambda\mathcal{A}_{\rm cl})$ in the bubble discussion, and the semiclassical expansion of the path integral corresponds to an expansion of the model integral in powers of α^2. We want to show that the lowest two orders of this expansion yield an imaginary part

$$\mathrm{Im}\, Z \sim e^{\lambda 4/27\alpha^2}\ \frac{1}{2}\frac{1}{\sqrt{|\lambda|}}, \tag{17.264}$$

where the exponential is the classical contribution and the factor contains the fluctuation correction. To derive (17.264), we continue the integral (17.261) analytically from $\alpha > 0$, where it is well defined, into the complex α-plane. It is convenient to introduce a new variable $t = \alpha\xi$. Then Z becomes

$$Z = \frac{1}{\alpha}\int_0^\infty \frac{dt}{\sqrt{2\pi}} \exp\left[\frac{\lambda}{\alpha^2}(t^2 + t^3)\right]. \tag{17.265}$$

Since $\lambda < 0$ this integral converges for $\alpha > 0$. To continue it to negative real values of α, we set $\alpha \equiv |\alpha|e^{i\varphi}$ and increase the angle φ from zero to $\pi/2$. While doing so,

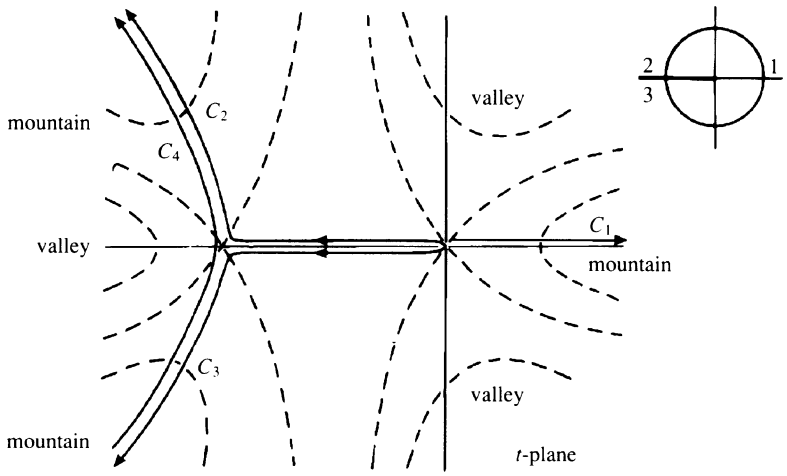

Figure 17.10 Lines of constant $\mathrm{Re}\,(t^2+t^3)$ in complex t-plane and integration contours C_i for various phase angles of α (shown in the insert) which maintain convergence of the integral (17.265).

we deform the contour in the t-plane in order to maintain convergence. Thus we introduce an auxiliary real variable t' and set

$$t = e^{i2\varphi/3}t', \quad t' \in (0,\infty). \tag{17.266}$$

The continued integral is then performed as $\int dt = e^{i2\varphi/3}\int_0^\infty dt'$. From the geometric viewpoint, the convergence is maintained for the following reason: For $\alpha > 0$, the real part of the "action" $-(\lambda/\alpha^2)(t^2+t^3)$ has asymptotically three mountains at azimuthal angles $\varphi = 0,\, 2\pi/3,\, 4\pi/3$, and three valleys at $\varphi = \pi/3,\, \pi,\, 5\pi/3$ (see Fig. 17.10). As α is rotated by the phase $e^{i\varphi}$, these mountains rotate with 2/3 of the angle φ anticlockwise in the t-plane. Since the contour keeps running up the same mountain, the integral continues to converge, rendering an analytic function of α. After α has been rotated to $e^{i\pi}\alpha = -\alpha$, the exponent in (17.265) takes back the original form, but the contour C runs up the mountain at $\varphi = 2\pi/3$. It does not matter which particular shape is chosen for the contour in the finite regime. We may deform the contour to the shape C_2 shown in Fig. 17.10. Next we observe that the point $-\alpha$ can also be reached by rotating α in the clockwise sense with $-\varphi$ increasing to π. In this case the final contour will run like C_3 in Fig. 17.10. The difference between the two analytic continuations is

$$\Delta Z \equiv Z(|\alpha|e^{-i\pi}) - Z(|\alpha|e^{i\pi}) = \frac{1}{|\alpha|}\int_{C_4}\frac{dt}{\sqrt{2\pi}}\exp\left\{\frac{\lambda}{\alpha^2}(t^2+t^3)\right\}, \tag{17.267}$$

where the contour $C_4 = C_2 - C_3$ connects the mountain at $\varphi = 4\pi/3$ with that at $\varphi = 2\pi/3$. The convergence of the combined integral is most rapid if the contour

C_4 is chosen to run along the line of steepest slope. This traverses the minimum at $t = -1$ vertically in the complex t-plane.

The fact that ΔZ is nonzero implies that the partition function has a cut in the complex α-plane along the negative real axis. Since Z is real for $\alpha > 0$, it is a real analytic function in the complex α-plane and the difference ΔZ gives a purely imaginary discontinuity across the cut:

$$\Delta Z \equiv \operatorname{disc} Z = Z(-|\alpha| - i\eta) - Z(-|\alpha| + i\eta). \tag{17.268}$$

Let us calculate the discontinuity in the limit of small α where the dominant contribution comes from the neighborhood of the point $t = -1$. While the action at this point has a local maximum along the real t-axis, it has a local minimum along the vertical contour in the complex t-plane. For small α^2, the integral can be found via the saddle point approximation calculating the local minimum in the quadratic approximation:

$$\begin{aligned} \operatorname{disc} Z &\approx e^{\lambda 4/27\alpha^2} \int_{-i\infty}^{i\infty} \frac{d\xi}{\sqrt{2\pi}} e^{\lambda(\xi-\xi_0)^2} \\ &= e^{\lambda 4/27\alpha^2} \frac{i}{\sqrt{-\lambda}}. \end{aligned} \tag{17.269}$$

Due to the real analyticity of Z, the imaginary part of Z is equal to one half of this:

$$\operatorname{Im} Z(-|\alpha| \mp i\eta) = \pm e^{\lambda 4/27\alpha^2} \frac{1}{2\sqrt{-\lambda}}. \tag{17.270}$$

The contour leading up to the extremal point adds only a real part to Z. The result (17.270) is therefore the exact leading contributing to the imaginary part in the limit $\alpha^2 \to 0$, corresponding to the semiclassical limit $\hbar \to 0$.

The exponent in (17.270) is the action of the model integral at the saddle point. The second factor produces the desired imaginary part. For a sequence of paths in functional space whose action depends on ξ as in Fig. 17.9, the result can be phrased as follows:

$$\begin{aligned} \int_0^\infty \frac{d\xi}{\sqrt{2\pi\hbar}} e^{-\mathcal{A}(\xi)/\hbar} &= \int_0^1 \frac{d\xi}{\sqrt{2\pi\hbar}} e^{-\mathcal{A}(\xi)/\hbar} + e^{-\mathcal{A}(1)/\hbar} \int_1^{1-i\infty} \frac{d\xi}{\sqrt{2\pi\hbar}} e^{-\mathcal{A}''(1)(\xi-1)^2/2\hbar} \\ &\approx \int_0^1 \frac{d\xi}{\sqrt{2\pi\hbar}} e^{-\mathcal{A}(\xi)/\hbar} + \frac{i}{2} e^{-\mathcal{A}(1)/\hbar} \frac{1}{\sqrt{-\mathcal{A}''(1)}}. \end{aligned} \tag{17.271}$$

After translating this result to the form (17.254), we conclude that the integration over the negative-eigenvalue mode

$$\int \frac{d\xi_{-1}}{\sqrt{2\pi\hbar}} e^{-\xi_{-1}^2 \lambda_{-1}/2\hbar} \tag{17.272}$$

becomes, for $\lambda_{-1} < 0$ and after a proper analytic continuation,

$$\int \frac{d\xi_{-1}}{\sqrt{2\pi\hbar}} e^{-\xi_{-1}^2 \lambda_{-1}/2\hbar} = \frac{i}{2} \frac{1}{\sqrt{|\lambda_{-1}|}}. \tag{17.273}$$

It is easy to give a physical interpretation to the factor 1/2 appearing in this formula, in contrast to the naively continued formula (17.287). At the extremum, the classical solution, which plays the role of a critical bubble, can equally well contract or expand in size. In the first case, the path $x(\tau)$ returns towards to the original valley and the bubble disappears. In the second case, the path moves more and more towards the lower valley at $x = -x_-$, thereby transforming the system into the stable ground state. The factor 1/2 accounts for the fact that only the *expansion* of the bubble solution produces a stable ground state, not the *contraction*.

The factor 1/2 multiplies the naively calculated imaginary part of the partition function which becomes

$$\operatorname{Im} Z(-|g| - i\eta) \approx \frac{1}{2}\sqrt{\mathcal{A}_{\rm cl}/2\pi\hbar}|K'|Le^{-\mathcal{A}_{\rm cl}/\hbar}. \tag{17.274}$$

The summation over an infinite number of bubble solutions moves the imaginary contribution to Z into the exponent as follows:

$$\operatorname{Re} Z + \operatorname{Im} Z = \operatorname{Re} Z(1 + \operatorname{Im} Z/\operatorname{Re} Z) \underset{\text{infinite sum}}{\longrightarrow} \operatorname{Re} Z e^{\operatorname{Im} Z/\operatorname{Re} Z} \tag{17.275}$$

as in Eqs. (17.195), (17.196). By comparison with (17.248), we obtain the correct semiclassical *tunneling rate formula* [rather than (17.257)]:

$$\frac{1}{\hbar}\Gamma = \sqrt{\frac{\mathcal{A}_{\rm cl}}{2\pi\hbar}}|K'|e^{-\mathcal{A}_{\rm cl}/\hbar}, \tag{17.276}$$

where K' is the square root of the eigenvalue ratios, with the zero-eigenvalue mode removed. The prefactor has the dimension of a frequency. It defines the *bubble decay frequency*

$$\omega_{\rm att} = \sqrt{\frac{\mathcal{A}_{\rm cl}}{2\pi\hbar}}\,|K'|. \tag{17.277}$$

The exponential in (17.276) is a "quantum Boltzmann factor" which suppresses the formation of a bubble triggering the tunneling process via its expansion. The subscript indicates that the frequency plays the role of an *attempt frequency* by which the metastable state attempts to tunnel through the barrier into the stable ground state.

17.10 Large-Order Behavior of Perturbation Expansions

The above semiclassical approach of the decay rate of a metastable state has an important fundamental application. At the end of Chapter 3 we have remarked that the perturbation expansion of the anharmonic oscillator has a zero radius of convergence. This property is typical for many quantum systems. The precise form of the divergence is controlled by the tunneling rate formula (17.276), as we shall see now.

17.10.1 Growth Properties of Expansion Coefficients

As a specific, but typical, example we consider the anharmonic oscillator with the action

$$\mathcal{A} = \int_{-L/2}^{L/2} d\tau \left[\frac{x'^2}{2} - \frac{\omega^2}{2} x^2 - \frac{g}{4} x^4 \right], \tag{17.278}$$

and study the partition function as an analytic function of g. It is given by the path integral at large L (which now represents the imaginary time $\beta = 1/k_B T$, setting $\hbar = 1$)

$$Z(g) = \int \mathcal{D}x(\tau) e^{\mathcal{A}}. \tag{17.279}$$

The L-dependence of the partition function follows from the spectral representation

$$Z(g) = \sum_n e^{-E^{(n)}(g)L}, \tag{17.280}$$

where $E^{(n)}(g)$ are the energy eigenvalues of the system. In the limit $L \to \infty$, this becomes an expansion for the ground state energy $E^{(0)}(g)$. In the limit $L \to \infty$, $Z(g)$ behaves like

$$Z(g) \to e^{-E^{(0)}(g)L}, \tag{17.281}$$

exhibiting directly the ground state energy.

Since the path integral can be done exactly at the point $g = 0$, it is suggestive to expand the exponential in powers of g and to calculate the perturbation series

$$Z(g) = \sum_{k=0} Z_k \left(\frac{g}{\omega^3} \right)^k. \tag{17.282}$$

As shown in Section 3.20, the expansion coefficients are given by the path integrals

$$\begin{aligned} Z_k &= \frac{(-g)^k}{k!} \int \mathcal{D}x(\tau) \left[\int_{-L/2}^{L/2} d\tau\, x^4(\tau) \right]^k \exp\left[- \int_{-L/2}^{L/2} d\tau \left(\frac{1}{2}\dot{x}^2 + \frac{\omega^2}{2} x^2 \right) \right] \\ &= Z^{-1} \frac{(-g)^k}{k!} \left\langle \int_{-L/2}^{L/2} d\tau\, x^4(\tau) \right\rangle_\omega . \end{aligned} \tag{17.283}$$

By selecting the connected Feynman diagrams in Fig. 3.7 contributing to this path integral, we obtain the perturbation expansion in powers of g for the free energy F. In the limit $L \to \infty$, this becomes an expansion for the ground state energy $E^{(0)}(g)$, in accordance with (17.281). By following the method in Section 3.18, we find similar expansions for all excited energies $E^{(n)}(g)$ in powers of g. For $g = 0$, the energies are, of course, those of a harmonic oscillator, $E_0^{(n)} = \omega(n + 1/2)$. In general, we find the series

$$E^{(n)}(g) = \sum_{k=0}^{\infty} E_k^{(n)} \left(\frac{g}{4} \right)^k. \tag{17.284}$$

Most perturbation expansions have the grave deficiency observed in Eq. (3C.27). Their coefficients grow for large order k like a factorial $k!$ causing a vanishing radius of convergence. They can yield approximate results only for very small values of g. Then the expansion terms $E_k^{(n)}\,(g/4)^k$ decrease at least for an initial sequence of k-values, say for $k = 0, \ldots, N$. For large k-values, the factorial growth prevails. Such series are called *asymptotic*. Their optimal evaluation requires a truncation after the smallest correction term. In general, the large-order behavior of perturbation expansions may be parametrized as

$$E_k = \gamma p^{\beta+1} k^\beta (-4a)^k (pk)! \left[1 + \frac{\gamma_1}{k} + \frac{\gamma_2}{k^2} + \ldots\right], \tag{17.285}$$

where the leading term $(pk)!$ grows like

$$(pk)! = (k!)^p (p^p)^k k^{(1-p)/2} \frac{\sqrt{p}}{(2\pi)^{(p-1)/2}} \left[1 + \mathcal{O}(1/k)\right]. \tag{17.286}$$

This behavior is found by approximating $n!$ via Stirling's formula (5.204). It is easy to see that the kth term of the series (17.284) is minimal at

$$k \approx k_{\min} \equiv \frac{1}{p(a|g|)^{1/p}}. \tag{17.287}$$

This is found by applying Stirling's formula once more to $(k!)^p$ and by minimizing $\gamma(k!)^p k^{\beta'}(p^p a|g|)^k$ with $\beta' = \beta + (1-p)/2$, which yields the equation

$$p \log k + \log(p^p a|g|) + (\beta + p/2)/k + \ldots = 0. \tag{17.288}$$

An equivalent way of writing (17.285) is

$$E_k = \gamma p (-4a)^k \Gamma(pk + \beta + 1) \left[1 + \frac{c_1}{pk+\beta} + \frac{c_2}{(pk+\beta)(pk+\beta-1)} + \ldots\right]. \tag{17.289}$$

The simplest example for a function with such strongly growing expansion coefficients can be constructed with the help of the exponential integral

$$E_1(g) = \int_g^\infty \frac{dt}{t} e^{-t}. \tag{17.290}$$

Defining

$$E(g) \equiv \frac{1}{g} e^{1/g} E_1(1/g) = \int_0^\infty dt \frac{1}{1+gt} e^{-t}, \tag{17.291}$$

this has the diverging expansion

$$E(g) = 1 - g + 2!g^2 - 3!g^3 + \ldots + (-1)^N N! g^N + \ldots\ . \tag{17.292}$$

At a small value of g, such as $g = 0.05$, the series can nevertheless be evaluated quite accurately if truncated at an appropriate value of N. The minimal correction

is reached at $N = 1/g = 20$ where the relative error with respect to the true value $E \approx 0.9543709099$ is equal to $\Delta E/E \approx 1.14 \cdot 10^{-8}$. At a somewhat larger value $g = 0.2$, on the other hand, the optimal evaluation up to $N = 5$ yields the much larger relative error $\approx 1.8\%$, the true value being $E \approx 0.852110880$.

The integrand on the right-hand side of (17.291), the function

$$B(t) = \frac{1}{1+t}, \tag{17.293}$$

is the so-called *Borel transform* of the function $E(g)$. It has a power series expansion which can be obtained from the divergent series (17.292) for $E(g)$ by removing in each term the catastrophically growing factor $k!$. This produces the convergent series

$$B(t) = 1 - t + t^2 - t^3 + \dots, \tag{17.294}$$

which sums up to (17.293). The integral

$$F(g) = \int_0^\infty \frac{dt}{g} e^{-t/g} B(t) \tag{17.295}$$

restores the original function by reinstalling, in each term t^k, the removed $k!$-factor.

Functions $F(g)$ of this type are called *Borel-resummable*. They possess a convergent Borel transform $B(t)$ from which $F(g)$ can be recovered with the help of the integral (17.295). The resummability is ensured by the fact that $B(t)$ has no singularities on the integration path $t \in [0, \infty)$, including a wedge-like neighborhood around it. In the above example, $B(t)$ contains only a pole at $t = -1$, and the function $E(g)$ is Borel-resummable. Alternating signs of the expansion coefficients of $F(g)$ are a typical signal for the resummability.

The best-known quantum field theory, *quantum electrodynamics*, has divergent perturbation expansions, as was first pointed out by Dyson [6]. The expansion parameter g in that theory is the *fine-structure constant*

$$\alpha = 1/137.035963(15) \approx 0.0073. \tag{17.296}$$

Fortunately, this is so small that an evaluation of observable quantities, such as the anomalous magnetic moment of the electron

$$a_{\rm e} = \frac{\Delta\mu}{\mu} = \frac{1}{2}\frac{\alpha}{\pi} - 0.328\,478\,965\,7\left(\frac{\alpha}{\pi}\right)^2 + 1.1765(13)\left(\frac{\alpha}{\pi}\right)^3 + \dots\ , \tag{17.297}$$

gives an extremely accurate result:

$$a_e^{\rm theor} = (1\,159\,652\,478 \pm 140) \cdot 10^{-12}. \tag{17.298}$$

The experimental value differs from this only in the last three digits, which are 200 ± 40. The divergence of the series sets in only after the 137th order.

A function $E(g)$ with factorially growing expansion coefficients cannot be analytic at the origin. We shall demonstrate below that it has a left-hand cut in the complex g-plane. Thus it satisfies a dispersion relation

$$E(g) = \frac{1}{2\pi i}\int_0^\infty dg' \frac{\text{disc}\, E(-g')}{g'+g}, \tag{17.299}$$

where $\text{disc}\, E(g')$ denotes the discontinuity across the left-hand cut

$$\text{disc}\, E(g) \equiv E(g-i\eta) - E(g+i\eta). \tag{17.300}$$

It is then easy to see that the above large-order behavior (17.289) is in one-to-one correspondence with a discontinuity which has an expansion, around the tip of the cut,

$$\text{disc}\, E(-|g|) = 2\pi i \gamma (a|g|)^{-(\beta+1)/p} e^{-1/(a|g|)^p} [1 + c_1 (a|g|)^{1/p} + c_2 (a|g|)^{2/p} + \ldots]\,. \tag{17.301}$$

The parameters are the same as in (17.289). The one-to-one correspondence is proved by expanding the dispersion relation (17.299) in powers of $g/4$, giving

$$E_k = (-4)^k \int_0^\infty \frac{dg'}{2\pi i} \frac{1}{g'^{k+1}}\, \text{disc}\, E(-g'). \tag{17.302}$$

The expansion coefficients are given by moment integrals of the discontinuity with respect to the inverse coupling constant $1/g$. Inserting (17.301) and using the integral formula[5]

$$\int_0^\infty dg \frac{1}{|g|^{\alpha+1}} e^{-1/(a|g|)^{(1/p)}} = a^\alpha p \Gamma(p\alpha), \tag{17.303}$$

we indeed recover (17.289).

From the strong-coupling limit of the ground state energy of the anharmonic oscillator Eq. (5.168) we see that the discontinuity grow for large g like $g^{1/3}$. In this case, the dispersion relation (17.304) needs a subtraction and reads

$$E(g) = E(0) + \frac{g}{2\pi i}\int_0^\infty \frac{dg'}{g'} \frac{\text{disc}\, E(-g')}{g'+g}. \tag{17.304}$$

This does not influence the moment formula (17.302) for the expansion coefficients, except that the lowest coefficient is no longer calculable from the discontinuity. Since the lowest coefficient is known, there is no essential restriction.

17.10.2 Semiclassical Large-Order Behavior

The large-order behavior of many divergent perturbation expansions can be determined with the help of the tunneling theory developed above. Consider the potential

[5] I.S. Gradshteyn and I.M. Ryzhik, *op. cit.*, Formula 3.478.

of the anharmonic oscillator at a small negative coupling constant g (see Fig. 17.11). The minimum at the origin is obviously metastable so that the ground state has only a finite lifetime. There are barriers to the right and left of the metastable minimum, which are very high for very small negative coupling constants. In this limit, the lifetime can be calculated accurately with the semiclassical methods of the last section. The fluctuation determinant yields an imaginary part of $Z(g)$ of the form (17.270), which determines the imaginary part of the ground state energy via (17.276), which is accurate near the tip of the left-hand cut in the complex g-plane. From this imaginary part, the dispersion relation (17.302) determines the large-order behavior of the perturbation coefficients.

The classical equation of motion as a function of τ is

$$x''(\tau) - V'(x(\tau)) = 0. \tag{17.305}$$

The differential equation is integrated as in (17.26), using the first integral of motion

$$\frac{1}{2}x'^2 - \frac{1}{2}\omega^2 x^2 - \frac{g}{4}x^4 = E = \text{const}\,, \tag{17.306}$$

from which we find the solutions for $E = 0$

$$\tau - \tau_0 = \pm\frac{1}{\omega}\int dx \frac{1}{x\sqrt{1-(|g|/2\omega^2)x^2}} = \mp\frac{1}{\omega}\text{arcosh}\left(\sqrt{\frac{2\omega^2}{|g|}}\frac{1}{x}\right), \tag{17.307}$$

or

$$x(\tau) = x_{\rm cl}(\tau) \equiv \pm\sqrt{\frac{2\omega^2}{|g|}}\frac{1}{\cosh[\omega(\tau-\tau_0)]}. \tag{17.308}$$

They represent excursions towards the abysses outside the barriers and correspond precisely to the bubble solutions of the tunneling discussion in the last section. The excursion towards the abyss on the right-hand side is illustrated in Fig. 17.11. The associated action is calculated as in (17.29):

$$\begin{aligned}\mathcal{A}_{\rm cl} &= \int_{-L/2}^{L/2} d\tau \left[\frac{1}{2}x_{\rm cl}'^2(\tau) + V(x_{\rm cl}(\tau))\right] = 2\int_0^{L/2} d\tau\,[x_{\rm cl}'^2(\tau) - E] \\ &= 2\int_0^{x_m} dx\sqrt{2(E+V)} - EL,\end{aligned} \tag{17.309}$$

where x_m is the maximum of the solution. The bubble solution has $E = 0$, so that

$$\mathcal{A}_{\rm cl} = 2\int_0^{x_m} dx\sqrt{2V} = \frac{4\omega^3}{3|g|}. \tag{17.310}$$

Inserting the fluctuating path $x(\tau) = x_{\rm cl}(\tau) + y(\tau)$ into the action (17.278) and expanding it in powers of $y(\tau)$, we find an action for the quadratic fluctuations of the same form as in Eq. (17.211), but with a functional matrix

$$\begin{aligned}\mathcal{O}_\omega(\tau,\tau') &= \left[-\frac{d^2}{d\tau^2} + \omega^2 + 3gx_{\rm cl}^2(\tau)\right]'\delta(\tau-\tau') \\ &= \left[-\frac{d^2}{d\tau^2} + \omega^2\left(1 - \frac{6}{\cosh^2[\omega(\tau-\tau_0)]}\right)\right]'\delta(\tau-\tau').\end{aligned} \tag{17.311}$$

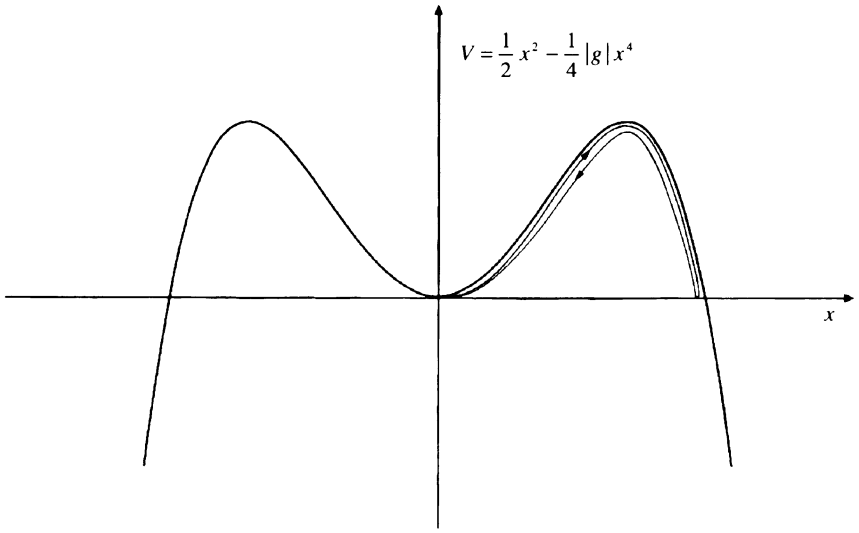

Figure 17.11 Potential of anharmonic oscillator (17.278) for small negative coupling g. The ground state centered at the origin is metastable. It decays via a classical solution which makes an excursion towards the abyss as indicated by the oriented curve.

This is once more the operator of the Rosen-Morse type encountered in Eq. (17.138) with $m = \omega, z = 1$, and $s = 2$. The subscript ω on the operator symbol indicates the asymptotic harmonic form of the potential. The potential accommodates again two bound states with the normalized wave functions[6] and energies (see Fig. 17.12)

$$y_0(\tau) = -\sqrt{\frac{3\omega}{2}}\frac{\sinh[\omega(\tau-\tau_0)]}{\cosh^2[\omega(\tau-\tau_0)]} \quad \text{with} \quad \lambda_0 = 0, \tag{17.312}$$

$$y_{-1}(\tau) = \sqrt{\frac{3\omega}{4}}\frac{1}{\cosh^2[\omega(\tau-\tau_0)]} \quad \text{with} \quad \lambda_{-1} = -3\omega^2. \tag{17.313}$$

These are the same functions as in (17.52), (17.53), apart from the fact that m is now ω rather than $\omega/2$. However, the energies are shifted with respect to the earlier case. Now the first excited state has a zero eigenvalue so that the ground state has a negative eigenvalue. This is responsible for the finite lifetime of the ground state.

The fluctuation determinant is obtained by any of the above procedures, for instance from the general formula (17.143),

$$\frac{\prod_n \lambda_n^0}{\prod_n \lambda_n} = \frac{\Gamma(\sqrt{z}-s)\Gamma(\sqrt{z}+s+1)}{\Gamma(\sqrt{z})\Gamma(\sqrt{z}+1)}, \tag{17.314}$$

[6]The sign of y_0 is chosen to agree with that of $x'_{\rm cl}(\tau)$ in accordance with (17.88).

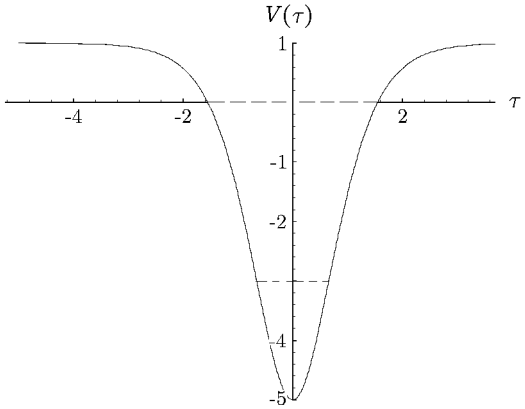

Figure 17.12 Rosen-Morse Potential for fluctuations around the classical bubble solution.

by inserting the parameters $z = 1$ and $s = 2$. The zero eigenvalue is removed by multiplying this with $(z-1)\omega^2$, resulting in the eigenvalue ratio

$$\frac{\prod_n \lambda_n^0}{\prod_n' \lambda_n} = \lim_{z\to 1}(\sqrt{z}-1)(\sqrt{z}+1)\omega^2 \left[\frac{\Gamma(\sqrt{z}-2)\Gamma(\sqrt{z}+3)}{\Gamma(\sqrt{z})\Gamma(\sqrt{z}+1)}\right] = -12\omega^2. \quad (17.315)$$

The negative sign due to the negative-eigenvalue solution in (17.313) accounts for the instability of the fluctuations.

Using formula (17.274), we find the imaginary part of the partition function

$$\mathrm{Im}\, Z(-|g| - i\eta) \approx \sqrt{\frac{6}{\pi}}\sqrt{\frac{4\omega^3}{3|g|}}\omega L e^{-4\omega^3/3|g|} e^{-\omega L/2}. \quad (17.316)$$

After summing over all bubble solutions, as in (17.275), we obtain the imaginary part of the ground state energy

$$\mathrm{Im}\, E^{(0)}(-|g| - i\eta) = -\omega\sqrt{\frac{6}{\pi}}\sqrt{\frac{4\omega^3}{3|g|}} e^{-4\omega^3/3|g|}. \quad (17.317)$$

A comparison of this with (17.301) fixes the growth parameters of the large-order perturbation coefficients to

$$a = 3/4\omega^3, \quad \beta = -\frac{1}{2}, \quad \gamma = -\frac{\omega}{\pi}\sqrt{\frac{6}{\pi}}, \quad p = 1. \quad (17.318)$$

Recalling the one-to-one correspondence between (17.301) and (17.289), we see that the large-order behavior of the perturbation coefficients of the ground state energy $E^{(0)}(g)$ is

$$E_k^{(0)} = -\frac{\omega}{\pi}\sqrt{\frac{6}{\pi}}(-3/\omega^3)^k \Gamma(k+1/2). \quad (17.319)$$

It is just as easy to find the large-k behavior of the excited states. Their decay is triggered by a periodic classical solution with a very long but finite Euclidean period L, which moves back and forth between positions $x_< \neq 0$ and $x_> < \sqrt{2\omega^2/|g|}$. Its action is approximately given by

$$\mathcal{A}'_{\rm cl} \approx \frac{4\omega^3}{3|g|}(1 - 12e^{-\omega L}). \tag{17.320}$$

In comparison with the limit $L \to \infty$, the Boltzmann-like factor $e^{-\mathcal{A}_{\rm cl}}$ of this solution is replaced by

$$e^{-\mathcal{A}'_{\rm cl}} = e^{-\mathcal{A}_{\rm cl}} \sum_{n=0}^{\infty} \mathcal{A}_{\rm cl}^n \frac{12^n}{n!} e^{-n\omega L}. \tag{17.321}$$

The exponentials in the sum raise the reference energies in the imaginary part of $Z(-|g|-i\eta)$ in (17.316) from $\omega/2$ to $\omega(n+1/2)$. The imaginary parts for the energies to the nth excited states become

$$\text{Im}\, E^{(n)}(-|g| - i\eta) = -\frac{12^n}{n!}\omega\sqrt{\frac{6}{\pi}}\sqrt{\frac{4\omega^3}{3|g|}}^{1+2n} e^{-4\omega^3/3|g|}, \tag{17.322}$$

implying an asymptotic behavior of the perturbation coefficients:

$$E_k^{(n)} = -\frac{\omega}{\pi}\sqrt{\frac{6}{\pi}}\frac{12^n}{n!}(-3/\omega^3)^k \Gamma(k + n + 1/2). \tag{17.323}$$

It is worth mentioning that within the semiclassical approximation, the dispersion integrals for the energies can be derived directly from the path integral (17.279). This can obviously be rewritten as

$$\begin{aligned} Z(g) &= \int_{-i\infty}^{i\infty} \frac{d\lambda}{2\pi i} \int_0^\infty \frac{da}{4} e^{-(ga+\lambda a)/4} \\ &\times \int \mathcal{D}x(\tau) \exp\left\{ -\int_{L/2}^{L/2} d\tau \left[\frac{1}{2}x'^2 + \frac{\omega^2}{2}x^2 - \frac{\lambda}{4}x^4 \right] \right\}. \end{aligned} \tag{17.324}$$

The integration over λ generates a δ-function $4\delta(\int d\tau\, x^4(\tau) - a)$ which eliminates the additionally introduced a-integration. The integral over a is easily performed. It yields a factor $1/(\lambda + g)$, so that we obtain the integral formula

$$Z(g) = \int_{-i\infty}^{i\infty} \frac{d\lambda}{2\pi i} \frac{1}{\lambda + g} Z(-\lambda). \tag{17.325}$$

The integrand has a pole at $\lambda = -g$ and a cut on the positive real λ-axis. We now deform the contour of integration in λ until it encloses the cut tightly in the clockwise sense. In the semiclassical approximation, the discontinuity across the cut is given by Eq. (17.316), i.e., with the present variable λ:

$$\text{Im}\, Z(-|\lambda| - i\eta) = \sqrt{\frac{6}{\pi}}\sqrt{\frac{4\omega^3}{3\lambda}} e^{-4\omega^3/3\lambda} e^{-\omega L/2}. \tag{17.326}$$

On the upper branch of the cut, $\sqrt{\lambda}$ is positive, on the lower negative. Thus we arrive at a simple dispersion integral from $\lambda = 0$ to $\lambda = \infty$:

$$Z(g)=2\omega \int_0^\infty \frac{d\lambda}{2\pi}\frac{1}{\lambda+g}\sqrt{\frac{6}{\pi}}\sqrt{\frac{4\omega^3}{3\lambda}}e^{-4\omega^3/3\lambda}e^{-\omega L/2}. \tag{17.327}$$

For the ground state energy, this implies

$$E^{(0)}(g)=-2\omega \int_0^\infty \frac{d\lambda}{2\pi}\frac{1}{\lambda+g}\sqrt{\frac{6}{\pi}}\sqrt{\frac{4\omega^3}{3\lambda}}e^{-4\omega^3/3\lambda}. \tag{17.328}$$

Of course, this expression is just an approximation, since the integrand is valid only at small λ. In fact, the integral converges only in this approximation. If the full imaginary part is inserted, the integral diverges. We shall see below that for large λ, the imaginary part grows like $\lambda^{1/3}$. Thus a subtraction is necessary. A convergent integral representation exists for $E^{(0)}(g) - E^{(0)}(0)$. With $E^{(0)}(0)$ being equal to $\omega/2$, we find the convergent dispersion integral

$$E^{(0)}(g)=\frac{\omega}{2}+2\omega g \int_0^\infty \frac{d\lambda}{2\pi}\frac{1}{\lambda(\lambda+g)}\sqrt{\frac{6}{\pi}}\sqrt{\frac{4\omega^3}{3\lambda}}e^{-4\omega^3/3\lambda}. \tag{17.329}$$

The subtraction is advantageous also if the initial integral converges since it suppresses the influence of the large-λ regime on which the semiclassical tunneling calculation contains no information.

After substituting $\lambda \to 4g/3t\omega^3$, the integral (17.329) is seen to become a Borel integral of the form (17.295).

By expanding $1/(\lambda+g)$ in a power series in g

$$\frac{1}{\lambda+g}=\sum_{k=0}^{\infty}(-1)^k g^k \lambda^{-k-1}, \tag{17.330}$$

we obtain the expansion coefficients as the moment integrals of the imaginary part as a function of $1/g$:

$$E_k^{(0)} = -2\omega\,(-4)^k \int_0^\infty \frac{d\lambda}{2\pi}\frac{1}{\lambda^{k+1}}\sqrt{\frac{6}{\pi}}\sqrt{\frac{4\omega^3}{3\lambda}}e^{-4\omega^3/3\lambda}. \tag{17.331}$$

This leads again to the large-k behavior (17.319).

The direct treatment of the path integral has the virtue that it can be generalized also to systems which do not possess a Borel-resummable perturbation series. As an example, one may derive and study the integral representation for the level splitting formula in Section 17.7.

17.10.3 Fluctuation Correction to the Imaginary Part and Large-Order Behavior

It is instructive to calculate the first nonleading term $c_1 a|g|$ in the imaginary part (17.301), which gives rise to a correction factor $1 + c_1/k$ in the large-order behavior

(17.289). As in Section 17.8, we expand the action around the classical solution. The interaction between the fluctuations $y(\tau)$ is the same as before in (17.215). The quadratic fluctuations are now governed by the differential operator

$$\mathcal{O}_\omega(\tau,\tau') = \left[-\frac{d^2}{d\tau^2} + \omega^2\left(1 - \frac{6}{\cosh^2\omega(\tau-\tau_0)}\right)\right]' \delta(\tau-\tau'), \tag{17.332}$$

the prime indicating the absence of the zero eigenvalue. Its removal gives rise to the factor

$$\mathcal{A}_{\rm e}^{\rm eff} = -\hbar\log\left[1 - \sqrt{\frac{3|g|}{4\omega^3}}\int d\tau\, y_0'(\tau)y(\tau)\right]. \tag{17.333}$$

After expanding, in the path integral, the exponential $e^{-(\mathcal{A}_{\rm fl}^{\rm int}+\mathcal{A}_e^{\rm eff})/\hbar}$ in powers of the interaction up to the second order, a perturbative evaluation of the correlation functions of the fluctuations $y(\tau)$ according to the rules of Section 3.20 yields a correction factor

$$C = \left[1 + (I_1+I_2+I_3)\frac{|g|\hbar}{\omega^3} + \mathcal{O}(g^2)\right], \tag{17.334}$$

with the same τ-integrals as in Eqs. (17.217), (17.219), (17.223), and (17.224), after replacing g by $|g|$. The correction parameter C has again a diagrammatic expansion (17.225), where the vertices stand for the same analytic expressions as in Fig. 17.5, except for the third vertex, which is now

$$\sqrt{\frac{3|g|}{4\omega^3}}y_0'(\tau). \tag{17.335}$$

The lines represent the subtracted Green function

$$G'_{\mathcal{O}_\omega}(\tau,\tau') = \langle y(\tau)y(\tau')\rangle_{\mathcal{O}_\omega} = \hbar\mathcal{O}_\omega^{-1}(\tau,\tau'), \tag{17.336}$$

where $\mathcal{O}_\omega^{-1}(\tau,\tau')$ is the inverse of the functional matrix (17.332).

In contrast to the level splitting calculation in Section 17.8, only the integral I_1 requires a subtraction,

$$I_1 = \frac{3\omega^3}{4\hbar^2}\int d\tau\, G'^2_{\mathcal{O}_\omega}(\tau,\tau) = L\frac{3\omega}{16} + \frac{3\omega^3}{4\hbar^2}\int d\tau\,\left[G'^2_{\mathcal{O}_\omega}(\tau,\tau) - \frac{\hbar^2}{4\omega^2}\right], \tag{17.337}$$

and Eq. (17.334) assumes that I_1 is subtracted, i.e., I_1 should be replaced by $I_1' \equiv I_1 - L3\omega/16$. The correction factor for the tunneling rate reads, therefore,

$$C' = \left[1 + (I_1'+I_2+I_3)\frac{|g|\hbar}{\omega^3} + \mathcal{O}(g^2)\right]. \tag{17.338}$$

The subtracted integral contributes only to the real part of the ground state energy which we know to be $(1/2 + 3g\hbar/16\omega^3)\hbar\omega$.

As in Section 17.8, the explicit Green function $G'_{\mathcal{O}_\omega}(\tau,\tau')$ is found from the amplitude (17.227). By a change of variables $x=\omega\tau$ and $\hbar^2/2\mu=\omega^2$, setting $s=2$, the Schrödinger operator in (17.226) coincides with that in (17.212), provided we set $E_{\mathcal{RM}}=0$. The amplitude (17.227) then yields the Green functions for $\tau>\tau'$

$$G_{\mathcal{O}_\omega}(\tau,\tau')=\frac{\hbar}{2\omega}\Gamma(m-2)\Gamma(m+3)\times P_2^{-m}(\tanh\omega\tau)P_2^{-m}(-\tanh\omega\tau'), \quad (17.339)$$

with $m=1$. Due to translational invariance along the τ-axis, this Green function has a pole at $E_{\mathcal{RM}}=0$ [just like the Green function (17.229)]. The pole must be removed before going to this energy, and the result is the subtracted Green function $G'_{\mathcal{O}_\omega}(\tau,\tau')$, given by

$$G'_{\mathcal{O}_\omega}(\tau,\tau')=\frac{1}{2m}\frac{d}{dm}(m^2-1)G_{\mathcal{O}_\omega}(\tau,\tau')\bigg|_{m=1}. \quad (17.340)$$

Using (17.231), we find the subtracted Green function

$$G'_{\mathcal{O}_\omega}(\tau,\tau')=\hbar[Y_0(\tau_>)y_0(\tau_<)+y_0(-\tau_>)Y_0(-\tau_<)], \quad (17.341)$$

with

$$y_0(\tau)=2\sqrt{\frac{3\omega}{2}}P_2^{-1}(-\tanh\omega\tau)=-\sqrt{\frac{3\omega}{2}}\frac{\sinh\omega\tau}{\cosh^2\omega\tau}, \quad (17.342)$$

$$\begin{aligned} Y_0(\tau) &= \sqrt{\frac{2}{3\omega}}\frac{1}{8\omega m}\left\{\frac{1}{2}\left[\frac{d}{dm}(m^2-1)\Gamma(m-2)\Gamma(m+3)\right]P_2^{-m}(\tanh\omega\tau)\right. \\ &\quad \left.+\left[(m^2-1)\Gamma(m-2)\Gamma(m+3)\right]\frac{d}{dm}P_2^{-m}(\tanh\omega\tau)\right\}\bigg|_{m=1} \\ &= -\sqrt{\frac{2}{3\omega^3}}\left[\frac{3}{4}\frac{1}{\cosh\omega\tau}+\left(-\frac{3}{4}\omega\tau-\frac{1}{8}\right)\frac{\sinh\omega\tau}{\cosh^2\omega\tau}-\frac{1}{4}e^{-\omega\tau}\right]. \end{aligned} \quad (17.343)$$

For $\tau=\tau'$

$$G'_{\mathcal{O}_\omega}(\tau,\tau) = \frac{\hbar}{2\omega}\frac{1}{\cosh^2\omega\tau}(\cosh^2\omega\tau-1)(\cosh^2\omega\tau-1/2). \quad (17.344)$$

The evaluation of the integrals $I_1', I_{21}, I_{22}, I_3$ proceeds as in Section 17.8 (performed in Appendix 17A), yielding [7]

$$I_1'=-\frac{11\cdot 29}{2^4\cdot 5\cdot 7}, \quad I_{21}=-\frac{71}{2^5\cdot 3\cdot 7}, \quad I_{22}=\frac{3\cdot 13}{2^4\cdot 7}, \quad I_3=-\frac{53}{2^4\cdot 5}. \quad (17.345)$$

The correction factor (17.338) is therefore

$$C'=\left[1-\frac{95}{72}\frac{3|g|\hbar}{4\omega^3}+\mathcal{O}(g^2)\right]. \quad (17.346)$$

Using the one-to-one correspondence between (17.289) and (17.301), this yields the large-k behavior of the expansion coefficients of the ground state energy:

$$E_k^{(0)}=-\frac{\omega}{\pi}\sqrt{\frac{6}{\pi}}(-3/\omega^3)^k\Gamma(k+1/2)[1-95/72k+\ldots]. \quad (17.347)$$

17.10.4 Variational Approach to Tunneling. Perturbation Coefficients to All Orders

The semiclassical calculations of tunneling amplitudes are valid only for very high barriers. It is possible to remove this limitation with the help of a variational approach [8] similar to the one described in Chapter 5. For simplicity, we discuss here only the case of an anharmonic oscillator at zero temperature. For the lowest energy levels we shall derive highly accurate imaginary parts over the entire left-hand cut in the coupling constant plane. The accuracy can be tested by inserting these imaginary parts into the dispersion relation (17.329) to recover the perturbation coefficients of the energies. These turn out to be in good agreement with the exact ones to all orders.

For the path integral of the anharmonic oscillator

$$Z(g) = \int \mathcal{D}x(\tau) \exp\left\{ - \int_{-L/2}^{L/2} d\tau \, \left[\frac{1}{2} x'^2 + \frac{\omega^2}{2} x^2 + \frac{g}{4} x^4 \right] \right\}, \tag{17.348}$$

the variational energy (5.32) at zero temperature is given by

ref(5.32)
lab(5.36)
est(5.43)

$$W_1 = \frac{\Omega}{2} + \frac{\omega^2 - \Omega^2}{2} a^2 + \frac{3g}{4} a^4, \tag{17.349}$$

with $a^2 = 1/2\Omega$. We have omitted the path average argument x_0 since, by symmetry of the potential, the minimum lies at $x_0 = 0$. The energy has to be extremized in Ω^2. This yields the cubic equation $\Omega^3 - \omega^2 \Omega - 3g/2 = 0$. The physically relevant solution starts out with ω at $g = 0$ and has two branches: For $g \in (-g^{(0)}, 0)$ with $g^{(0)} = 4\omega^3/9\sqrt{3}$ [compare (5.163)], it is given by

$$\Omega = \frac{2\omega}{\sqrt{3}} \cos\left[\frac{\pi}{3} - \frac{1}{3} \arccos\left(-g/g^{(0)}\right) \right]. \tag{17.350}$$

For large negative coupling constants $g < -g^{(0)}$, the solution is

$$\Omega^{\rm re} = \frac{\omega}{\sqrt{3}} \cosh(\gamma/3), \quad \Omega^{\rm im} = \omega \sinh(\gamma/3); \qquad \gamma = \operatorname{arcosh}\left(-g/g^{(0)}\right). \tag{17.351}$$

In this regime, the ground state energy acquires an imaginary part

$$\operatorname{Im} W_1 = \frac{1}{4} \Omega^{\rm i} (1 - 1/|\Omega|^2) - \frac{3g}{4} \Omega^{\rm re} \Omega^{\rm im} / 2|\Omega|^4. \tag{17.352}$$

This imaginary part describes the instability of the system to *slide* down into the two abysses situated at large positive and negative x. In this regime of coupling constants, the barriers to the right and left of the origin are no obstacle to the decay since they are smaller than the zero-point energy.

In the first regime of small negative coupling constants $g \in (-g^{(0)}, 0)$, the barriers are high enough to prevent at least one long-lived ground state from sliding down. Its energy is approximately given by the minimum of (17.349). It can decay towards

the abysses via an extremal excursion across the trial potential $\Omega^2 x^2/2 + gx^4/4$. The associated bubble solution reads, according to (17.308),

$$x(\tau) = x_{\rm cl}(\tau) \equiv \pm\sqrt{2\Omega^2/|g|}\frac{1}{\cosh[\Omega(\tau-\tau_0)]}. \tag{17.353}$$

It has the action $\mathcal{A}_{\rm cl} = 4\Omega^3/3|g|$. Its fluctuation determinant is given by (17.315), if ω is replaced by the trial frequency Ω. Translations contribute a factor $\beta\Omega\sqrt{\mathcal{A}_{\rm cl}/2\pi}$. Thus, the partition function has an imaginary part

$$\mathrm{Im}\, Z(-|g| - i\eta) = \beta\Omega\sqrt{\frac{6}{\pi}}\sqrt{\frac{4\Omega^3}{3|g|}}e^{-\beta\Omega/2 - 4\Omega^3/3|g|}. \tag{17.354}$$

In the variational approach, this replaces the semiclassical expression (17.316), which will henceforth be denoted by $Z^{\rm im}_{\rm sc}(g)$.

The expression (17.354) receives fluctuation corrections. To lowest order, they produce a factor $\exp(-\langle \mathcal{A}^{\rm int}_{\rm fl,tot}\rangle_{\mathcal{O}_\Omega})$, where the action $\mathcal{A}^{\rm int}_{\rm fl,tot}$ contains the interaction terms (17.215) and (17.213) of the fluctuations, with ω replaced by Ω, plus additional terms arising from the variational ansatz. They compensate for the fact that we are using the trial potential $\Omega^2 x^2/2$ rather than the proper $\omega^2 x^2/2$ as the zeroth-order potential for the perturbation expansion. These compensation terms have the action

$$\begin{aligned}\mathcal{A}^{\rm int}_{\rm fl,var} &= \int_{-\infty}^{\infty} d\tau\, \frac{\omega^2-\Omega^2}{2} x^2(\tau) \\ &= \int_{-\infty}^{\infty} d\tau\, \frac{\omega^2-\Omega^2}{2}[x^2_{\rm cl}(\tau) + 2x_{\rm cl}(\tau)y(\tau) + y^2(\tau)].\end{aligned} \tag{17.355}$$

The expectations $\langle \ldots\rangle_{\mathcal{O}_\Omega}$ in the perturbation correction are calculated with respect to fluctuations governed by the operator (17.332), in which ω is replaced by Ω. As before, all correlation functions are expanded by Wick's rule into sums of products of the simple correlation functions $G'_{\mathcal{O}_\Omega}(\tau,\tau')$ of (17.336). Using the integral formula (17.54), we have

$$\int_{-\infty}^{\infty} d\tau\, x^2_{\rm cl}(\tau) = 4\Omega/|g|. \tag{17.356}$$

The expectation of $\int_{-\infty}^{\infty} d\tau\, y(\tau)^2$ is found with the help of (17.344) as

$$\begin{aligned}\int_{-\infty}^{\infty} d\tau\, \langle y^2(\tau)\rangle_{\mathcal{O}_\Omega} &= L\frac{1}{2\Omega} + \frac{1}{\Omega}\int_{-\infty}^{\infty} d\tau\, \left[G'_{\mathcal{O}_\Omega}(\tau,\tau) - 1/2\right] \\ &= L\frac{1}{2\Omega} - \frac{7}{6\Omega^2}.\end{aligned} \tag{17.357}$$

The second term can be obtained quite simply by differentiating the logarithm of (17.314) with respect to $\Omega^2 z$.

The linearly divergent term $L/2\Omega$ contributes to the earlier-calculated term proportional to L in the integral (17.337) (with ω replaced by Ω); together they yield

L-times W_1 of (17.349). Thus we can remove a factor e^{-LW_1} from $\mathrm{Im}\, Z$, write Z as $\approx \mathrm{Re}\, Z e^{\mathrm{Im}Z/\mathrm{Re}Z} = e^{-LW_1+\mathrm{Im}Z/\mathrm{Re}Z}$ [as in (17.275)], and deduce the imaginary part of the energy from the exponent.

We now go over to the cumulants in accordance with the rules of perturbation theory in Eqs. (3.483)–(3.487) involving the integrals (17.217) (with g and ω replaced by $|g|$ and Ω, respectively). Using (17.345) we find the correction factor $e^{-A_0-A_1}$ with

ref(3.483) lab(2.42cd4) est(3.175) ref(3.487) lab(3.fvers) est(3.179)

$$A_0 = \frac{95}{96}\frac{|g|}{\Omega^3}, \qquad A_1 = \frac{1}{2}(\omega^2-\Omega^2)\left(\frac{4\Omega}{|g|}-\frac{7}{6\Omega^2}\right). \tag{17.358}$$

If we want to find all terms contributing to the imaginary part up to the order g, we must continue the perturbation expansion to the next order. This yields a further factor

$$\exp\left\{\frac{1}{2}[\langle \mathcal{A}^{\mathrm{int}\,2}_{\mathrm{fl,tot}}\rangle_{\mathcal{O}_\Omega} - \langle \mathcal{A}^{\mathrm{int}}_{\mathrm{fl,tot}}\rangle^2_{\mathcal{O}_\Omega}]\right\} = \exp(-A_2-A_3-A_4), \tag{17.359}$$

with the integrals

$$\begin{aligned}
A_2 &= -\frac{1}{2}(\omega^2-\Omega^2)^2\int d\tau d\tau'\, x_{\mathrm{cl}}(\tau)\langle y(\tau)y(\tau')\rangle_{\mathcal{O}_\Omega} x_{\mathrm{cl}}(\tau'),\\
A_3 &= -(\omega^2-\Omega^2)\sqrt{\frac{3|g|}{4\Omega^3}}\int d\tau d\tau'\, y_0'(\tau)\langle y(\tau)y(\tau')\rangle_{\mathcal{O}_\Omega} x_{\mathrm{cl}}(\tau'),\\
A_4 &= (\omega^2-\Omega^2)|g|\int d\tau d\tau'\, x_{\mathrm{cl}}(\tau)\langle y(\tau)y^3(\tau')\rangle_{\mathcal{O}_\Omega} x_{\mathrm{cl}}(\tau').
\end{aligned} \tag{17.360}$$

Performing the Wick contractions in the correlation functions, the integrals are conveniently rewritten as

$$\begin{aligned}
A_2 &= -\frac{1}{2}(\omega^2-\Omega^2)^2\frac{1}{\Omega|g|}a_2,\\
A_3 &= -(\omega^2-\Omega^2)\frac{1}{\Omega^2}a_3,\\
A_4 &= (\omega^2-\Omega^2)\frac{1}{\Omega^2}a_4,
\end{aligned} \tag{17.361}$$

where a_2, a_3, a_4 are given by

$$\begin{aligned}
a_2 &= |g|\Omega\int d\tau d\tau'\, x_{\mathrm{cl}}(\tau)G'_{\mathcal{O}_\Omega}(\tau,\tau')x_{\mathrm{cl}}(\tau'),\\
a_3 &= \Omega^2\sqrt{\frac{3|g|}{4\Omega^3}}\int d\tau d\tau'\, y_0'(\tau)G'_{\mathcal{O}_\Omega}(\tau,\tau')x_{\mathrm{cl}}(\tau'),\\
a_4 &= 3|g|\Omega^2\int d\tau d\tau'\, x_{\mathrm{cl}}(\tau)G'_{\mathcal{O}_\Omega}(\tau,\tau')G'_{\mathcal{O}_\Omega}(\tau',\tau')x_{\mathrm{cl}}(\tau').
\end{aligned} \tag{17.362}$$

In terms of these, the imaginary part of the energy reads

$$\begin{aligned}
\mathrm{Im}\, E(-|g|-i\eta) = &-\Omega\sqrt{\frac{6}{\pi}}\sqrt{\frac{4\Omega^3}{3|g|}}e^{-4\Omega^3/3|g|-c_1 3|g|/4\Omega^3}\\
&\times\exp\left[-\frac{\omega^2-\Omega^2}{2}\left(\frac{4\Omega}{|g|}-\frac{7}{6\Omega^2}-2\frac{a_3-a_4}{\Omega^2}\right)+\frac{(\omega^2-\Omega^2)^2}{2\Omega|g|}a_2\right],
\end{aligned} \tag{17.363}$$

evaluated at the Ω-value (17.350).

To best visualize the higher-order effect of fluctuations, we factorize (17.363) into the semiclassical part (17.317) and a correction factor $\varepsilon_{\rm i}(g)$,

$$\mathrm{Im}\, E(-|g| - i\eta) = -\omega\sqrt{\frac{6}{\pi}}\sqrt{\frac{4\omega^3}{3|g|}}e^{-4\omega^3/3|g|}\varepsilon_{\rm i}(g), \tag{17.364}$$

where

$$\begin{aligned}\varepsilon_{\rm i}(g) &= \left(\frac{\Omega}{\omega}\right)^{5/2}\exp\Big[-4\frac{\Omega^3-\omega^3}{3|g|} - c_1\frac{3|g|}{4\Omega^3} \\ &- \frac{\omega^2-\Omega^2}{2}\left(\frac{4\Omega}{|g|} - \frac{7}{6\Omega^2} - 2\frac{a_3-a_4}{\Omega^2}\right) + \frac{(\omega^2-\Omega^2)^2}{2\Omega|g|}a_2\Big].\end{aligned} \tag{17.365}$$

The calculation of the integrals (17.362) proceeds as in Appendix 17A, yielding

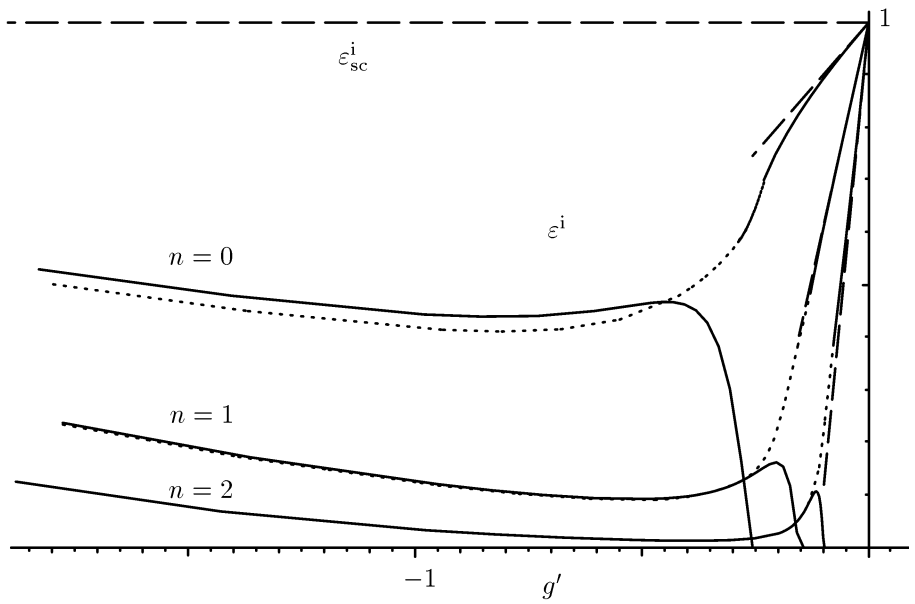

Figure 17.13 Reduced imaginary part of lowest three energy levels of anharmonic oscillator for negative couplings plotted against $g' \equiv g/\omega^3$. The semiclassical limit corresponds to $\varepsilon_{\rm i} \equiv 1$. The small-$|g'|$ branch is due to tunneling, the large-$|g'|$ branch to direct decay (sliding). Solid and dotted curves show the imaginary parts of the variational approximations W_1 and W_3, respectively; dashed straight lines indicate the exactly known slopes.

$a_2 = -1, a_3 = 3/4, a_4 = 1/12$.

The result is shown in Fig. 17.13. The slope of $\varepsilon_{\rm i}(g)$ at $g = 0$ maintains the first-order value $c_1 3/4 = 95/96$, i.e., the additional terms in the exponent of (17.365) cancel each other to first order in g.

There exists a short derivation of this result using the same method as in the
ref(5.190) derivation of Eq. (5.190). We take the fluctuation-corrected semiclassical approxi-
lab(5.r0)
est(5.149)

mation at the frequency ω

$$\operatorname{Im} E(-|g| - i\eta) = -\omega\sqrt{\frac{6}{\pi}}\sqrt{\frac{4\omega^3}{3|g|}}e^{-4\omega^3/3|g|-3c_1|g|/4\omega^3}, \tag{17.366}$$

move the ω-dependent prefactor into the exponent with the help of the logarithm, replace everywhere ω by $\sqrt{\Omega^2-(\Omega^2-\omega^2)}=\sqrt{\Omega^2-gr^2/2}$ with $r^2=2(\Omega^2-\omega^2)/g$, and expand the exponent in powers of g including all orders of g to which the exponent of (17.366) is known (treating r as a quantity of order unity). This leads again to (17.364) with (17.365).

The imaginary part is inserted into the dispersion relation (17.329) and yields for positive g the energy

$$E^{(0)}(g)=\frac{\omega}{2}+2\omega g\int_0^\infty\frac{d\lambda}{2\pi}\frac{1}{\lambda(\lambda+g)}\sqrt{\frac{6}{\pi}}\sqrt{\frac{4\omega^3}{3\lambda}}e^{-4\omega^3/3\lambda}\varepsilon_{\rm i}(\lambda). \tag{17.367}$$

Expanding the integrand in powers of g gives an integral formula for the perturbation coefficients analogous to (17.331). Its evaluation yields the numbers shown in Table 17.1. They are compared with exact previous larger-order values (17.319) which follow from $\varepsilon_{\rm i}\equiv 1$. The improvement of our knowledge on the imaginary part of the energy makes it possible to extend the previous large-order results to low orders. Even the lowest coefficient with $k=1$ is reproduced very well [9].

The high degree of accuracy of the low-order coefficients is improved further by going to the higher variational approximation W_3 of Eq. (5.192) and extracting from it the imaginary part $\operatorname{Im} W_3(0)$ at zero temperature [10]. When continuing the coupling constant g to the sliding regime, we obtain the dotted curve in Fig. 17.13. It merges rather smoothly into the tunneling branch at $g\approx -0.24$. Plotting the merging regime with more resolution, we find two closely lying intersections at $g'=-0.229$ and $g'=-0.254$. We choose the first of these to cross over from one branch to the other. After inserting the imaginary part into the integral (17.331), we obtain the fifth column in Table 17.1. For $k=1$, the accuracy is now better than 0.05%. To make the approximation completely consistent, the tunneling amplitude should also be calculated to the corresponding order. This would yield a further improvement in the low-order coefficients.

It is instructive to test the accuracy of our low-order results by evaluating the dispersion relation (17.367) for the g-dependent ground state energy $E^{(0)}(g)$. The results shown in Fig. 17.14 compare well with the exact curves. They are only slightly worse than the original Feynman-Kleinert approximation W_1 evaluated at positive values of g. We do not show the approximation W_3 since it is indistinguishable from the exact energy on this plot.

The approximation obtained from the dispersion relation has the advantage of possessing the properly diverging power series expansion and a reliable information on the analytic cut structure in the complex g-plane. Also here, the third-order result $E^{(0)}_{\rm var3+disp}$ based on the imaginary part of W_3 for $g<0$ is so accurate that it cannot be distinguished from the exact ones on the plot.

Table 17.1 Comparison between exact perturbation coefficients, semiclassical ones, and those obtained from moment integrals over the imaginary parts consisting of (17.363) in the tunneling regime and the analytic continuation of the variational approximations W_1 and W_3 in the sliding regime. An alternating sign $(-1)^{k-1}$ is omitted and ω is set equal to 1.

k	E_k	$E_k^{\rm sc}$	$E_k^{\rm var1+disp}$	$E_k^{\rm var3+disp}$
1	0.75	1.16954520	0.76306206	0.74932168
2	2.625	5.26295341	2.49885978	2.61462012
3	20.8125	39.4721506	18.3870038	20.7186128
4	241.289063	414.457581	205.886443	240.857317
5	3580.98047	5595.17734	3093.38043	3590.69587
6	63982.8135	92320.4261	57436.2852	64432.5387
7	1329733.73	1800248.43	1244339.99	1342857.03
8	31448214.7	40505587.0	30397396.0	31791078.0
9	833541603	1032892468	822446267	842273537
10	24478940700	29437435332	24420208763	24703889150

The strong-coupling behavior is well reproduced by our curves. Recall the limiting expression for the middle curve given in Eq. (5.77) and the exact one (5.226) with the coefficients of Table 5.9.

The calculation of the imaginary part in the sliding regime can be accelerated by removing from the perturbation coefficients the portion which is due to the imaginary part of the tunneling amplitude. By adding the energy associated with this portion in the form of a dispersion relation it is possible to find variational approximations which for positive coupling constants are not only numerically accurate but which also have power series expansions with the correct large-order behavior [which was not the case for the earlier approximations $W_N(g)$].

The entire treatment can be generalized to excited states. The variational energies are then replaced by the minima of the expressions derived in Section 5.19,

$$W_1^{(n)} = \Omega n_2 + \frac{\omega^2 - \Omega^2}{2}\frac{n_2}{\Omega} + \frac{g}{4}\frac{n_4}{\Omega^2}, \tag{17.368}$$

with $n_2 = n + 1/2$ and $n_4 = (3/2)(n^2 + n + 1/2)$. The optimal Ω-values are given by the solutions (17.350), (17.351), with $g^{(0)}$ replaced by $g^{(n)} = 2n_2/3\sqrt{3}n_4$. For $g \in (-g^{(n)}, 0)$, the energies are real; for $g < -g^{(n)}$ they possess the imaginary part

$$\mathrm{Im}\, W_1^{(n)} = \frac{1}{2}\Omega^{\rm i}\left(1 - \frac{\omega^2}{|\Omega|^2}\right)n_2 - \frac{g}{2}\Omega^{\rm re}\Omega^{\rm im}\frac{n_4}{|\Omega|^4}. \tag{17.369}$$

For $g \in (-g^{(n)}, 0)$, the imaginary part arises from the bubble solution. In the semiclassical limit it produces a factor $12^n \mathcal{A}_{\rm cl}^n/n!$ for $n > 0$ as in Eq. (17.322) (with ω replaced by Ω). Also here, the variational approach can easily be continued higher order approximations W_2, W_3, ...

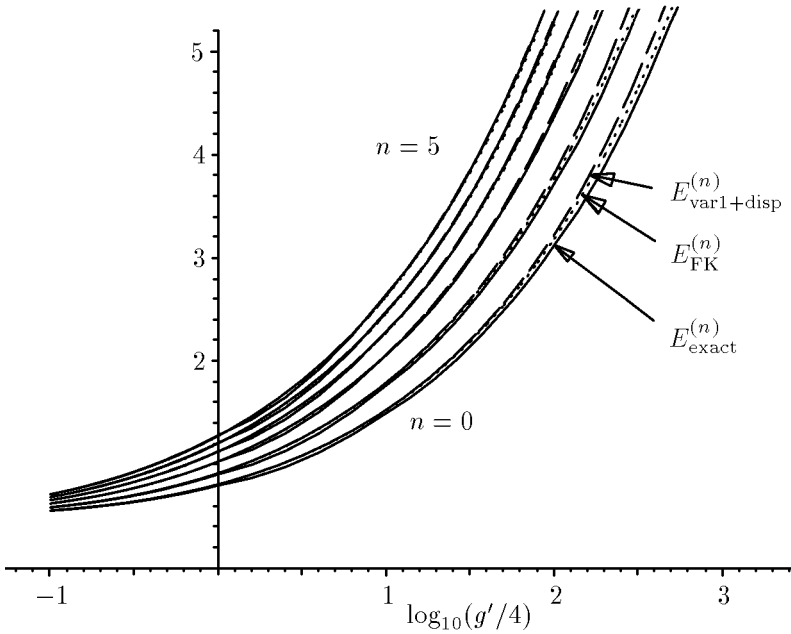

Figure 17.14 Energies of anharmonic oscillator as function of $g' \equiv g/\omega^3$, obtained from variational imaginary part, and the dispersion relation (17.328) as a function of the coupling constant g. Comparison is made with the exact curve and the Feynman-Kleinert variational energy for $g > 0$.

To first order in g, the imaginary part is known from a WKB calculation [11]. It reads

$$\mathrm{Im}\, E^{(n)}(-|g| - i\eta) = -\frac{12^n}{n!}\omega\sqrt{\frac{6}{\pi}}\sqrt{\frac{4\omega^3}{3|g|}}^{1+2n} e^{-4\omega^3/3|g| - c_1^{(n)} 3|g|/4\omega^3}, \tag{17.370}$$

with the slope parameter

$$c_1^{(n)} = \frac{d\,\varepsilon_{\rm i}^{(n)}}{d(g/\omega^3)} = \left(\frac{95}{96} + \frac{29}{16}n + \frac{17}{16}n^2\right)\omega^{-3}. \tag{17.371}$$

Following the procedure described after Eq. (17.366), we obtain from this a variational expression for the imaginary part which generalizes Eq. (17.364) to any n:

$$\mathrm{Im}\, E^{(n)}(-|g| - i\eta) = -\frac{12^n}{n!}\omega\sqrt{\frac{6}{\pi}}\sqrt{\frac{4\omega^3}{3|g|}}^{1+2n} e^{-4\omega^3/3|g|\,\varepsilon_{\rm i}^{(n)}(g)}, \tag{17.372}$$

with a correction factor

$$\begin{aligned}\varepsilon_{\rm i}^{(n)}(g) \;=\; & \left(\frac{\Omega}{\omega}\right)^{3n+5/2} \exp\Big[-4\frac{\Omega^3-\omega^3}{3|g|} - c_1^{(n)}\frac{3|g|}{4\Omega^3} \\ & - \frac{\omega^2-\Omega^2}{2}\left(\frac{4\Omega}{|g|} - \frac{3n+5/2}{\Omega^2}\right) - \frac{(\omega^2-\Omega^2)^2}{2\Omega|g|}\Big].\end{aligned} \tag{17.373}$$

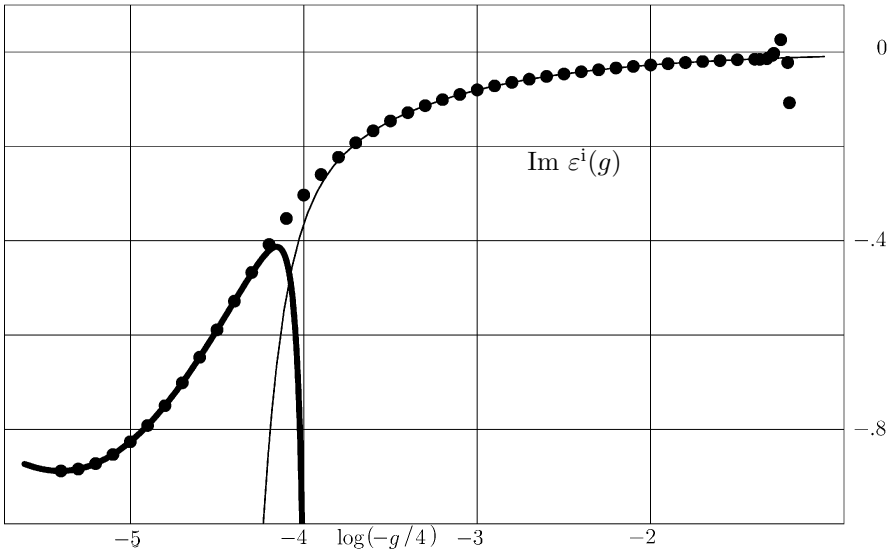

Figure 17.15 Reduced imaginary part of ground state energy of anharmonic oscillator from variational perturbation theory plotted for small negative g against $\log(-g/4)$. The fat curve is the analytic continuation of the strong-coupling expansion (5.226) with the expansion coefficients up to the 22nd order listed in Table 5.9. The thin curve is the divergent semiclassical expansion of the contribution of the classical solution in Eq. (17.374).

Inserting for Ω the optimal value $\Omega^{(n)}$, we obtain the solid curves shown in Fig. 17.13. Their slopes have the exact values (17.371).

The sliding regime for the excited states can be obtained from an analytic continuation of the variational energies. For $n = 1, 2$ the resulting imaginary parts are shown as dotted curves in Fig. 17.13. They merge smoothly with the corresponding tunneling branches obtained from W_1.

If we extend the variational evaluation of the perturbation expansions to high orders in g, we find the imaginary part over the left-hand cut extending deeper and deeper into the regime dominated by the classical solution and the fluctuations around it [10]. This is shown in the double-logarithmic plot of Fig. 17.15.

The result may be compared with the the divergent semiclassical expansion around the classical solution [13]

$$\log \varepsilon^{\rm i}(g) = -\frac{4}{3g} + k_1 \frac{g}{4} + k_2 \left(\frac{g}{4}\right)^2 + \dots \ . \tag{17.374}$$

also plotted in Fig. 17.15. The coefficients are listed in Table 17.2.

Table 17.2 Coefficients k_n of semiclassical expansion (17.374) around classical solution.

1	2	3	4	5
3.95833	19.3437500	174.2092014	2177.286133	34045.58329
6	7	8	9	10
632817.0536	1.357206×10^7	3.2924×10^8	8.92×10^9	2.65×10^{11}

The inclusion of finite temperatures is possible by summing over the imaginary parts of the energies weighted by a Boltzmann factor with these energies. This opens the road to applications in many branches of physics where tunneling phenomena are relevant.

It will be interesting to generalize this procedure to quantum field theories, where it can give rise to the development of much more efficient resummation techniques for perturbation series. One will be able to set up system-dependent basis functions in terms of which these series possess a convergent re-expansion. The critical exponents of the O(N)-symmetric φ^4-theory should then be calculable from the presently known five-loop results [14] with a much greater accuracy than before.

17.10.5 Convergence of Variational Perturbation Expansion

The knowledge of the discontinuity across the left-hand makes it possible to understand roughly the convergence properties of the variational perturbation expansion developed in Section 5.14. The ground state energy satisfies the subtracted dispersion relation [compare (17.299)]

$$E^{(0)}(g) = \frac{\omega}{2} - \frac{g}{2\pi i}\int_0^{-\infty} \frac{dg'}{g'} \frac{\text{disc}\, E^{(0)}(g')}{g'-g}, \tag{17.375}$$

where $\text{disc}\, E^{(0)}(g')$ denotes the discontinuity across the left-hand cut in the complex g-plane. An expansion of the integrand in powers of g yields the perturbation series

$$E^{(0)}(g) = \omega \sum_{k=0}^{N} E_k^{(0)} \left(\frac{g}{4\omega^3}\right)^k. \tag{17.376}$$

The associated variational energy has the form [compare (5.206)]

$$W_N^{\Omega}(g) = \Omega \sum_{k=0}^{N} \varepsilon_k^{(0)} \left(\frac{g}{4\Omega^3}\right)^k. \tag{17.377}$$

It is obtained from (17.376) by the replacement (5.188) and a re-expansion in powers of g. In the present context, we write this replacement as

$$\omega \longrightarrow \Omega(1-\sigma\hat{g})^{1/2}, \tag{17.378}$$

where $\hat{g}$ is the dimensionless coupling constant g/Ω^3, and

$$\sigma = \Omega(\Omega^2-1)/g \tag{17.379}$$

[recall Eqs. (5.213) and (5.208)].

There is a simple way of obtaining the same re-expansion from the dispersion relation (17.375). Introducing the dimensionless coupling constant $\bar{g} \equiv g/\omega^3$, the replacement (17.378) amounts to

$$\bar{g} \longrightarrow \tilde{g}(\hat{g}) \equiv \frac{\hat{g}}{(1-\sigma\hat{g})^{3/2}}. \tag{17.380}$$

Since Eq. (17.375) represents an energy, it can be written as ω times a dimensionless function of $\bar{g}$. Apart from the replacement (17.380) in the argument, it receives an overall factor $\Omega/\omega = (1-\sigma\hat{g})^{1/2}$. We introduce the reduced energies

$$\hat{E}(\hat{g}) \equiv E(g)/\Omega, \tag{17.381}$$

which depends only on the reduced coupling constant $\hat{g}$, the dispersion relation (17.375) for $E^{(0)}(g)$ implies a dispersion relation for $\hat{E}^{(0)}(\hat{g})$:

$$\hat{E}^{(0)}(g) = (1-\sigma\hat{g})^{1/2}\left[\frac{1}{2} + \frac{\tilde{g}(\hat{g})}{2\pi i}\int_0^{-\infty}\frac{d\bar{g}'}{\bar{g}'}\frac{\mathrm{disc}\,\bar{E}^{(0)}(\bar{g}')}{\bar{g}'-\tilde{g}(\hat{g})}\right]. \tag{17.382}$$

The resummed perturbation series is obtained from this by an expansion in powers of $\hat{g}/4$ up to order N.

It should be emphasized that only the truncation of the expansion causes a difference between the two expressions (17.375) and (17.382), since $\bar{g}$ and $\tilde{g}$ are the same numbers, as can be verified by inserting (17.379) into the right-hand side of (17.380).

To find the re-expansion coefficients we observe that the expression (17.382) satisfies a dispersion relation in the complex $\hat{g}$-plane. If C denotes the cuts in this plane and $\mathrm{disc}_C E(\hat{g})$ is the discontinuity across these cuts, the dispersion relation reads

$$\hat{E}^{(0)}(\hat{g}) = \frac{1}{2} + \frac{\hat{g}}{2\pi i}\int_C \frac{d\hat{g}'}{\hat{g}'}\frac{\mathrm{disc}_C\hat{E}^{(0)}(\hat{g}')}{\hat{g}'-\hat{g}}. \tag{17.383}$$

We have changed the argument of the energy from $\bar{g}$ to $\hat{g}$ since this will be the relevant variable in the sequel.

When expanding the denominator in the integrand in powers of $\hat{g}/4$, the expansion coefficients $\varepsilon_l^{(0)}$ are found to be moment integrals with respect to the inverse coupling constant $1/\hat{g}$ [compare (17.302)]:

$$\varepsilon_k^{(0)} = -\frac{4^k}{2\pi i}\int_C \frac{d\hat{g}}{\hat{g}^{k+1}}\mathrm{disc}_C\hat{E}^{(0)}(\hat{g}). \tag{17.384}$$

In the complex $\hat{g}$-plane, the integral (17.382) has in principle cuts along the contours $C_1, C_{\bar{1}}, C_2, C_{\bar{2}}$, and C_3, as shown in Fig. 17.16. The first four cuts are the images of the left-hand cut in the complex g-plane; the curve C_3 is due to the square root of $1-\sigma\hat{g}$ in the mapping (17.380) and the prefactor of (17.382).

Let $\bar{D}(\bar{g})$ abbreviate the reduced discontinuity in the original dispersion relation (17.375):

$$\bar{D}(\bar{g}) \equiv \mathrm{disc}\;\bar{E}^{(0)}(\bar{g}) = 2i\mathrm{Im}\,\bar{E}^{(0)}(\bar{g}-i\eta), \quad \bar{g}\le 0. \tag{17.385}$$

Then the discontinuities across the various cuts are

$$\underset{C_{1,\bar{1},2,\bar{2}}}{\mathrm{disc}}\;\hat{E}^{(0)}(\hat{g}) \;=\; (1-\sigma\hat{g})^{1/2}\bar{D}(\hat{g}(1-\sigma\hat{g})^{-3/2}), \tag{17.386}$$

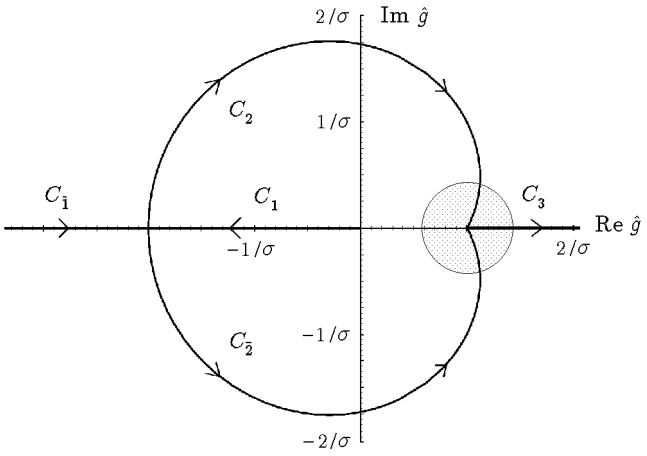

Figure 17.16 Cuts in complex $\hat{g}$-plane whose moments with respect to inverse coupling constant determine re-expansion coefficients. The cuts inside the shaded circle happen to be absent due to the convergence of the strong-coupling expansion for $g > g_{\rm s}$.

$$\begin{aligned} \operatorname*{disc}_{C_3} \hat{E}^{(0)}(\hat{g}) &= -2i(\sigma\hat{g}-1)^{1/2} \\ &\quad \times\Big[\frac{1}{2} - \int_0^\infty \frac{d\bar{g}'}{2\pi}\frac{\hat{g}(\sigma\hat{g}-1)^{-3/2}}{\bar{g}'^2+\hat{g}^2(\sigma\hat{g}-1)^{-3}}\bar{D}(-\bar{g}')\Big]. \end{aligned} \tag{17.387}$$

For small negative $\bar{g}$, the discontinuity is given by the semiclassical limit (17.317):

$$\bar{D}\bar{g}) \approx -2i\sqrt{\frac{6}{\pi}}\sqrt{\frac{4}{-3\bar{g}}}e^{4/3\bar{g}}. \tag{17.388}$$

We denote by $\varepsilon_k^{(0)}(C_i)$ the contributions of the different cuts to the integral (17.384) for the coefficients. After inserting (17.388) into Eq. (17.386), we obtain from the cut along C_1 the semiclassical approximation

$$\varepsilon_k^{(0)}(C_1) \approx -2\,4^k \int_{C_1}\frac{d\hat{g}}{2\pi}\frac{1}{\hat{g}^{k+1}}\sqrt{\frac{6}{\pi}}\sqrt{-\frac{4(1-\sigma\hat{g})^{5/2}}{3\hat{g}}}e^{4(1-\sigma\hat{g})^{3/2}/3\hat{g}}. \tag{17.389}$$

For the kth term S_k of the series this yields an estimate

$$S_k \propto \left[\int_{C_\gamma}\frac{d\gamma}{2\pi}e^{f_k(\gamma)}\right](\sigma\hat{g})^k, \tag{17.390}$$

where $f_k(\gamma)$ is the function of $\gamma \equiv \sigma\hat{g}$

$$f_k(\gamma) = -\left(k+\frac{3}{2}\right)\log(-\gamma) + \frac{4\sigma}{3\gamma}(1-\gamma)^{3/2}. \tag{17.391}$$

For large k, the integral may be evaluated via the saddle point approximation of Subsection 4.2.1. The extremum of $f_k(\gamma)$ satisfies the equation

$$-k+\frac{3}{2} = \frac{4\sigma}{3\gamma}(1-\gamma)^{1/2}\left(1+\tfrac{1}{2}\gamma\right), \tag{17.392}$$

which is solved by

$$\gamma \xrightarrow[k\to\infty]{} \gamma_k = -4\sigma/3k. \tag{17.393}$$

At the extremum, $f_k(\gamma)$ has the value

$$f_k \xrightarrow[k\to\infty]{} k\log(3k/4e\sigma) - 2\sigma. \tag{17.394}$$

The constant -2σ in this limiting expression arises when expanding the second term of Eq. (17.391) into a Taylor series, $(4\sigma/3\gamma)(1-\gamma)^{3/2} = 4\sigma/3\gamma_k - 2\sigma + \dots$. Only the first two terms survive the large-k limit.

Thus, to leading order in k, the kth term of the re-expanded series becomes

$$S_k \propto e^{-2\sigma}\left(\frac{-3k}{e}\right)^k \left(\frac{\hat{g}}{4}\right)^k. \tag{17.395}$$

The corresponding re-expansion coefficients are

$$\varepsilon_k^{(0)} \propto e^{-2\sigma} E_k^{(0)}. \tag{17.396}$$

They have the remarkable property of growing in precisely the same manner with k as the initial expansion coefficients $E_k^{(0)}$, except for an overall suppression factor $e^{-2\sigma}$. This property was found empirically in Fig. 5.20b.

In order to estimate the convergence of the variational perturbation expansion, we note that with

$$\sigma = \frac{\Omega(\Omega^2-1)}{g} \tag{17.397}$$

and $\hat{g}$ from (5.213), we have

$$\sigma\hat{g} = 1 - \frac{1}{\Omega^2}. \tag{17.398}$$

For large Ω, this expression is smaller than unity. Hence the powers $(\sigma\hat{g})^k$ alone yield a convergent series. An optimal re-expansion of the energy can be achieved by choosing, for a given large maximal order N of the expansion, a parameter σ proportional to N:

$$\sigma \approx \sigma_N \equiv cN. \tag{17.399}$$

Inserting this into (17.391), we obtain for large $k = N$

$$f_N(\gamma) \approx N\left[-\log(-\gamma) + \frac{4c}{3\gamma}(1-\gamma)^{3/2}\right]. \tag{17.400}$$

The extremum of this function lies at

$$1 + \frac{4c}{3\gamma}(1-\gamma)^{1/2}(1+\tfrac{1}{2}\gamma) = 0. \tag{17.401}$$

The constant c is now chosen in such a way that the large exponent proportional to N in the exponential function $e^{f_N(\gamma)}$ due to the first term in (17.400) is canceled by an equally large contribution from the second term, i.e., we require at the extremum

$$f_N(\gamma) = 0. \tag{17.402}$$

The two equations (17.401) and (17.402) are solved by

$$\gamma = -0.242\,964\,029\,973\,520\ldots, \qquad c = 0.186\,047\,272\,987\,975\ldots\,. \tag{17.403}$$

In contrast to the extremal γ in Eq. (17.393) which dominates the large-k limit, the extremal γ of the present limit, in which k is also large but of the order of N, remains finite (the previous estimate holds for $k \gg N$). Accordingly, the second term $(4c/3\gamma)(1-\gamma)^{3/2}$ in $f_N(\gamma)$ contributes in full, not merely via the first two Taylor expansion terms of $(1-\gamma)^{3/2}$, as it did in (17.394).

Since $f_N(\gamma)$ vanishes at the extremum, the Nth term in the re-expansion has the order of magnitude

$$S_N \propto (\sigma_N \hat{g}_N)^N = \left(1 - \frac{1}{\Omega_N^2}\right)^N. \tag{17.404}$$

According to (17.397) and (17.399), the frequency Ω_N grows for large N like

$$\Omega_N \sim \sigma_N^{1/3} g^{1/3} \sim (cNg)^{1/3}. \tag{17.405}$$

As a consequence, the last term of the series decreases for large N like

$$S_N(C_1) \propto \left[1 - \frac{1}{(\sigma_N g)^{2/3}}\right]^N \approx e^{-N/(\sigma g)^{2/3}} \approx e^{-N^{1/3}/(cg)^{2/3}}. \tag{17.406}$$

This estimate does not yet explain the convergence of the variational perturbation expansion in the strong-coupling limit observed in Figs. 5.21 and 5.22. For the contribution of the cut C_1 to S_N, the derivation of such a behavior requires including a little more information into the estimate. This information is supplied by the empirically observed property, that the best Ω_N-values lie for finite N on a curve [recall Eq. (5.211)]:

$$\sigma_N \sim cN\left(1 + \frac{6.85}{N^{2/3}}\right). \tag{17.407}$$

Thus the asymptotic behavior (17.399) receives, at a finite N, a rather large correction. By inserting this σ_N into $f_N(\gamma)$ of (17.400), we find an extra exponential factor

$$\begin{aligned} e^{\Delta f_N} &\approx \exp\left[N\frac{4c}{3}\frac{(1-\gamma)^{3/2}}{\gamma}\frac{6.85}{N^{2/3}}\right] \\ &= \exp\left[-N\log(-\gamma)\frac{6.85}{N^{2/3}}\right] \approx e^{-9.7N^{1/3}}. \end{aligned} \tag{17.408}$$

This reduces the size of the last term due to the cut C_1 in (17.406) to

$$S_N(C_1) \propto e^{-[9.7+(cg)^{-2/3}]N^{1/3}}, \tag{17.409}$$

which agrees with the convergence seen in Figs. 5.21 and 5.22.

There is no need to evaluate the effect of the shift in the extremal value of γ caused by the correction term in (17.407), since this would be of second order in $1/N^{2/3}$.

How about the contributions of the other cuts? For $C_{\bar{1}}$, the integrals in (17.384) run from $\hat{g} = -2/\sigma$ to $-\infty$ and decrease like $(-2/\sigma)^{-k}$. The associated last term $S_N(C_{\bar{1}})$ is of the negligible order $e^{-N \log N}$. For the cuts $C_{2,\bar{2},3}$, the integrals (17.384) start at $\hat{g} = 1/\sigma$ and have therefore the leading behavior

$$\varepsilon_k^{(0)}(C_{2,\bar{2},3}) \sim \sigma^k. \tag{17.410}$$

This implies a contribution to the Nth term in the re-expansion of the order of

$$S_N(C_{2,\bar{2},3}) \sim (\sigma\hat{g})^N, \tag{17.411}$$

which decreases merely like (17.406) and does not explain the empirically observed convergence in the strong-coupling limit. As before, an additional information produces a better estimate. The cuts in Fig. 17.16 do not really reach the point $\sigma\hat{g} = 1$. There exists a small circle of radius $\Delta\hat{g} > 0$ in which $\hat{E}^{(0)}(\hat{g})$ has no singularities at all. This is a consequence of the fact unused up to this point that the strong-coupling expansion (5.231) converges for $g > g_s$. For the reduced energy, this expansion reads:

$$\hat{E}^{(0)}(\hat{g}) = \left(\frac{\hat{g}}{4}\right)^{1/3} \left\{ \alpha_0 + \alpha_1 \left[\frac{\hat{g}}{4\omega^3}\frac{1}{(1-\sigma\hat{g})^{3/2}}\right]^{-2/3} + \alpha_2 \left[\frac{\hat{g}}{4\omega^3}\frac{1}{(1-\sigma\hat{g})^{3/2}}\right]^{-4/3} + \dots \right\}. \tag{17.412}$$

The convergence of (5.231) for $g > g_s$ implies that (17.412) converges for all $\sigma\hat{g}$ in a neighborhood of the point $\sigma\hat{g} = 1$ with a radius

$$\Delta(\sigma\hat{g}) \sim \left(\frac{\hat{g}}{-\bar{g}_s}\right)^{2/3} = \left\{\frac{1}{-\sigma\bar{g}_s}[1+\Delta(\sigma\hat{g})]\right\}^{2/3}, \tag{17.413}$$

where $\bar{g}_s \equiv g_s/\omega^3$. For large N, $\Delta(\sigma\hat{g})$ goes to zero like $1/(N|\bar{g}s|c)^{2/3}$. Thus the integration contours of the moment integrals (17.384) for the contributions $\varepsilon_k^{(0)}(C_i)$ of the other cuts do not begin at the point $\sigma\hat{g} = 1$, but a little distance $\Delta(\sigma\hat{g})$ away from it. This generates an additional suppression factor

$$(\sigma\hat{g})^{-N} \sim [1+\Delta(\sigma\hat{g})]^{-N}. \tag{17.414}$$

Let us set $-\bar{g}_s = |\bar{g}_s|\exp(i\varphi_s)$ and $x_s \equiv (-\hat{g}/\bar{g}_s)^{2/3} = -|x_s|\exp(i\theta)$, and introduce the parameter $a \equiv 1/[|\bar{g}_s|c]^{2/3}$. Since there are two complex conjugate contributions we obtain, for large N a last term of the re-expanded series the order of

$$S_N(C_{2,\bar{2},3}) \approx e^{-N^{1/3}a\cos\theta}\cos(N^{1/3}a\sin\theta). \tag{17.415}$$

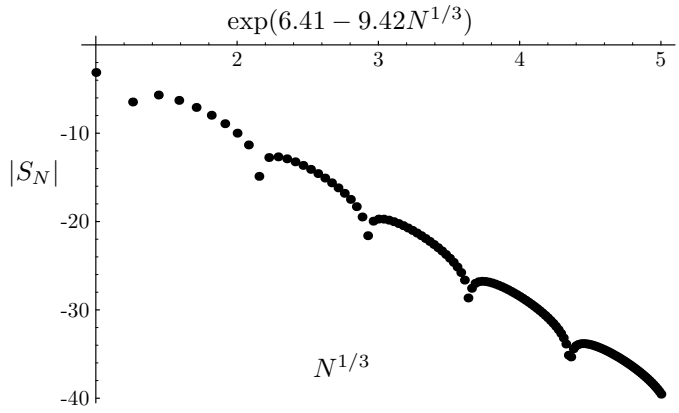

Figure 17.17 Theoretically obtained convergence behavior of Nth approximants for α_0, to be compared with the empirically found behavior in Fig. 5.21.

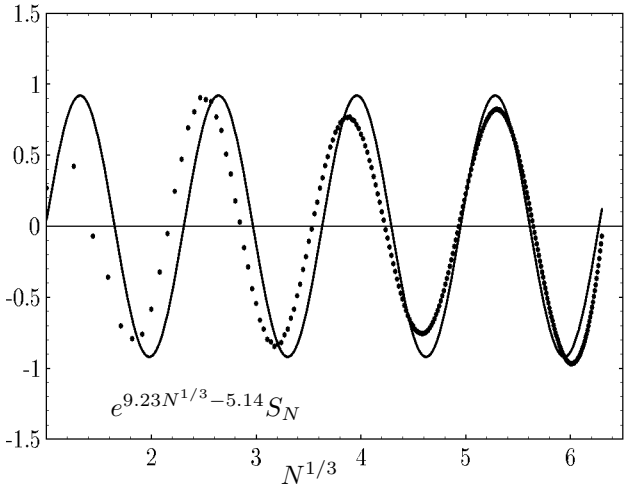

Figure 17.18 Theoretically obtained oscillatory behavior around exponentially fast asymptotic approach of α_0 to its exact value as a function of the order N of the approximant, to be compared with the empirically found behavior in Fig. 5.22, averaged between even and odd orders.

By choosing

$$|\bar{g}_{\rm s}| \sim 0.160, \qquad \theta \sim -0.467, \tag{17.416}$$

we obtain the curves shown in Figs. 17.17 and 17.18 which agree very well with the observed Figs. 5.21 and 5.22. Their envelope has the asymptotic falloff $e^{-9.23N^{1/3}}$.

Let us see how the positions of the leading Bender-Wu singularities determined by (17.416) compare with what we can extract directly from the strong-coupling series (5.231) up to order 22. For a pair of square root singularities at $x_{\rm s} = -|x_{\rm s}| \exp(\pm i\theta)$, the coefficients of a power series $\sum \alpha_n x^n$ have the asymptotic ratios $R_n \equiv \alpha_{n+1}/\alpha_n \sim$

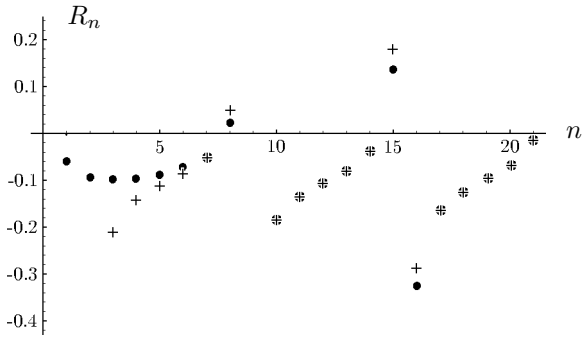

Figure 17.19 Comparison of ratios R_n between successive expansion coefficients of strong-coupling expansion (dots) with ratios $R_n^{\rm as}$ of expansion of superposition of two singularities at $g = 0.156 \times \exp(\pm 0.69)$ (crosses).

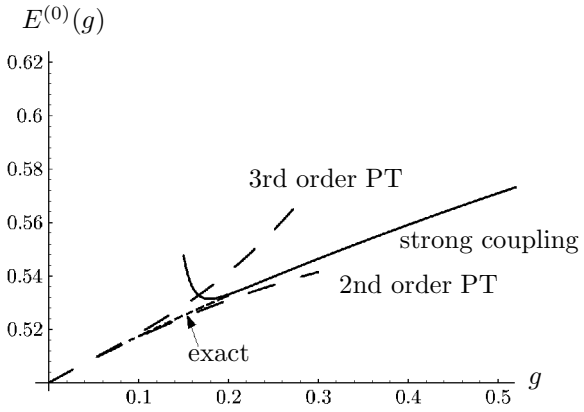

Figure 17.20 Strong-coupling expansion of ground state energy in comparison with exact values and perturbative results of 2nd and 3rd order. The convergence radius in $1/g$ is larger than $1/0.2$.

$R_n^{\rm as} \equiv -\cos[(n+1)\theta+\delta]/|x_{\rm s}|\cos(n\theta+\delta)$. In Fig. 17.19 we have plotted these ratios against the ratios R_n obtained from the coefficients α_n of Table 5.9 . For large n, the agreement is good if we choose

$$|x_{\rm s}| = 1/0.117, \quad \theta = -0.467, \tag{17.417}$$

with an irrelevant phase angle $\delta = -0.15$. The angle θ is in excellent agreement with the value found in (17.416). From $|x_{\rm s}|$ we obtain $|\bar{g}_{\rm s}| = 4|1/x_{\rm s}|^{3/2} = 0.160$, again in excellent agreement with (17.416).

This convergence radius is compatible with the heuristic convergence of the strong-coupling series up to order 22, as can be seen in Fig. 17.19 by comparing the curves resulting from the series with the exact curve.

It is possible to extend the convergence proof to the more general divergent power series discussed in Section 5.17, whose strong-coupling expansions have the more general growth parameters p and q [15]. The convergence is assured for $1/2 < 2/q < 1$ [16]. If the interaction of the anharmonic oscillator is $\int d\tau\, x^n(\tau)$ with $n \neq 4$, the dimensionless expansion parameter for the energies is $g/\omega^{n/2+1}$ rather than g/ω^3. Then $q = n/2+1$, such that for $n \geq 6$ the convergence is lost. This can be verified by trying to resum the expansions for the ground state energies of $n = 6$ and $n = 8$, for example. For $n = 6$, the cut in Fig. 17.16 becomes circular such that there is no more shaded circle C_3 in which the strong-coupling series converges.

17.11 Decay of Supercurrent in Thin Closed Wire

An important physical application of the above tunneling theory explains the temperature behavior of the resistance of a thin[7] superconducting wire. The superconducting state is described by a complex order parameter $\psi(z)$ depending on the spatial variable z along the wire. We then speak of an *order field*. The variable z plays the role of the Euclidean time τ in the previous sections. We shall consider a closed wire where $\psi(z)$ satisfies the periodic boundary condition

$$\psi(z) = \psi(z+L). \tag{17.418}$$

The energy density of the system is described approximately by a *Ginzburg-Landau expansion* in powers of ψ and its gradients containing only the terms

$$\varepsilon(z) = |\partial_z\psi(z)|^2 + m^2|\psi(z)|^2 + \frac{g}{4}|\psi(z)|^4. \tag{17.419}$$

The total fluctuating energy is given by the functional

$$E[\psi^*,\psi] = \int_{-L/2}^{L/2} dz\, \varepsilon(z), \tag{17.420}$$

[7] A superconducting wire is called *thin* if it is much smaller than the coherence length to be defined in Eq. (17.425).

and the probability of each fluctuation is determined by the Boltzmann factor $\exp\{-E[\psi^*,\psi]/k_BT\}$. The parameter m^2 in front of $|\psi(z)|^2$ is called the *mass term* of the field. It vanishes at the critical temperature T_c and behaves near T_c like

$$m^2 \approx m_0^2 \left(\frac{T}{T_c} - 1\right). \tag{17.421}$$

Below T_c, the square mass is negative and the wire becomes superconducting. One can easily estimate, that each term in the Landau expansion is of the order of $|1 - T/T_c|^2$ and any higher expansion term in (17.419) would be smaller than that by at least a power $|1 - T/T_c|^{1/2}$.

The partition function of the system is given by the path integral

$$Z = \int \mathcal{D}\psi^*(z)\mathcal{D}\psi(z) e^{-E[\psi^*,\psi]/k_BT}. \tag{17.422}$$

If T does not lie too close to T_c [although close enough to justify the Landau expansion, i.e., the neglect of higher expansion terms in (17.419) suppressed by a factor $|1-T/T_c|^{1/2}$], this path integral can be treated semiclassically in the way described earlier in this chapter [17].

The basic microscopic mechanism responsible for the phenomenon of superconductivity will be irrelevant for the subsequent discussion. Let us only recall the following facts: A superconductor is a metal at low temperatures whose electrons near the surface of the Fermi sea overcome their Coulomb repulsion due to *phonon exchange*. This enables them to form bound states between two electrons of opposite spin orientations in a relative s-wave, the celebrated *Cooper pairs*.[8] The attraction which binds the Cooper pairs is extremely weak. This is why the temperature has to be very small to keep the pairs from being destroyed by thermal fluctuations. The critical temperature T_c, where the pairs break up, is related to the binding energy of the Cooper pairs by $E_{\text{pair}} = k_BT_c$. The field-theoretic process called phonon exchange is a way of describing the accumulation of positive ions along the path of an electron which acts as an attractive potential wake upon another electron while screening the Coulomb repulsion. The attraction is very weak and leads to a bound state only in the s-wave (the centrifugal barrier $\propto l(l+1)/r^2$ preventing the formation of a bound state in higher partial waves). The potential between the electrons may well be approximated by a δ-function potential $V(x) \approx -g\delta(r)$. The critical temperature T_c, usually a few degrees Kelvin, is found to satisfy the characteristic exponential relation

$$T_c k_B = \mu e^{-1/g}. \tag{17.423}$$

The parameter μ denotes the upper energy cutoff of the phonon spectrum $T_D k_B$, where T_D is the Debye temperature of the lattice vibration.

[8] We consider here only with old-fashioned superconductivity which sets in below a very small critical temperature of a few-degree Kelvin. The physics of the recently discovered high-temperature superconductors is at present not sufficiently understood to be discussed along the same lines.

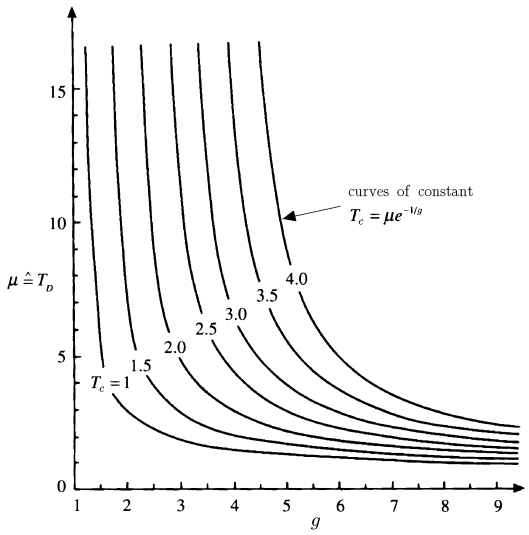

Figure 17.21 Renormalization group trajectories in the g, μ plane of superconducting electrons (g=attractive coupling constant, μ=Debye temperature, $k_B = 1$). Curves with same T_c imply identical superconducting properties. The renormalization group determines the reparametrizations of a fixed superconductive system along any of these curves.

An important result of the theory, confirmed by experiment, is that all T-dependent characteristic equilibrium properties of the superconductor near T_c depend only on the single parameter T_c. Thus, many quite different systems with different microscopic parameters $\mu \equiv T_D$ and g will have the *same* superconducting properties (see Fig. 17.21). The critical temperature is an important prototype for the understanding of the so-called *dimensionally transmuted coupling constant* in quantum field theories, which plays a completely analogous role in specifying the system. In quantum field theory, an arbitrary mass parameter μ is needed to define the coupling strength of a renormalized theory and physical quantities depend only on the combination[9]

$$M_c = \mu e^{-1/g(\mu)}. \tag{17.424}$$

The set of all changes μ which are accompanied by a simultaneous change of $g(\mu)$ such as to stay on a fixed curve with M_c from the *renormalization group*. The curve $\mu, g(\mu)$ is called the *renormalization group trajectory* [16].

If one works in natural units with $\hbar = k_B = M = 1$, the critical temperature corresponds to a length of $\approx 1000\text{Å}$. This length sets the scale for the spatial correlations of the Cooper pairs near the critical point via the relation

$$\xi(T) = \frac{\text{const.}}{T_c}\left(1 - \frac{T}{T_c}\right)^{-1/2} \approx 1000\text{Å}\left(1 - \frac{T}{T_c}\right)^{-1/2}. \tag{17.425}$$

[9]In quantum chromodynamics, this dimensionally transmuted coupling constant is of the order of the pion mass and usually denoted by Λ.

The Cooper pairs are much larger than the lattice spacing, which is of the order of 1Å. Their size is determined by the ratio $\hbar^2 k_F/m_e \pi k_B T_c$, where k_F is the wave number of electrons of mass m_e on the surface of the Fermi sphere. The temperature T_c in conventional superconductors of the order of 1 K corresponds to 1/11604.447 eV. Thus the thermal energy $k_B T_c$ is smaller than the atomic energy $E_H = 27.210\,\text{eV}$ (recall the atomic units defined on p. 13.7) by a factor 2.345×10^{-3}, and we find that $\hbar^2/m_e \pi k_B T_c$ is of the order of $10^2 a_H^2$. Since a_H is of the order of $1/k_F$, we estimate the size of the Cooper pairs as being roughly 100 times larger than the lattice spacing.

This justifies a posteriori the δ-function approximation for the attractive potential, whose range is just a few lattice spacings, i.e., much smaller than $\xi(T)$. The presence of such large bound states causes the superconductor to be coherent over the large distance $\xi(T)$. For this reason, $\xi(T)$ is called the *coherence length*.

Similar Cooper pairs exist in other low-temperature fermion systems such as ^{3}He, where they give rise to the phenomenon of *superfluidity*. There, the interatomic potential contains a hard repulsive core for $r < 2.7$Å. This prevents the formation of an s-wave bound state. In addition it produces a strong spin-spin correlation in the almost fully degenerate Fermi liquid, with a preference of parallel spin configurations. Because of the necessary antisymmetry of the pair wave function of the electrons, this amounts to a repulsion in any even partial wave. For this reason, Cooper pairs can only exist in the p-wave spin triplet state. The binding energy is much weaker than in a superconductor, suppressing the critical temperature by roughly a factor thousand. Experimentally, one finds $T_c = 27$mK at a pressure of $p = 35$ bar. Since the masses of the ^{3}He atoms are larger than those of the electrons by about the same factor thousand, the coherence length ξ has the same order of magnitude in both systems, i.e., $1/T_c$ has the same length when measured in units of Å.

The theoretical description of the behavior of the condensate is greatly simplified by re-expressing the fundamental Euclidean action in terms of a Cooper *pair field* which is the composite field

$$\psi_{\text{pair}}(\mathbf{x}) = \psi_{\text{e}}(\mathbf{x})\psi_{\text{e}}(\mathbf{x}). \tag{17.426}$$

Such a change of field variables can easily be performed in a path integral formulation of the field theory. The method is very similar to the introduction of the auxiliary field $\varphi(\mathbf{x})$ in the polymer field theory of Section 15.12. Since this subject has been treated extensively elsewhere[10] we shall not go into details. The partition function of the system reads

$$Z = \int \mathcal{D}\psi_{\text{e}}^*(\mathbf{x})\mathcal{D}\psi_{\text{e}}(\mathbf{x}) e^{-\mathcal{A}[\psi_{\text{e}}^*,\psi_{\text{e}}]}. \tag{17.427}$$

[10]The way to describe the pair formation by means of path integrals is explained in H. Kleinert, *Collective Quantum Fields*, Fortschr. Phys. *26*, 565 (1978) (`http://www.physik.fu-berlin.de/~kleinert/55`).

By going from integration variables $\psi_{\rm e}$ to $\psi_{\rm pair}$, we can derive the alternative pair partition function

$$Z = \int \mathcal{D}\psi^*_{\rm pair}(\mathbf{x})\mathcal{D}\psi_{\rm pair}(\mathbf{x})e^{-\mathcal{A}[\psi^*_{\rm pair},\psi_{\rm pair}]}, \tag{17.428}$$

where $\psi_{\rm pair}$ is the Cooper pair field (17.426).

In general, the new action is very complicated. For temperatures close to T_c, however, it can be expanded in powers of the field $\psi_{\rm pair}$ and its derivatives, leading to a Landau expansion of the type (17.419). For static fields the Euclidean field action is

$$\begin{aligned}\mathcal{A}[\psi^*_{\rm pair},\psi_{\rm pair}] &= E/k_BT = \frac{1}{k_BT}\int d^3x\,\varepsilon(\mathbf{x}) \qquad (17.429)\\ &= \frac{1}{k_BT}\int d^3x\left[\left(-\log\frac{\mu}{T}+\frac{1}{g^2}\right)|\psi_{\rm pair}|^2+\frac{1}{2T_c^2}|\psi_{\rm pair}|^4+\frac{1}{T_c^2}|\boldsymbol{\nabla}\psi_{\rm pair}|^2+\dots\right],\end{aligned}$$

where the dots denote the omitted higher powers of $\psi_{\rm pair}$ and of their derivatives, each accompanied by an additional factor $1/T_c$.

Let us discuss the path integral (17.429) first in the classical limit. We observe that with the critical temperature (17.423), the mass term in the energy can be written as

$$-\log\frac{T_c}{T}\,|\psi_{\rm pair}|^2 \sim -\left(1-\frac{T}{T_c}\right)|\psi_{\rm pair}|^2. \tag{17.430}$$

It has the "wrong sign" for $T < T_c$, so that the field has no stable minimum at $\psi_{\rm pair} = 0$. It fluctuates around one of the infinitely many nonzero values with the fixed absolute value

$$|\psi_{\rm pair,0}| = T_c\sqrt{1-\frac{T}{T_c}}. \tag{17.431}$$

It is then useful to take a factor $T_c\,(1-T/T_c)^{1/2}$ out of the field $\psi_{\rm pair}$, define

$$\psi(\mathbf{x}) \equiv \psi_{\rm pair}(\mathbf{x})\frac{1}{T_c(1-T/T_c)^{1/2}}, \tag{17.432}$$

and write the renormalized energy density as

$$\varepsilon(\mathbf{x}) = |\boldsymbol{\nabla}\psi|^2 - |\psi|^2 + \frac{1}{2}|\psi|^4. \tag{17.433}$$

Here we have made use of the coherence length (17.425) to introduce a dimensionless space variable $\mathbf{x}$, replacing $\mathbf{x} \to \mathbf{x}\,\xi$. We also have dropped an overall energy density factor proportional to $(1-T/T_c)^2\,T_c^2$.

In the rescaled form (17.433), the minimum of the energy lies at $|\psi_0| = 1$, where it has the density

$$\varepsilon = \varepsilon_c = -1/2. \tag{17.434}$$

The negative energy accounts for the binding of the Cooper pairs in the condensate (in the present natural units) and is therefore called the *condensation energy*. In terms of (17.433), the partition function in equilibrium can be written as

$$Z = \int \mathcal{D}\psi^*(\mathbf{x})\mathcal{D}\psi(\mathbf{x})e^{-(1/T)\int d^3x\,\varepsilon(\mathbf{x})}. \tag{17.435}$$

We are now prepared to discuss the flow properties of an electric current of the system carried by the Cooper pairs. It is carried by the divergenceless pair current [compare (1.102)]

$$\mathbf{j}(\mathbf{x}) = \frac{1}{2i}\psi^*(\mathbf{x}) \overset{\leftrightarrow}{\boldsymbol{\nabla}} \psi(\mathbf{x}) \tag{17.436}$$

associated with the transport of the number of pairs, apart from a charge factor of the pairs, which is equal to twice the electron charge.

The important question to be understood by the theory is: How can this current become "super", and stay alive for a very long time (in practice ranging from hours to years, as far as the patience of the experimentalist may last) [18]. To see this let us set up a current in a long circular wire and assume that the wire thickness is much smaller than the coherence length $\xi(T)$. Then transverse variations of the pair field $\psi(\mathbf{x})$ are strongly suppressed with respect to longitudinal ones (by the gradient terms $|\boldsymbol{\nabla}\psi(\mathbf{x})|^2$ in the Boltzmann factor) and the system depends mainly on the coordinate z *along* the wire, so that the above formalism can be applied. If the cross section of the wire is absorbed into the inverse temperature prefactor in the Boltzmann factor in (17.435), we may simply study the partition function (17.435) for a one-dimensional problem along the z-axis. The energy density (17.433) is precisely of the form announced in the beginning in Eq. (17.419). It is convenient to decompose the complex field $\psi(z)$ into polar coordinates

$$\psi(z) = \rho(z)e^{i\gamma(z)}, \tag{17.437}$$

in terms of which the energy density reads

$$\varepsilon(z) = -\rho^2 + \frac{1}{2}\rho^4 + \rho_z^2 + \rho^2\gamma_z^2, \tag{17.438}$$

where the subscript z indicates a derivative with respect to z. The field equations are

$$j(z) = \rho^2(z)\gamma_z(z) = \text{const} \tag{17.439}$$

and

$$\rho_{zz} = -\rho + \rho^3 + \frac{j^2}{\rho^3}. \tag{17.440}$$

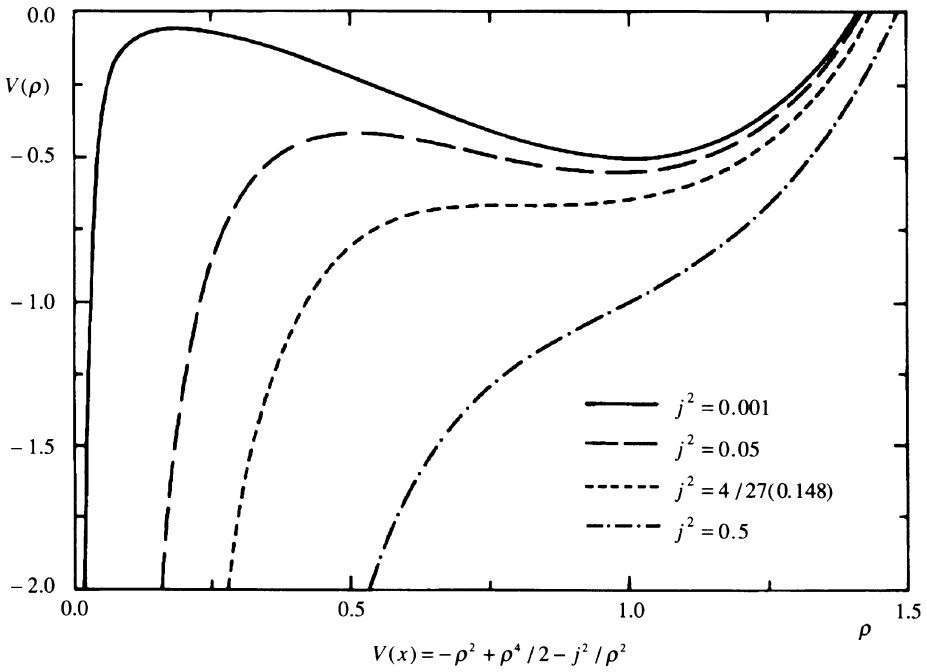

Figure 17.22 Potential $V(\rho) = -\rho^2 + \rho^4/2 - j^2/\rho^2$ showing barrier in superconducting wire to the left of ρ_0 to be penetrated if the supercurrent is to relax.

If z is reinterpreted as an imaginary "time", the latter equation can be interpreted as describing the mechanical motion of a mass point at the position $\rho(z)$ moving as a function of the "time" z in the potential

$$-V(\rho) \equiv \rho^2 - \frac{1}{2}\rho^4 + \frac{j^2}{\rho^2}, \tag{17.441}$$

which is the potential shown in Fig. 17.22 turned upside down.

Certainly, the time-sliced path integral in ρ would suffer from the phenomenon of path collapse described in Chapter 8. At the level of the semiclassical approximation to be performed here, however, this does not happen. There are two types of extremal solutions. The trivial solutions are

$$\gamma(z) = kz, \qquad \rho(z) \equiv \rho_0 = \sqrt{1-k^2}. \tag{17.442}$$

Since the wire is closed, the phase $\gamma(z)$ has to be periodic over the total length L of the wire. This implies the quantization of the wave number k,

$$k_n = \frac{2\pi}{L}n, \quad n = 0, \pm 1, \pm 2, \ldots \ . \tag{17.443}$$

The current associated with these solutions is

$$j = \rho_0^2 k = (1-k^2)k. \tag{17.444}$$

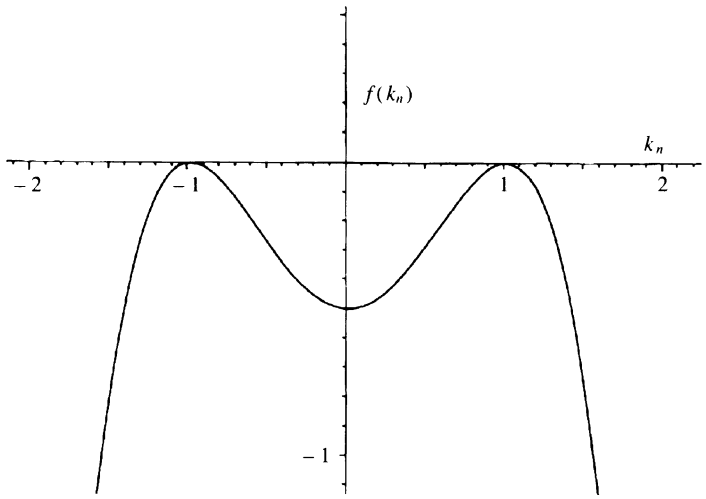

Figure 17.23 The condensation energy as function of velocity parameter $k_n = 2\pi n/L$.

As a function of k, this has an absolute maximum at the so-called *critical current* j_c, i.e.,

$$|j| < j_c \equiv \frac{2}{3\sqrt{3}}. \tag{17.445}$$

No solution of the field equations can carry a larger current than this. The critical wave number is

$$k_c \equiv \frac{1}{\sqrt{3}}, \tag{17.446}$$

and the energy density:

$$e_c(k) = V(\rho_0) = -\frac{1}{2}(1-k^2)^2. \tag{17.447}$$

It is plotted in Fig. 17.23. Note that the k-values (17.446) for which a supercurrent can exist between the turning points. The energy $e_c(k)$ represents the negative condensation energy of the state in the presence of the current. For $k \to 0$ it goes against the current-free value (17.434).

We can now understand why all states of current j_n smaller than j_c are, in fact, "super" in the sense of having an extremely long lifetime. At each value of k_n, the wire carries a metastable current which can only decay by a slow tunneling. To see this, we picture the field configuration as a spiral of radius ρ wound around the wire with the azimuthal angle representing the phase $\gamma(z) = k_n z$ (see Fig. 17.24). At zero temperature, the size ρ of the order parameter is frozen at ρ_0 and the winding number is *absolutely stable* on topological grounds. Then, each metastable state with wave number k_n has an infinite lifetime. If the current is to relax by one unit of n it is necessary that at some place z, thermal fluctuations carry $\rho(z)$ to zero. There

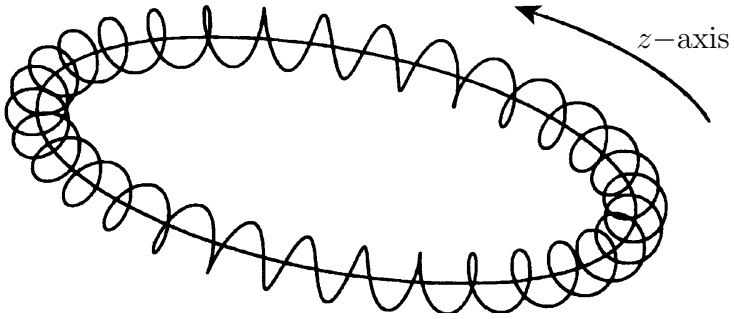

Figure 17.24 Order parameter $\Delta(z) = \rho(z)e^{i\gamma(z)}$ of superconducting thin circular wire neglecting fluctuations. The order parameter is pictured as a spiral of radius ρ_0 and pitch $\partial\gamma(z)/\partial z = 2\pi n/L$ winding around the wire. At $T = 0$, the supercurrent is absolutely stable since the winding number n is fixed topologically.

the phase becomes undefined and may slip by 2π. At the typical low temperatures of these systems, such *phase slips* are extremely rare. To have a local excursion of $\rho(z)$ to $\rho \approx 0$ at one place z, with an appreciable measure in the functional integral (17.435), it must start from a nontrivial solution of the equations of motion which carries $\rho(z)$ as closely as possible to zero. From our experience with the mechanical motion of a mass point in a potential such as $-V(\rho)$ of Eq. (17.441), it is easily realized that there exists such a solution. It carries $\rho(z)$ from $\rho_0 = \sqrt{1-k^2}$ at $z = -\infty$ across the potential barrier to the small value $\rho_1 = \sqrt{2}k$ and back once more across the barrier to ρ_0 at $z = \infty$ (see Fig. 17.25). Using the first integral of

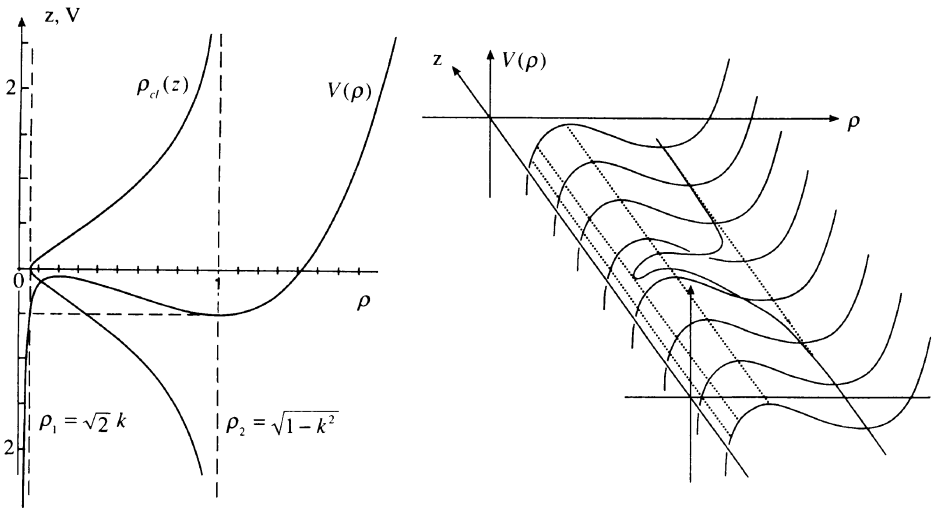

Figure 17.25 Extremal excursion of order parameter in superconducting wire. It corresponds to a mass point starting out at ρ_0, rolling under the influence of "negative gravity" up the mountain unto the point $\rho_1 = \sqrt{2}k$, and returning back to ρ_0, with the variable z playing the role of a time variable.

motion of the differential equation (17.440), the law of energy conservation

$$\frac{1}{2}\rho_z^2 - \frac{1}{2}V(\rho) = E = -\frac{1}{2}V(\rho_0) = \frac{1}{4}\rho_0(\rho_0 + 2\rho_1) \tag{17.448}$$

leads to the equation

$$\rho_z = \sqrt{2E + V(\rho)}. \tag{17.449}$$

This is solved by the integral

$$\begin{aligned} z - z_1 &= \sqrt{2}\int_{\rho_1}^{\rho} \frac{\rho d\rho}{\sqrt{\rho^6 - 2\rho^4 + 4E\rho^2 - 2j^2}} \\ &= \frac{1}{\sqrt{2}}\int_{\rho_1^2}^{\rho^2} \frac{d\rho^2}{\sqrt{(\rho^2 - \rho_1^2)(\rho^2 - \rho_0^2)}}, \end{aligned} \tag{17.450}$$

yielding

$$z - z_1 = -\frac{2}{\sqrt{2(\rho_0^2 - \rho_1^2)}}\text{arctanh}\sqrt{\frac{\rho^2 - \rho_1^2}{\rho_0^2 - \rho_1^2}}. \tag{17.451}$$

Inverting this, we find the bubble solution

$$\rho_{\rm cl}^2(z) = 1 - k^2 - \frac{\omega^2/2}{\cosh^2[\omega(z - z_1)/2]}, \tag{17.452}$$

where

$$\omega = \sqrt{2(\rho_0^2 - \rho_1^2)} \tag{17.453}$$

is the curvature of $V(\rho)$ close to ρ_0, i.e.,

$$V(\rho) \approx \omega^2(\rho - \rho_0)^2 + \dots \ . \tag{17.454}$$

The extra energy of the bubble solution is

$$E_{\rm cl} = \int_0^L dz\,[e(\rho_{\rm cl}) - e_c(k)] = \frac{4}{3}\omega = \frac{4}{3}\sqrt{2(1 - 3k^2)}. \tag{17.455}$$

The explicit solution (17.452) reaches the point of smallest ρ at z_1, where its value is

$$\rho_1 \equiv \rho(z_1) = \sqrt{2}k. \tag{17.456}$$

This value is still nonzero and does not yet permit a phase slip. However, we shall now demonstrate that quadratic fluctuations around the solution (17.456) do, in fact, to reduce the current. For this, we insert the fluctuating order field

$$\rho(z) = \rho_{\rm cl}(z) + \delta\rho(z) \tag{17.457}$$

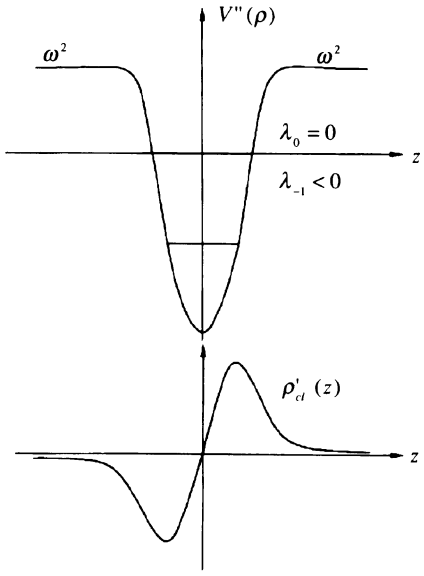

Figure 17.26 Infinitesimal translation of critical bubble yields antisymmetric wave function of zero energy $\rho'_{\rm cl}$ solving differential equation (17.509). Since this wave function has a node, there must be a negative-energy bound state.

into the free energy. With $\rho_{\rm cl}$ being extremal, the lowest variation of E is of second order in $\delta\rho(z)$

$$\delta^2 E = \int_0^L dz\ \delta\rho(z)[-\partial_z^2 + V''(\rho)]\delta\rho(z). \tag{17.458}$$

This expression is not positive definite as can be verified by studying the eigenvalue problem

$$[-\partial_z^2 + V''(\rho_{\rm cl})]\psi_n(z) = \left[-\partial_z^2 - 1 + 3\rho_{\rm cl}^2 - 3\frac{j^4}{\rho_{\rm cl}^4}\right]\psi_n(z) = \lambda_n\psi(z). \tag{17.459}$$

The potential $V''(\rho_{\rm cl}(z))$ has asymptotically the value ω^2. When approaching $z = z_1$ from the right, it develops a minimum at a negative value (see Fig. 17.26). After that it goes again against ω^2. The energy eigenvalues λ_0 and λ_{-1} lie as indicated in the figure. The fact that there is precisely one negative eigenvalue λ_{-1} can be proved without an explicit solution by the same physical argument that was used to show the instability of the fluctuation problem (17.253): A small temporal translation of the classical solution corresponds to a wave function which has no energy and a zero implying the existence of precisely one lower wave function with $\lambda_{-1} < 0$ and no zero.

The negative eigenvalue makes the critical bubble solution unstable against contraction or expansion. The former makes the fluctuation return to the spiral classical solution (17.452) of Fig. 17.24, the second removes one unit from the winding number of the spiral and reduces the supercurrent. For the precise calculation of the

decay rate, the reader is referred to the references quoted at the end of the chapter. Here we only give the final result which is [19]

$$\text{rate} = \text{const} \times L\,\omega(k) e^{-E_{\rm cl}/k_B T}, \tag{17.460}$$

with the k-dependent prefactor

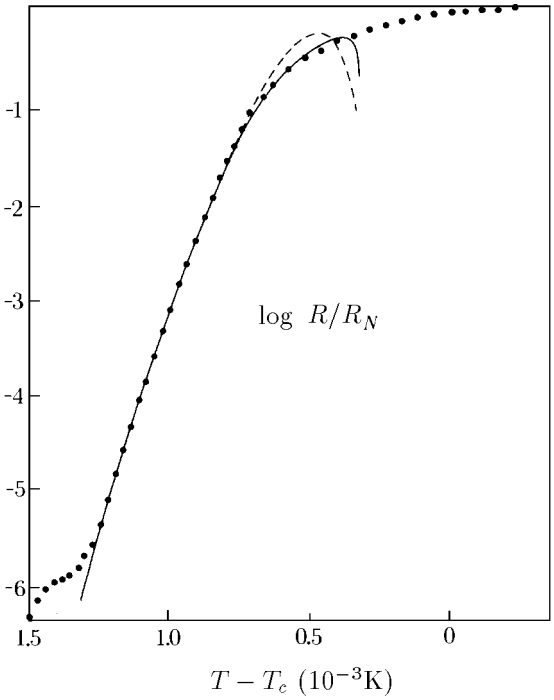

Figure 17.27 Logarithmic plot of resistance of thin superconducting wire as function of temperature at current 0.2μA in comparison with experimental data (vertical axis is normalized by the Ohmic resistance $R_n = 0.5\Omega$ measured at $T > T_c$, see papers quoted at end of chapter).

$$\omega(k) = 2|\lambda'_{-1}| \frac{(1-3k^2)^{7/4}}{(1-k^2)^{1/2}} \exp\left[-\frac{3\sqrt{2}k}{\sqrt{1-3k^2}} \arctan\left(\frac{\sqrt{1-3k^2}}{\sqrt{2}k}\right)\right], \tag{17.461}$$

where

$$\lambda'_{-1} \equiv -\frac{1}{2}\left\{\left[(1+k^2)^2 + 3(1-3k^2)^2\right]^{1/2} - (1+k^2)\right\} < 0 \tag{17.462}$$

is the negative eigenvalue of the fluctuations in the complex field $\psi(z)$ [which is not directly related to λ_{-1} of Eq. (17.459) and requires a separate discussion of the initial path integral (17.435)]. This complicated-looking expression has a simple quite accurate approximation which had previously been deduced from a numerical evaluation of the fluctuation determinant [20]:

$$\omega(k) \approx (1-\sqrt{3}k)^{15/4}(1+k^2/4). \tag{17.463}$$

Both expressions vanish at the critical value $k = k_c = 1/\sqrt{3}$.

The resistance of a thin superconducting wire following from this calculation is compared with experimental data in Fig. 17.27.

17.12 Decay of Metastable Thermodynamic Phases

A generalization of this decay mechanism can be found in the first-order phase transitions of many-particle systems. These possess some order parameter with an effective potential which has two minima corresponding to two different thermodynamic phases. Take, for instance, water near the boiling point. At the boiling temperature, the liquid and gas phases have the same energy. This situation corresponds to the symmetric potential. At a slightly higher temperature, the liquid phase is overheated and becomes metastable. The potential is now slightly asymmetric. The decay of the overheated phase proceeds by the formation of critical bubbles [4]. Their outside consists of the metastable water phase, their inside is filled with vapor lying close to the stable minimum of the potential. The radius of the critical bubble is determined by the equilibrium between the gain in volume energy and the cost in surface energy. If σ is the surface tension and ϵ the difference in energy density, the energy of bubble solution depends on the radius as follows:

$$E \propto \sigma\, 4\pi R^2 - \epsilon \frac{4\pi}{3} R^3. \tag{17.464}$$

A plot of this energy in Fig. 17.28 looks just like that of the action $\mathcal{A}(\xi)$ in Fig. 17.8. Thus the role of the deformation parameter ξ is played here by the bubble radius R.

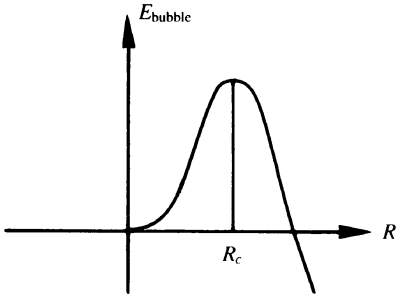

Figure 17.28 Bubble energy as function of its radius R.

At the critical bubble, the energy has a maximum. The fluctuations of the critical bubble must therefore have a negative eigenvalue. This negative eigenvalue mode accounts for the fact that the critical bubble is unstable against expansion and contraction. When expanding, the bubble transforms the entire liquid into the stable gas phase. When contracting, the bubble disappears and the liquid remains in the overheated phase. Only the first half of the fluctuations have to be counted when calculating the lifetime of the overheated phase.

It is instructive to take a comparative look at the instability of a critical bubble to see how the different spatial dimensions modify the properties of the solution. We shall discuss first the case of three space dimensions. As in the case of superconductivity, the description of the liquid-vapor phase transition makes use of a space-dependent order parameter, the real order field $\varphi(\mathbf{x})$. The two minima of the

potential $V(\varphi)$ describe the two phases of the system. The kinetic term $\mathbf{x}'^2$ in the path integral is now a field gradient term $[(\partial_{\mathbf{x}}\varphi(\mathbf{x}))^2]$ which ensures finite correlations between neighboring field configurations. The Euclidean action controlling the fluctuations is therefore of the form

$$\mathcal{A}[\varphi] = \int d^3x \left\{ \frac{1}{2}[\boldsymbol{\nabla}\varphi(\mathbf{x})]^2 + V(\varphi) \right\}, \tag{17.465}$$

where $V(\varphi)$ is the same potential as in Eq. (17.1), but it is extended by the asymmetric energy (17.243). Within classical statistics, the thermal fluctuations are controlled by the path integral for the partition function

$$Z = \int \mathcal{D}\varphi(\mathbf{x}) e^{-\mathcal{A}[\varphi]/T}. \tag{17.466}$$

Here T is the temperature measured in multiples of the Boltzmann constant k_B. The path integral $\int \mathcal{D}\varphi(\mathbf{x})$ is defined by cutting the three-dimensional space into small cubes of size ϵ and performing one field integration at each point.

The critical bubble extremizes the action. Assuming spherical symmetry, the bubble satisfies in D dimensions the classical Euler-Lagrange field equation

$$\left(-\frac{d^2}{dr^2} - \frac{D-1}{r}\frac{d}{dr} \right) \varphi_{\rm cl} + V'(\varphi_{\rm cl}(r)) = 0. \tag{17.467}$$

This differs from the equation (17.305) for the one-dimensional bubble solution by the extra gradient term $-[(D-1)/r]\partial_r\varphi_{\rm cl}(r)$. Such a term is an obstacle to an exact solution of the equation via the energy conservation law (17.306). The relevant qualitative properties of the solution can nevertheless be seen in a similar way as for the bubble solution. As in Fig. 17.11 we plot the reversed potential and imagine the solution $\varphi(r)$ to describe the motion of a mass point in this potential with $-r$ playing the role of a "time". Setting $\varphi_{\rm cl}(r) = x(-t)$, the field equation (17.467) takes the form

$$\ddot{x}(t) - \frac{D-1}{t}\dot{x}(t) - V'(x(t)) = 0. \tag{17.468}$$

In this notation, the second term, i.e., the term $-[(D-1)/r]\partial_r\varphi_{\rm cl}(r)$ in (17.467) plays the role of a negative "friction" accelerating motion of the particle along $x(t)$. This effect decreases with time like $1/t$. With our everyday experience of mechanical systems, the qualitative behavior of the solution can immediately be plotted qualitatively as shown in Fig. 17.29. For $D = 1$, the energy conservation makes the particle reach the right-hand zero of the potential. For $D > 1$, the "antifriction" makes the trajectory overshoot. At $r = 0$, the solution is closest to the stable minimum (the maximum of the reversed potential) on the left-hand side. In the superheated water system, this corresponds to the inside of the bubble being filled with vapor. As r moves outward in the bubble, the state moves closer to the metastable state, i.e., it becomes more and more liquid. The antifriction term has the effect that the

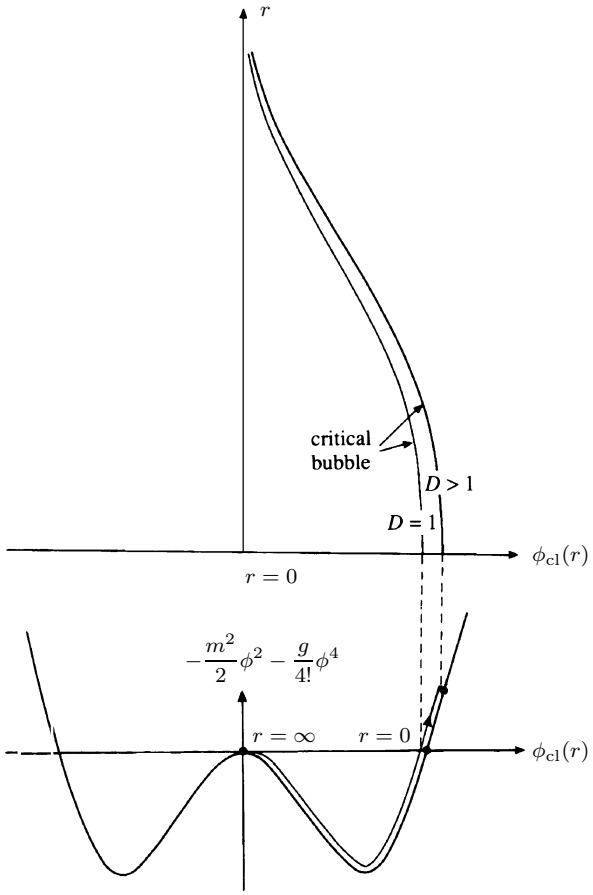

Figure 17.29 Qualitative behavior of critical bubble solution as function of its radius.

point of departure on the left-hand side lies energetically below the final value of the metastable state.

Consider now the fluctuations of such a critical bubble in $D = 3$ dimensions. Suppose that the field deviates from the solution of the field equation (17.467) by $\delta\varphi(\mathbf{x})$. The deviations satisfy the differential equation

$$\left[-\frac{d^2}{dr^2} - \frac{2}{r}\frac{d}{dr} + \frac{\hat{L}^2}{r^2} + V''(\varphi_{\rm cl}(r))\right]\delta\varphi(\mathbf{x}) = \lambda\,\delta\varphi(\mathbf{x}), \tag{17.469}$$

where $\hat{L}^2$ is the differential operator of orbital angular momentum (in units $\hbar = 1$). Taking advantage of rotational invariance, we expand $\delta\varphi(\mathbf{x})$ into eigenfunctions of angular momentum φ_{nlm}, the spherical harmonics $Y_{lm}(\hat{\mathbf{x}})$:

$$\phi(\mathbf{x}) = \sum_{nlm} \varphi_{nlm}(r) Y_{lm}(\hat{\mathbf{x}}). \tag{17.470}$$

The coefficients φ_{nlm} satisfy the radial differential equation

$$\left[-\frac{d^2}{dr^2} - \frac{2}{r}\frac{d}{dr} + \frac{l(l+1)}{r^2} + V''(\varphi_{\rm cl}(r))\right]\varphi_{nlm}(r) = \lambda_{nl}\varphi_{nlm}(r), \tag{17.471}$$

with

$$V''(\varphi_{\rm cl}(r)) = -\frac{\omega^2}{2} + \frac{3}{2}\frac{\omega^2}{a^2}\varphi_{\rm cl}^2(r). \tag{17.472}$$

One set of solutions is easily found, namely those associated with the translational motion of the classical solution. Indeed, if we take the bubble at the origin,

$$\varphi_{\rm cl}(\mathbf{x}) = \varphi_{\rm cl}(r), \tag{17.473}$$

to another place $\mathbf{x}+\mathbf{a}$, we find, to lowest order in $\mathbf{a}$,

$$\begin{aligned} \varphi_{\rm cl}(\mathbf{x}+\mathbf{a}) &= \varphi_{\rm cl}(\mathbf{x}) + \mathbf{a}\partial_{\mathbf{x}}\varphi_{\rm cl}(\mathbf{x}) \\ &= \varphi_{\rm cl}(r) + \mathbf{a}\hat{\mathbf{x}}\partial_r\varphi_{\rm cl}(r). \end{aligned} \tag{17.474}$$

But $\hat{\mathbf{x}}$ is just the Cartesian way of writing the three components of the spherical harmonics $Y_{1m}(\hat{x})$. If we introduce the *spherical components* of a vector as follows

$$\begin{pmatrix} x_0 \\ x_1 \\ x_{-1} \end{pmatrix} \equiv \begin{pmatrix} x_3 \\ (x_1+ix_2)/\sqrt{2} \\ -(x_1-ix_2)/\sqrt{2} \end{pmatrix}, \tag{17.475}$$

we see that

$$\hat{x}_m = \sqrt{\frac{4\pi}{3}}Y_{1m}(\hat{\mathbf{x}}). \tag{17.476}$$

Thus, $\delta\varphi(\mathbf{x}) = \mathbf{a}\hat{\mathbf{x}}\partial_r\varphi(\mathbf{x})$ must be a solution of Eq. (17.469) with zero eigenvalue λ. This can easily be verified directly: The factor $\hat{\mathbf{x}}$ causes $\hat{L}^2$ to have the eigenvalue 2, and the accompanying radial derivative $\delta\varphi(\mathbf{x}) = \partial_r\varphi_{\rm cl}(r)$ is a solution of Eq. (17.471) for $l=1$ and $\lambda_{nl}=0$, as is seen by differentiating the Euler-Lagrange equation (17.467) with respect to r. Choosing the principal quantum number of these translational modes to be $n=1$, we assign the three components of $\hat{\mathbf{x}}\partial_r\varphi_{\rm cl}(r)$ to represent the eigenmodes $\varphi_{1,1,m}$.

As long as the bubble radius is large compared to the thickness of the wall, which is of the order $1/\omega$, the $1/r^2$ -terms will be very small. There exists then an entire family of solutions $\varphi_{1lm}(\mathbf{x})$ with all possible values of l which all have approximately the same radial wave function $\partial_r\varphi_{\rm cl}(r)$. Their eigenvalues are found by a perturbation expansion. The perturbation consists in the centrifugal barrier but with the $l=1$ barrier subtracted since it is already contained in the derivative $\partial_r\varphi_{\rm cl}(r)$, i.e.,

$$V_{\rm pert} = [l(l+1)-2]/2r^2. \tag{17.477}$$

The bound-state wave functions φ_{1lm} are normalizable and differ appreciably from zero only in the neighborhood of the bubble wall. To lowest approximation, the perturbation expansion produces therefore an energy

$$\lambda_{nl} \approx \frac{l(l+1)-2}{r_c^2}, \tag{17.478}$$

where r_c is the radius of the critical bubble. As a consequence, the lowest $l = 0$ eigenstate has a negative energy

$$\lambda_{00} \approx -\frac{1}{r_c^2}. \tag{17.479}$$

Physically, this single $l = 0$ -mode corresponds to an infinitesimal radial vibration of the bubble. As already explained above it is not astonishing that a radial vibration has a negative eigenvalue. The critical bubble lies at a maximum of the action. Expansion or contraction is energetically favorable. Since $Y_{00}(\mathbf{x})$ is a constant, the wave function is proportional to $(d/dr)\varphi_{\rm cl}(r)$ itself without an angular factor. This is seen directly by performing an infinitesimal radial contraction

$$\varphi_{\rm cl}((1-\epsilon)r) = \varphi_{\rm cl}(r) - \epsilon r \partial_r \varphi_{\rm cl}(r). \tag{17.480}$$

The variation $r\partial_r\varphi_{\rm cl}(r)$ is almost zero except in the vicinity of the critical radius r_c, so that $r\partial_r\varphi_{\rm cl}(r) \approx r_c\partial_r\varphi_{\rm cl}(r)$ which is the above wave function. Being the ground state of the Schrödinger equation (17.469), it should be denoted by $\varphi_{000}(r)$. Since it solves approximately the Schrödinger equation (17.471) with $l = 1$, it also solves this equation approximately with $l = 0$ and the energy (17.479).

Finally let us point out that in $D > 1$ dimensions, the value of the negative eigenvalue can be calculated very simply from a phenomenological consideration of the bubble action. Since the inside of the bubble is very close to the true ground state of the system whose energy density lies lower than that of the metastable one by ϵ, the volume energy of a bubble of an arbitrary radius R is

$$E_V = -S_D \frac{R^D}{D}\epsilon, \tag{17.481}$$

where $S_D R^{D-1}$ is the surface of the bubble and $S_D R^D/D$ its volume. The surface energy can be parametrized as

$$E_S = S_D R^{D-1}\sigma, \tag{17.482}$$

where σ is a constant proportional to the surface tension. Adding the two terms and differentiating with respect to R, we obtain a critical bubble radius at

$$R = r_c = (D-1)\sigma/\epsilon, \tag{17.483}$$

with a critical bubble energy

$$E_c = \frac{S_D}{D}R_c^{D-1}\sigma = \frac{S_D}{D(D-1)}R_c^D\epsilon = \frac{S_D}{D}(D-1)^{D-1}\frac{\sigma^D}{\epsilon^{D-1}}. \tag{17.484}$$

The second derivative with respect to the radius R is, at the critical radius,

$$\frac{d^2E}{dR^2}\Big|_{R=r_c} = -DE_c\frac{D-1}{r_c^2}. \tag{17.485}$$

Identifying the critical bubble energy E_c with the classical Euclidean action $\mathcal{A}_{\rm cl}$ we find the variation of the bubble action as

$$\delta^2\mathcal{A}_{\rm cl} \approx -\frac{1}{2}(\delta R)^2 D\,\mathcal{A}_{\rm cl}\frac{D-1}{r_c^2}. \tag{17.486}$$

We now express the dilational variation of the bubble radius in terms of the normal coordinate of (17.470). The normalized wave function is obviously

$$\varphi_{000}(r) = \frac{\partial_r\varphi_{\rm cl}(r)}{\sqrt{\int d^Dx(\partial_r\varphi_{\rm cl})^2}}. \tag{17.487}$$

But the expression under the square root is exactly D times the action of the critical bubble

$$\int d^Dx(\partial_r\varphi_{\rm cl})^2 = D\mathcal{A}_{\rm cl}. \tag{17.488}$$

To prove this we introduce a scale factor s into the solution of the bubble and evaluate the action

$$\begin{aligned}\tilde{\mathcal{A}}_{\rm cl} &= \int d^Dx\left\{\frac{1}{2}([\partial_r\varphi_{\rm cl}(sr)]^2 + V(\varphi_{\rm cl}(sr))\right\}\\ &= \frac{1}{s^D}\int d^Dx\left\{\frac{s^2}{2}[\partial_r\varphi_{\rm cl}(r)]^2 + V(\varphi_{\rm cl}(r))\right\}.\end{aligned} \tag{17.489}$$

Since $\tilde{\mathcal{A}}_{\rm cl}$ is extremal at $s=1$, it has to satisfy

$$\frac{\partial\tilde{\mathcal{A}}_{\rm cl}}{\partial s}\Big|_{s=1} = 0, \tag{17.490}$$

or

$$\int d^Dx\left\{(D-2)\frac{1}{2}[\partial_r\varphi_{\rm cl}]^2 + DV(\varphi_{\rm cl}(r))\right\} = 0. \tag{17.491}$$

Hence

$$\int d^DxV(\varphi_{\rm cl}(r)) = -\frac{D-2}{D}\int d^Dx\frac{1}{2}[\partial_r\varphi_{\rm cl}(r)]^2, \tag{17.492}$$

implying that

$$\begin{aligned}\mathcal{A}_{\rm cl} &= \left(\frac{1}{2} - \frac{D-2}{2D}\right)\int d^Dx[\partial_r\varphi_{\rm cl}(r)]^2\\ &= \frac{1}{D}\int d^Dx[\partial_r\varphi_{\rm cl}(r)]^2.\end{aligned} \tag{17.493}$$

With (17.487), the φ_{000} contribution to $\delta\varphi(\mathbf{x})$ reads

$$\delta\varphi(\mathbf{x}) = \xi_{000}\varphi_{000}(r) = \xi_{000}\frac{\partial_r\varphi}{\sqrt{D\mathcal{A}_{\rm cl}}}, \tag{17.494}$$

and we arrive at

$$\delta R = \frac{\xi_{000}}{\sqrt{D\mathcal{A}_{\rm cl}}}. \tag{17.495}$$

Inserting this into (17.486) shows that the second variation of the Euclidean action $\delta^2\mathcal{A}_{\rm cl}$ can be written in terms of the normal coordinates associated with the normalized fluctuation wave function φ_{000} as

$$\delta^2\mathcal{A}_{\rm cl} = -\xi_{000}^2\frac{D-1}{2r_c^2}. \tag{17.496}$$

From this relation, we read off the negative eigenvalue

$$\lambda_{00} = -\frac{D-1}{2r_c^2}. \tag{17.497}$$

For $D = 3$, this is in agreement with the $D = 3$ value (17.479). For general D, the eigenvalue corresponding to (17.479) would have been derived with the arguments employed there from the derivative term $-[(D-1)/r]d/dr$ in the Lagrangian and would also have resulted in (17.497).

All other multipole modes φ_{nlm} have a positive energy. Close to the bubble wall (as compared with the radius), the classical solutions $(1/r)\varphi_{nlm}(r)$ can be taken approximately from the solvable one-dimensional equation

$$\left[-\frac{1}{2}\frac{d^2}{dr^2} + \frac{\omega^2}{2}\left(1 - \frac{3}{2}\frac{1}{\cosh^2[\omega(r-r_c)/2]}\right)\right]\left(\frac{1}{r}\varphi_{nlm}\right) \approx \tilde{\lambda}_n\left(\frac{1}{r}\varphi_{nlm}\right). \tag{17.498}$$

The wave functions with $n = 0$ are

$$\varphi_{0lm} \approx \sqrt{\frac{3\omega}{8}}\frac{1}{\cosh^2[\omega(r-r_c)/2]}, \tag{17.499}$$

and have the eigenvalues

$$\lambda_{0l} \approx \frac{l(l+1)-2}{2r_c^2}. \tag{17.500}$$

The $n = 1$ -bound states are

$$\varphi_{1lm} \approx \sqrt{\frac{3\omega}{4}}\frac{\sinh[\omega(r-r_c)/2]}{\cosh^2[\omega(r-r_c)/2]}, \tag{17.501}$$

with eigenvalues

$$\lambda_{1l} \approx \frac{3}{8}\omega^2 + \frac{l(l+2)-2}{2r_c^2}. \tag{17.502}$$

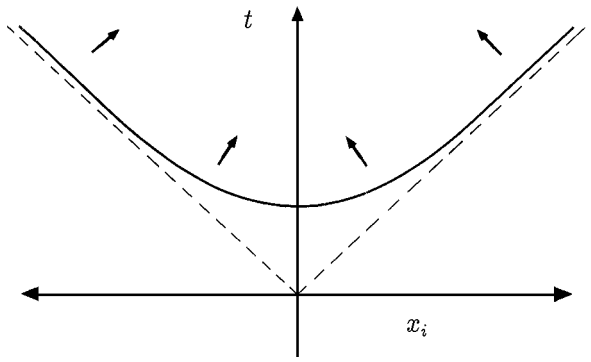

Figure 17.30 Decay of metastable false vacuum in Minkowski space. It proceeds as a shock wave which after some time traverses the world almost with light velocity, converting the false into the true vacuum.

17.13 Decay of Metastable Vacuum State in Quantum Field Theory

The theory of decay presented in the last section has an interesting quantum field-theoretic application. Consider a metastable scalar field system in a D-dimensional Euclidean spacetime at temperature zero. At a fixed time, there will be a certain average number of bubbles, regulated by the "quantum Boltzmann factor" $\exp(-\mathcal{A}_{\rm cl}/\hbar)$. If the bubble gas is sufficiently dilute (i.e., if the distances between bubbles is much larger than the radii), each bubble is described quite accurately by the classical solution. In Minkowski space, a Euclidean radius $r = \sqrt{\mathbf{x}^2 + c^2\tau^2}$ corresponds to $r = \sqrt{\mathbf{x}^2 - c^2t^2}$, where c is the light velocity. The critical bubble has therefore the spacetime behavior

$$\varphi_{\rm cl}(\mathbf{x}, t) = \varphi_{\rm cl}(r = \sqrt{\mathbf{x}^2 - c^2t^2}). \tag{17.503}$$

From the above discussion in Euclidean space we know that φ will be equal to the metastable false vacuum in the outer region $r > r_c$, i.e., for

$$\mathbf{x}^2 - c^2t^2 > r_c^2. \tag{17.504}$$

The inside region

$$\mathbf{x}^2 - c^2t^2 < r_c^2 \tag{17.505}$$

contains the true vacuum state with the lower energy. Thus a critical bubble in spacetime has the hyperbolic structure drawn in Fig. 17.30. Therefore, the Euclidean critical bubble describes in Minkowski space the growth of a bubble as a function of time. The bubble starts life at some time $t = r_c/c$ and expands almost instantly to a radius of order r_c. The position of the shock wave is described by

$$\mathbf{x}^2 - c^2t^2 = r_c^2. \tag{17.506}$$

This implies that a shock wave that runs through space with a velocity

$$v = \frac{|\mathbf{x}|}{t} = \frac{c}{\sqrt{1 - r_c^2/c^2t^2}} \tag{17.507}$$

and converts the metastable into the stable vacuum — a global catastrophe. A Euclidean bubble centered at another place $\mathbf{x}_b, \tau_b$ would correspond to the same process starting at $\mathbf{x}_b$ and a time

$$t_b = r_c/c + \tau_b. \tag{17.508}$$

A finite time after the creation of a bubble, of the order r_c/c, the velocity of the shock wave approaches the speed of light (in many-body systems the speed of sound). Thus, we would hardly be able to see precursors of such a catastrophe warning us ahead of time. We would be annihilated with the present universe before we could even notice.

17.14 Crossover from Quantum Tunneling to Thermally Driven Decay

For completeness, we discuss here the difference between a decay caused by a quantum-mechanical tunneling process at $T = 0$, and a pure thermally driven decay at large temperatures. Consider a one-dimensional system possessing, at some place x_*, a high potential barrier, much higher than the thermal energy k_BT, with a shape similar to Fig. 17.10. Let the well to the left of the barrier be filled with a grand-canonical ensemble of noninteracting particles of mass M in a nearly perfect equilibrium. Their distribution of momenta and positions in phase space is governed by the Boltzmann factor $e^{-\beta[p^2/2M+V(x)]}$. The rate, at which the particles escape across the barrier, is given by the classical statistical integral

$$\Gamma_{\rm cl} = Z_{\rm cl}^{-1} \int dx \int \frac{dp}{2\pi\hbar} e^{-\beta[p^2/2M+V(x)]} \delta(x - x_*) \frac{p}{M} \Theta(p), \tag{17.509}$$

where $Z_{\rm cl}$ is the classical partition function

$$Z_{\rm cl} = \int dx \int \frac{dp}{2\pi\hbar} e^{-\beta[p^2/2M+V(x)]}. \tag{17.510}$$

The step function $\Theta(p)$ selects the particles running to the right across the top of the potential barrier. Performing the phase space path integral in (17.509) yields

$$\Gamma_{\rm cl} = \frac{Z_{\rm cl}^{-1}}{2\pi\hbar\beta} e^{-V(x_*)}. \tag{17.511}$$

If the metastable minimum of the potential is smooth, $V(x)$ can be replaced approximately in the neighborhood of x_0 by the harmonic expression

$$V(x) \approx \frac{M}{2}\omega_0^2 (x - x_0)^2. \tag{17.512}$$

The classical partition function is then given approximately by

$$Z_{\rm cl} \approx \frac{1}{\hbar\beta\omega_0}, \tag{17.513}$$

and the decay rate follows the simple formula

$$\Gamma_{\rm cl} \approx \frac{\omega_0}{2\pi} e^{-\beta V(x_*)}. \tag{17.514}$$

Let us compare this result with the decay rate due to pure quantum tunneling. In the limit of small temperatures, the decay proceeds from the ground state, and the partition function is approximately equal to

$$Z \approx e^{-\beta(E^{(0)} - i\hbar\Gamma/2)}. \tag{17.515}$$

The decay rate is given by the small imaginary part of the partition function:

$$\Gamma \xrightarrow[T\to 0]{} \frac{2}{\hbar\beta} \frac{{\rm Im}\, Z}{{\rm Re}\, Z}. \tag{17.516}$$

In contrast to this, the thermal rate formula (17.511) implies for the high-temperature regime, where Γ becomes equal to $\Gamma_{\rm cl}$, the relation:

$$\Gamma \xrightarrow[T\to\infty]{} \frac{\omega_*}{\pi} \frac{{\rm Im}\, Z_{\rm cl}}{{\rm Re}\, Z_{\rm cl}}. \tag{17.517}$$

The frequency ω_* is determined by the curvature of the potential at the top of the barrier, where it behaves like

$$V(x) \approx -\frac{M}{2}\omega_*^2 (x - x_*)^2. \tag{17.518}$$

The relation (17.517) follows immediately by calculating in the integral (17.510) the contribution of the neighborhood of the top of the barrier in the saddle point approximation. As in the integral, this is done (17.261) by rotating the contour of integration which starts at $x = x_*$ into the upper complex half-plane. Writing $x = x_* + iy$ this leads to the following integral:

$${\rm Im}\, Z_{\rm cl} \approx \int_0^\infty \frac{dy}{\sqrt{2\pi\hbar^2\beta/M}} e^{-\beta\left[V(x_*) + \frac{M}{2}\omega_*^2 y^2\right]} \approx \frac{1}{2\hbar\beta\omega_*} e^{-\beta V(x_*)}. \tag{17.519}$$

Since the real part is given by (17.513) we find the ratio

$$\frac{{\rm Im}\, Z_{\rm cl}}{{\rm Re}\, Z_{\rm cl}} \approx \frac{\omega_0}{2\omega_*} e^{-\beta V(x_*)}, \tag{17.520}$$

so that (17.511) is equivalent to (17.517).

The two formulas (17.516) and (17.517) are derived for the two extreme regimes $T \gg T_0$ and $T \ll T_0$, respectively, where T_0 denotes the characteristic temperature

associated with the curvature of the potential at the metastable minimum $T_0 = \hbar\omega_0/k_B$. Numerical studies have shown that the applicability extends into the close neighborhood of T_0 on each side of the temperature axis. The crossover regime is quite small, of the order $\mathcal{O}(\hbar^{3/2})$.

Note that given the knowledge of the imaginary parts of all excited states, which can be obtained as in Section 17.9, it will be possible to calculate the average lifetime of a metastable state at all temperatures without the restrictions of the semiclassical approximation. This remains to be done.

Appendix 17A Feynman Integrals for Fluctuation Correction

For the integral (17.219) we obtain with (17.237) immediately the result stated in Eq. (17.240)

$$I_1' = \frac{97}{560}. \tag{17A.1}$$

To calculate the remaining three double integrals I_{21}, I_{22}, I_3 in (17.223) and (17.224) we observe that because of the symmetry of the Green function $G_{\mathcal{O}_\omega}(\tau,\tau')$ in τ,τ' the measure of integration can be rewritten as $2\int_{-\infty}^{\infty} d\tau \int_{-\infty}^{t} d\tau'$. We further introduce the dimensionless classical functions

$$\begin{aligned} \tilde{x}_{\rm cl}(\tau) &\equiv \sqrt{\frac{g}{2\omega^2}}x_{\rm cl}(\tau) = \tanh(\tau/2), \\ \tilde{y}_0(\tau) &\equiv \sqrt{\frac{8}{3\omega}}y_0(\tau) = \frac{1}{\cosh^2(\omega\tau/2)}, \end{aligned} \tag{17A.2}$$

use natural units with $\omega = 1, g = 1$, since these quantities cancel in all integrals, and define

$$\begin{aligned} x_{\rm G}(\tau) &\equiv \tilde{x}_{\rm cl}(\tau)G_{\mathcal{O}_\omega}(\tau,\tau) \\ x_{\rm KG}(\tau) &\equiv \left[\int_{-\infty}^{\tau} G_{\mathcal{O}_\omega}(\tau,\tau')x_{\rm G}(\tau')d\tau'\right]_{\rm A} \\ x_{\rm K3G}(\tau) &\equiv \left[\int_{-\infty}^{\tau} G^3_{\mathcal{O}_\omega}(\tau,\tau')x_{\rm G}(\tau')dt'\right]_{\rm A}, \end{aligned} \tag{17A.3}$$

where the subscript A denotes the antisymmetric part in τ. Because of the antisymmetry of $x_{\rm cl}$, the symmetric part gives no contribution to the integrals which can be written as

$$I_{21} = 6\int_0^\infty d\tau\, \tilde{x}_{\rm cl}(\tau)x_{\rm K3G}(\tau), \tag{17A.4}$$

$$I_{22} = 9\int_0^\infty d\tau\, x_{\rm G}(\tau)x_{\rm KG}(\tau), \tag{17A.5}$$

$$I_3 = 24\int_0^\infty d\tau\, y_0'(\tau)x_{\rm KG}(\tau). \tag{17A.6}$$

When evaluating the integrals in (17A.3) the antisymmetry of $y_0(\tau)$ is useful. We easily find

$$x_{\rm KG}(\tau) = \frac{1}{4}\frac{12\tau + \tanh(\tau/2)}{12\cosh^2(\tau/2)}. \tag{17A.7}$$

Inserting this into I_{22} and I_3 we encounter integrals of two types

$$\int_0^\infty d\tau\, \sinh^m(\tau/2)/\cosh^n(\tau/2) \quad \text{and} \quad \int_0^\infty \tau \sinh^m(\tau/2)/\cosh^n(\tau/2).$$

The former can be performed with the help of formula (17.54), the latter require integrations by parts of the type

$$\int_0^\infty f(\tau/2)\tanh\frac{\tau}{2}\,d\tau = -\int_0^\infty f'(\tau/2)\ln(2\,\cosh\frac{\tau}{2})\,d\tau, \tag{17A.8}$$

which lead to a finite sum of integrals of the first type plus integrals of the type[11]

$$\int_0^\infty \log\cosh(\tau/2)\sinh^m(\tau/2)/\cosh^n(\tau/2).$$

These, in turn, are equal to $-\partial_\nu \int_0^\infty d\tau\,\sinh^m(\tau/2)/\cosh^{\nu+1}(\tau/2)$ so that it is evaluated again via (17.54). After performing the subtraction in I_{22} we obtain the values given in Eq. (17.240).

The evaluation of the integral I_{21} is more tedious since we must integrate over the third power of the Green function, which is itself a lengthy function of τ. It is once more useful to exploit the symmetry properties of the integrand. We introduce the abbreviations

$$\begin{aligned} f_n^{\rm S/A}(\tau) &\equiv \frac{1}{2}[H_{\rm R}^n(\tau) \pm H_{\rm R}^n(-\tau)]y_0^{3-n}(\tau), \\ F_n^{\rm S/A}(\tau) &\equiv \int_0^\tau f_n^{\rm S/A}(\tau')\tilde{x}_{\rm cl}(\tau')d\tau', \\ N_n &\equiv \int_0^\infty H_{\rm R}^n(\tau)y_0^{3-n}(\tau')\tilde{x}_{\rm cl}(\tau')d\tau', \end{aligned} \tag{17A.9}$$

and find $x_{\rm K3G}$ in the form

$$\begin{aligned} x_{\rm K3G}(\tau) &= f_3^{\rm A}(\tau)[N_0 - F_0^{\rm S}(\tau)] + 3f_2^{\rm A}(\tau)[N_1 - F_1^{\rm S}(\tau)] + 3f_1^{\rm A}(\tau)[N_2 - F_2^{\rm S}(\tau)] \\ &\quad +3f_2^{\rm S}(\tau)F_1^{\rm A}(\tau) + 3f_1^{\rm S}(\tau)F_2^{\rm A}(\tau) + f_0^{\rm S}(\tau)F_3^{\rm A}(\tau), \end{aligned} \tag{17A.10}$$

with

$$N_0 = \frac{3}{32}\ , \quad N_1 = -\frac{7}{128}\ , \quad N_2 = \frac{203}{512} - \frac{\log 2}{2}. \tag{17A.11}$$

Explicitly:

$$\begin{aligned} x_{\rm K3G}(\tau) &= \frac{\mathrm{sech}^7\frac{\tau}{2}}{3\cdot 2^9}\left[3\,\tau\,\left(58\,\cosh\frac{\tau}{2} - 27\,\cosh\frac{3\,\tau}{2} - 3\,\cosh\frac{5\,\tau}{2}\right)\right. \\ &\quad - \left(753\,\sinh\frac{\tau}{2} + 48\,\sinh\frac{3\,\tau}{2} + 22\,\sinh\frac{5\,\tau}{2} + \sinh\frac{7\,\tau}{2}\right) \\ &\quad + 36\,\cosh\frac{\tau}{2}\,\ln(2\,\cosh\frac{\tau}{2})\,(6\,\tau + 8\,\sinh\tau + \sinh 2\tau) \\ &\quad \left. - 108\,\cosh\frac{\tau}{2}\,\left(\int_0^\tau d\tau'\,\tau'\,\tanh\frac{\tau'}{2}\right)\right]. \end{aligned} \tag{17A.12}$$

The integrals to be performed are of the same types as before, except for the one involving the last term which requires one further partial integration:

$$\begin{aligned} -\int_0^\infty d\tau\,\tilde{x}_{\rm cl}(\tau)\mathrm{sech}^6\frac{\tau}{2}\int_0^\tau d\tau'\,\tau'\tanh\frac{\tau'}{2} &= \frac{1}{3}\int_0^\infty d\tau\,\frac{d}{d\tau}\left[\mathrm{sech}^6\frac{\tau}{2}\right]\int_0^\tau d\tau'\,\tau'\tanh\frac{\tau'}{2} \\ &= -\frac{1}{3}\int_0^\infty d\tau\,\mathrm{sech}^6\frac{\tau}{2}\,\tau\tanh\frac{\tau}{2} = -\frac{16}{135}. \end{aligned} \tag{17A.13}$$

[11] I.S. Gradshteyn and I.M. Ryzhik, *op. cit.*, Formulas 2.417.

After the necessary subtraction of the divergent term we find the value of I_{21} given in Eq. (17.240).

The final result for the first coefficient of the Taylor expansion of the subtracted fluctuation factor C' in Eq. (17.222) is therefore

$$c_1 = \frac{71}{24} \approx 2.958. \tag{17A.14}$$

This number was calculated in Ref. [13] by solving the Schrödinger equation [21].

With the help of the WKB approximation he derived a recursion relation for the higher coefficients c_k of the expansion of C':

$$C' = \left[1 - c_1 \frac{g\hbar}{\omega^3} - c_2 \left(\frac{g\hbar}{\omega^3}\right)^2 - c_3 \left(\frac{g\hbar}{\omega^3}\right)^3 + \dots\right]. \tag{17A.15}$$

From this he calculated the next nine coefficients

$$c_2 = \frac{315}{32} \approx 9.84376, \quad c_3 = \frac{65953}{1152} \approx 57.2509. \tag{17A.16}$$

Their large behavior is

$$c_k \sim \frac{9}{\pi} \left(\frac{3}{2}\right)^k k![\ln(6k) + \gamma]. \tag{17A.17}$$

Notes and References

The path integral theory of tunneling was first discussed by
A.I. Vainshtein, *Decaying Systems and the Divergence of Perturbation Series*, Novosibirsk Report (1964), in Russian (unpublished),
and in the context of the nucleation of first-order phase transitions by
J.S. Langer, Ann. Phys. **41**, 108 (1967).
The subject was studied further in the field-theoretic literature:

M.B. Voloshin, I.Y. Kobzarev, L.B. Okun, Yad. Fiz. **20**. 1229 (1974); Sov. J. Nucl. Phys. **20**, 644 (1975);
R. Rajaraman, Phys. Rep. **21**, 227 (1975),
R. Rajaraman, Phys. Rep. **21**, 227 (1975),
P. Frampton, Phys. Rev. Lett. **37**, 1378 (1976) and Phys. Rev. D **15**, 2922 (1977),
S. Coleman, Phys. Rev. D **15**, 2929 (1977); also in *The Whys of Subnuclear Physics*, Erice Lectures 1977, Plenum Press, 1979, ed. by A. Zichichi,
I. Affleck, Phys. Rev. Lett. **46**, 388 (1981).

For a finite-temperature discussion see
L. Dolan and J. Kiskies, Phys. Rev. D **20**, 505-513 (1979).

For multidimensional tunneling processes see
H. Kleinert and R. Kaul, J. Low Temp. Phys. **38**, 539 (1979) (`http://www.physik.fu-berlin.de/~kleinert/66`),
A. Auerbach and S. Kivelson, Nucl. Phys. B **257**, 799 (1985).

The fact that tunneling calculations can be used to derive the growth behavior of large-order perturbation coefficients was first noticed by
A.I. Vainshtein, Novosibirsk Preprint 1964, unpublished.
A different but closely related way of deriving this behavior was proposed by
L.N. Lipatov, JETP Lett. **24**, 157 (1976); **25**, 104 (1977); **44**, 216 (1977); **45**, 216 (1977).

A review on this subject is given in
J. Zinn-Justin, Phys. Rep. **49**, 205 (1979), and in *Recent Advances in Field Theory and Statistical Mechanics*, Les Houches Lectures 1982, Elsevier Science 1984, ed. by J.-B. Zuber and R. Stora.
J. Zinn-Justin, *Quantum Field Theory and Critical Phenomena*, Clarendon, Oxford, 1990.

The important applications to the ϵ-expansion of critical exponents in O(N)-symmetric φ^4 field theories were made by
E. Brezin, J.C. Le Guillou, and J. Zinn-Justin, Phys. Rev. D **15**, 1544, 1558 (1977).
E. Brezin and G. Parisi, J. Stat. Phys. **19**, 269 (1978).
The perturbation expansion of the φ^4-theory up to fifth-order was calculated in Ref. [14].
For two quartic interactions of different symmetries (one O(N)-symmetric, the other of cubic symmetry) see:
H. Kleinert and V. Schulte-Frohlinde, Phys. Lett. B **342**, 284 (1995) (cond-mat/9503038)
A detailed discussion and a comprehensive list of the references to the original papers are contained in the textbook [16].

The calculation of the anomalous magnetic moments in quantum electrodynamics is described in
T. Kinoshita and W.B. Lindquist, Phys. Rev. D **27**, 853 (1983).
M.J. Levine and R. Roskies, in *Proceedings of the Second International Conference on Precision Measurements and Fundamental Constants*, ed. by B.N. Taylor and W.D. Phillips, Natl. Bur. Std. US, Spec. Publ. **617** (1981).

The analytic result for the semiclassical decay rate of a supercurrent in a thin wire was found by
I.H. Duru, H. Kleinert, and N. Ünal, J. Low Temp. Phys. **42**, 137 (1981) (*ibid.*`http/74`),
H. Kleinert and T. Sauer, J. Low Temp. Physics **81**, 123 (1990) (*ibid.*`http/204`).
The experimental situation is explained in
M. Tinkham, *Introduction to Superconductivity*, McGraw-Hill, New York, 1975.
See, in particular, Chapter 7, Sections 7.1–7.3.
For quantum corrections to the decay rate see
N. Giordano, Phys. Rev. Lett. **61**, 2137 (1988);
N. Giordano and E.R. Schuler, Phys. Rev. Lett. **63**, 2417 (1989).

For thermally driven tunneling processes see the review article
P. Hänggi, P. Talkner, and M. Borkovec, Rev. Mod. Phys. **62**, 251 (1990).
Tunneling processes with dissipation were first discussed at $T = 0$ by
A.O. Caldeira and A.J. Leggett, Ann. Phys. **149**, 374 (1983), **153**, 445 (1973) (Erratum)
and for $T \neq 0$ by
H. Grabert, U. Weiss and P. Hänggi, Phys. Rev. Lett. **52**, 2193 (1984),
A.I. Larkin and Y.N. Ovchinnikov, Sov. Phys. JETP **59**, 420 (1984).
Papers on coherent tunneling:
A.J. Leggett, S. Chakravarty, A.T. Dorsey, M.P.A. Fisher, A. Garg, and W. Zwerger, Rev. Mod. Phys. **59**, 1 (1987),
U. Weiss, H. Grabert, P. Hänggi, and P. Riseborough, Phys. Rev. B **35**, 9535 (1987),
H. Grabert, P. Olschowski, and U. Weiss, Phys. Rev. B **36**, 1931 (1987),
On the use of periodic orbits see:
P. Hänggi and W. Hontscha, Ber. Bunsen-Ges. Phys. Chemie **95**, 379 (1991).

The individual citations refer to

[1] For the derivation see
N. Levinson, Kgl. Danske Videnskab. Selskab, Mat.-fys. Medd., **25** (9) (1949).

It is also closely related to Friedel's sum rule:
J. Friedel, Nuovo Cim. Suppl. **7**, 287 (1958).

[2] See also the solutions in textbooks such as
L.D. Landau and E.M. Lifshitz, *Quantum Mechanics*, Pergamon, London, 1965, §25, PROBLEM 4.

[3] L.D. Faddeev and V.N. Popov, Phys. Lett. B **25**, 29 (1967).

[4] J.S. Langer, Ann. Phys. **41**, 108 (1967).

[5] For a general proof see
S. Coleman, Nucl. Phys. B **298**, 178 (1988).

[6] F.J. Dyson, Phys. Rev. **85**, 631 (1952).

[7] Compare the result in Eq. (17.345) with
J.C. Collins and D.E. Soper, Ann. Phys. **112**, 209 (1978).

[8] The variational approach to tunneling was initiated in
H. Kleinert, Phys. Lett. B **300**, 261 (1993).
It has led to very precise tunneling rates in subsequent work by
R. Karrlein and H. Kleinert, Phys. Lett. A **187**, 133 (1994);
H. Kleinert and I. Mustapic, Int. J. Mod. Phys. A **11**, 4383 (1995), most precisely in Ref. [12].

[9] H. Kleinert, Phys. Lett. B **300**, 261 (1993) (*ibid.*`http/214`).

[10] R. Karrlein and H. Kleinert, Phys. Lett. A **187**, 133 (1994) (hep-th/9504048).

[11] C.M. Bender and T.T. Wu, Phys. Rev. D *7*, 1620 (1973), Eq. (5.22).

[12] B. Hamprecht and H. Kleinert, *Tunneling Amplitudes by Perturbation Theory*, Phys. Lett. B **564**, 111 (2003) (hep-th/0302124).

[13] J. Zinn-Justin, J. Math. Phys. **22**, 511 (1981); Table III.

[14] H. Kleinert, J. Neu, V. Schulte-Frohlinde, K.G. Chetyrkin, and S.A. Larin, Phys. Lett. B **272**, 39 (1991) (hep-th/9503230).

[15] H. Kleinert, Phys. Rev. D **57** , 2264 (1998); Addendum: Phys. Rev. D **58** , 107702 (1998) (cond-mat/9803268).

[16] For details and applications to see the textbook
H. Kleinert and V. Schulte-Frohlinde, *Critical Phenomena in ϕ^4-Theory*, World Scientific, Singapore, 2001 (*ibid.*`http/b8`).

[17] The path integral treatment of the decay rate of a supercurrent in a thin wire was initiated by
J.S. Langer and V. Ambegaokar, Phys. Rev. **164**, 498 (1967),
D.E. McCumber and B.I. Halperin, Phys. Rev. B **1**, 1054 (1970).

[18] M. Tinkham, *Introduction to Superconductivity*, McGraw-Hill, New York, 1975.

[19] H. Kleinert and T. Sauer, J. Low Temp. Physics **81**, 123 (1990) (*ibid.*`http/204`).

[20] D.E. McCumber and B.I. Halperin Phys. Rev. B **1**, 1054 (1970).

[21] Divide the numbers in the Table IV of Ref. [13] by $6n4^n$ to get our c_n.